UNIVERSIDAD DE GRANADA

FACULTAD DE CIENCIAS

Departamento de Química Inorgánica

MATERIALES BASADOS EN EL METABOLISMO DEL HIERRO

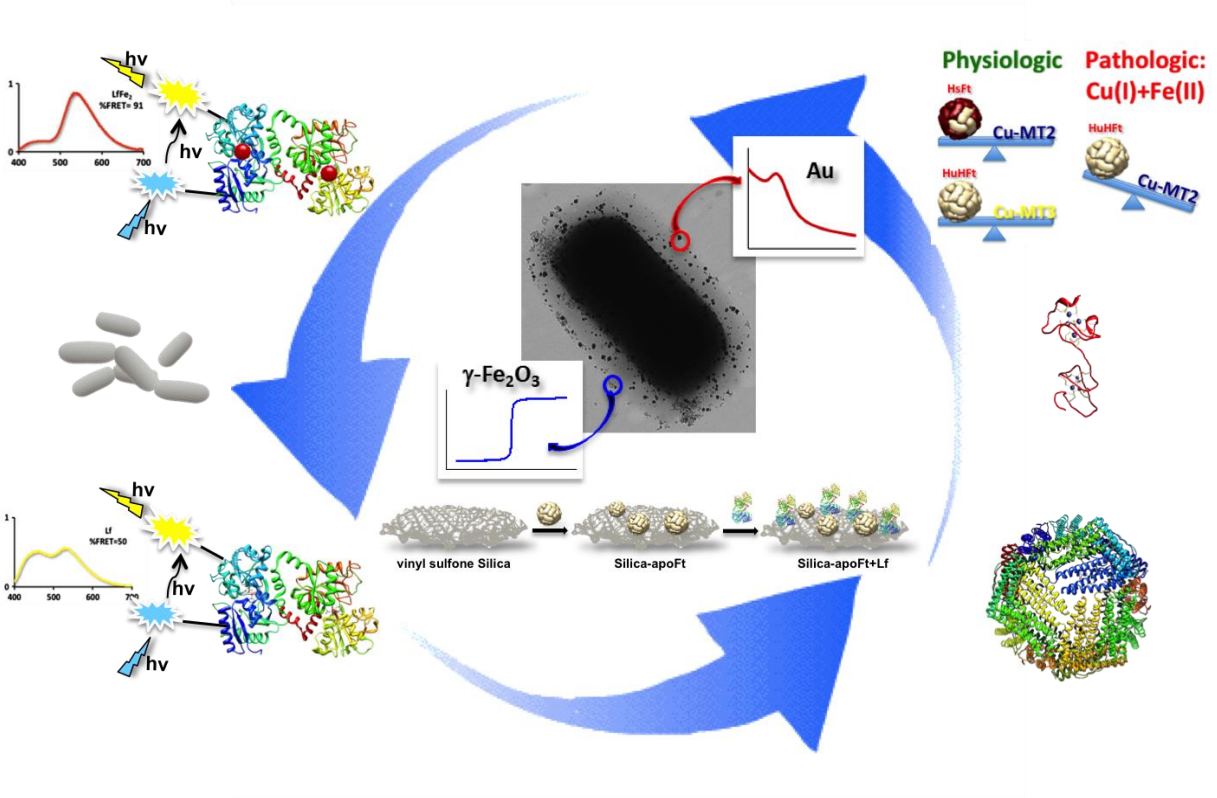

Fernando Carmona Rodríguez-Acosta

24/06/2014

UNIVERSIDAD DE GRANADA

FACULTAD DE CIENCIAS

Departamento de Química Inorgánica

PROGRAMA OFICIAL DE DOCTORADO EN QUÍMICA

TESIS DOCTORAL

MATERIALES BASADOS EN EL METABOLISMO DEL HIERRO

Fernando Carmona Rodríguez-Acosta

Granada, junio 2014

MATERIALES BASADOS EN EL METABOLISMO DEL HIERRO

Memoria de Tesis Doctoral presentada por
Fernando Carmona Rodríguez-Acosta
para aspirar al título de Doctor por la
Universidad de Granada

Fdo. Fernando Carmona Rodríguez-Acosta

EL DIRECTOR DE LA TESIS DOCTORAL:

José Manuel Domínguez Vera
Catedrático del Departamento de Química Inorgánica
Instituto de Biotecnología
Universidad de Granada

El doctorando Fernando Carmona Rodríguez-Acosta y el director de la Tesis José Manuel Domínguez Vera garantizamos, al firmar esta Tesis Doctoral, que el trabajo ha sido realizado por el doctorando bajo la dirección del director de la Tesis y hasta donde nuestro conocimiento alcanza, en la realización del trabajo, se han respetado los derechos de otros autores a ser citados, cuando se han utilizado sus resultados o publicaciones.

Granada, junio de 2014

El Doctorando

Fdo.: Fernando Carmona Rodríguez-Acosta

El Director de la Tesis

Fdo.: José Manuel Domínguez Vera

Catedrático del Departamento de Química Inorgánica. Instituto de Biotecnología

Universidad de Granada

a Papá, Mamá, Miguel y Rosalía,
las personas que más quiero
en este mundo

Esta Tesis Doctoral se ha llevado a cabo en los laboratorios del Departamento Química Inorgánica de la Universidad de Granada, en el grupo BIONANOMET (FQM-368), gracias al Ministerio de Ciencia e Innovación por la concesión de mi beca FPI y a la financiación de los proyectos CTQ2009-09344 y CTQ2012-32236, así como al proyecto POSTBIO financiado por BIOSEARCH S. A. y a la Junta de Andalucía (grupo FQM-368).

Gracias a todos los componentes de mi grupo de investigación, al que me siento extremadamente afortunado de formar parte. En especial gracias a ti Josema, mi director de Tesis, por confiar en mí y por formarme ya no sólo como investigador, sino también como persona. Tu vocación investigadora, tu trabajo y los valores humanos que me has transmitido durante estos años son para mí lo más valioso que me llevo de esta Tesis. Gracias por ser siempre tan atento y cariñoso conmigo.

Gracias Nati por ser una bellísima persona, siempre tan cercana y dispuesta a ayudarme cuando lo he necesitado, es una suerte poder trabajar contigo.

Gracias Rafa, por ser el mejor compañero de fatigas en los congresos y por tus espectaculares diseños en las imágenes que presento en mi Tesis Doctoral.

Gracias también a mis compañeros de laboratorio, en especial a Elsa, Daniela, Migue, Ana, Rocío y Manu. Sois todos geniales. ¡Estoy deseando estrenar el nuevo laboratorio con vosotros!.

Esta Tesis Doctoral no habría sido posible sin ti, Puri, que mostraste una enorme confianza en mi, cuando aún apenas había terminado la carrera, y me presentaste a Josema y al resto de componentes del grupo de investigación donde posteriormente realicé mi Tesis.

Gracias a todos los miembros del Departamento de Química Inorgánica de la Universidad de Granada, muy en especial al grupo de “Coordinación”, dirigido por el Profesor D. Enrique Colacio, a quienes guardo un especial cariño por todos los momentos que hemos pasado juntos, por tratarme siempre como a un miembro más de su grupo. Gracias a Enrique, Juanma, Antoñillo, Antonio Mota y, muy en especial gracias a ti, Pepe, a quien siempre recordaré con un profundo cariño y apego.

A todas las personas que han colaborado en el desarrollo de mi investigación durante estos cuatro años:

Gracias a la Profesora Mercè Capdevila, del Departamento de Química de la Universidad Autónoma de Barcelona y a la Profesora Sílvia Atrian, del Departamento de Genética de la Universidad de Barcelona, por la síntesis y purificación de las metalotioneínas y su estrecha colaboración y disponibilidad durante todos estos años. Gracias Mercè por tu incondicional apoyo durante mi estancia.

Gracias a BIOSEARCH S. A. por suministrarnos los liofilizados de bacterias probióticas y a la ayuda recibida de muchos de sus miembros durante estos años.

Gracias al Profesor Francisco Santoyo y su grupo de investigación, del Departamento de Química Orgánica de la Universidad de Granada por la síntesis del sólido sílica – vinilsulfona y por su magnífica colaboración durante estos años.

I thank Paolo Arosio and Michela Asperti for providing us the recombinant H-ferritin homopolymer.

Gracias al Profesor D. Claudio Fernández, del Instituto Max Planck de Rosario, Argentina, por el tiempo dedicado a mi investigación durante mi estancia.

Gracias a Jean-Didier Maréchal y a Víctor Muñoz por el estudio computacional que llevaron a cabo en las lactoferrinas marcadas con fluoróforos.

RESUMEN Y ESTRUCTURA DE LA TESIS DOCTORAL

La presente Tesis Doctoral se enmarca en el estudio de aspectos concretos del metabolismo de hierro, por una parte con un enfoque más clásico, que pretende entender mejor la función de determinadas metaloproteínas de hierro y por otra parte, con un enfoque más innovador, intentando recrear escenarios biológicos complejos compuestos de varias metaloproteínas donde poder estudiar las consecuencias patológicas que una disfunción en alguna de ellas podría desencadenar.

Además, aprovechando el conocimiento generado, hemos llevado a cabo el desarrollo de nuevos materiales bioinspirados en el metabolismo del hierro, con el objetivo de que puedan ser conceptualmente útiles para intervenir en dichos desajustes y actuar a nivel terapéutico en las patologías que de ello se derivan.

Los resultados experimentales obtenidos y la discusión de los mismos se presentan en esta Memoria divididos en 6 capítulos.

En el **primer capítulo,** se revisan los conceptos básicos del tema de investigación en el que se ha trabajado en la Tesis Doctoral y la motivación del mismo en el contexto actual. Inicialmente, se exponen las principales características de la maquinaria química que define el metabolismo y la homeostasis del hierro en los seres vivos. Seguidamente, se aborda un estudio detallado de dos proteínas cruciales en el metabolismo del hierro: la ferritina y la lactoferrina, donde se abordan cuestiones estructurales, funcionales y patológicas de éstas así como su interacción con otras biomoléculas presentes en su entorno. Posteriormente, se lleva a cabo una revisión del metabolismo del hierro en bacterias, tanto infecciosas como beneficiosas, en el marco de la defensa inmune del organismo debida al hierro. Finalmente, se concluye el capítulo con los objetivos que se han pretendido alcanzar en esta Tesis Doctoral.

En el **segundo capítulo**, se han puesto de manifiesto las discrepancias sobre los mecanismos de actuación del centro ferroxidasa de la ferritina, haciendo hincapié en cómo la propia función de la ferritina viene regulada por la composición de su cápside proteica, concretamente en la relación entre subunidades H y L. Hemos pretendido mostrar las implicaciones biológicas que podría tener una elección "inadecuada" por parte de la célula en la síntesis de la cápside proteica, especialmente a nivel cerebral.

En el **tercer capítulo**, hemos pretendido ir más allá de la controversia existente entre los diferentes mecanismos de actuación del centro ferroxidasa de la ferritina y hemos querido poner de manifiesto, por primera vez, que la alta actividad ferroxidasa y baja capacidad de almacenamiento de hierro de las ferritinas ricas en subunidades H, tiene implicaciones biológicas en un contexto más amplio que engloba a otras metaloproteínas presentes en la célula. Este enfoque novedoso se ha llevado a cabo estudiando la actividad ferroxidasa y la capacidad de almacenamiento de diferentes ferritinas (con diferente relación H/L) en presencia de metalotioneínas, proteínas de especial interés a nivel neurológico por encargarse de la homeóstasis de otros metales, como cobre y cinc.

Este capítulo trata en definitiva de abrir un debate sobre las consecuencias de los diferentes mecanismos de actuación de la ferritina en presencia de otras metaloproteínas existentes en su entorno como las metalotioneínas, recreando así un escenario biológico más real y preciso.

En el **cuarto capítulo**, hemos diseñado una serie de materiales con actividad antimicrobiana bioinspirados en las proteínas presentes en la leche materna, donde la ferritina es predominantemente H y existen elevadas concentraciones de lactoferrina, proteína encargada de captar Fe(III) para privar a los microorganismos patógenos de este metal esencial para su proliferación.

La existencia de este "tándem" lactoferrina – ferritina H en leche materna es coherente con los resultados obtenidos en el capítulo anterior y nos inspiró para llevar a cabo la preparación de materiales formados por ambas proteínas que combinaran de manera sinérgica las funciones de éstas, es decir, un alto poder detoxificante de Fe(II), por parte de la ferritina H, y una rápida incorporación del Fe(III) en la lactoferrina. Estos materiales actúan captando hierro del medio en cualquiera de sus estados de oxidación, llevando a cabo por tanto una acción antimicrobiana completa.

Es oportuno señalar que el estudio del metabolismo de hierro en bacterias adquiere una dimensión extraordinaria en el contexto de la búsqueda de nuevos agentes antibióticos. Puesto que todas las bacterias patógenas requieren hierro para su proliferación, cualquier vía de inhibir esta captación de hierro conlleva una acción antibacteriana.

En el **quinto capítulo,** pretendemos explorar una vía en la que podamos entender cómo, al mismo tiempo que nuestro organismo priva de hierro a microorganismos infecciosos, existen bacterias probióticas beneficiosas capaces de nutrirse de hierro a expensas del "host" donde proliferan. En particular hemos demostrado, mediante una nueva metodología, que la lactoferrina no sólo no tiene acción bacteriostática frente a estas bacterias beneficiosas, sino que además promueve su proliferación actuando como dadora de hierro.

Concretamente, hemos podido usar el fenómeno de FRET para demostrar que la lactoferrina cede hierro a bacterias probióticas y que además lo hace sin ser internalizada en la bacteria, a diferencia del mecanismo generalizado en el que las proteínas transportadoras de hierro, como la transferrina, ceden hierro a las células a través de su internalización por endocitosis.

En el **sexto capítulo,** y como fruto del estudio del metabolismo de hierro en bacterias probióticas, hemos podido constatar la presencia una molécula reductora emitida por estas bacterias capaz de reducir Fe(III) a Fe(II). Este poder de reducción ha sido aplicado a otros iones metálicos y en particular hemos demostrado que estas bacterias probióticas son capaces de reducir Au(III) a Au(0) con la consiguiente formación de nanopartículas de Au que se quedan fijadas en el biofilm de la bacteria.

Por otra parte, trabajos llevados a cabo en el grupo de investigación en los que he participado, mostraron que estas bacterias probióticas son capaces de incorporar en su superficie nanopartículas de maghemita.

Hemos pretendido combinar ambas propiedades de estas bacterias probióticas: poder de reducción de Au(III) y capacidad de incorporar nanopartículas de óxido de hierro en su membrana exterior, para generar bacterias vivas compuestas simultáneamente por nanopartículas con propiedades ópticas (debido a la presencia de nanopartículas de Au) y magnéticas (debido a la presencia de nanopartículas de maghemita). Esto nos ha permitido crear el primer material vivo con propiedades magneto-ópticas.

Los resultados del trabajo de investigación realizado durante el desarrollo de esta Tesis Doctoral han dado lugar hasta la actualidad, a 5 artículos ya publicados:

- Carmona, F., Palacios, Ò., Gálvez, N., Cuesta, R., Atrian, S., Capdevila, M., & Domínguez-Vera, J. M. (2013). Ferritin iron uptake and release in the presence of metals and metalloproteins: chemical implications in the brain. ***Coordination Chemistry Reviews*, *257*(19), 2752-2764**.

- Fernando Carmona, Daniela Mendoza, Scheghajegh Kord, Michela Asperti, Paolo Arosio, Sílvia Atrian, Mercè Capdevila, Jose M. Dominguez-Vera. (2014). Chemically and biologically harmless vs. harmful ferritin/copper-metallothionein couples. ***Chemistry: A European JournaL. Accepted.*** *DOI: 10.1002/chem.201404660*

- Fernando Carmona, Daniela Mendoza, Alicia Megía-Fernández, Francisco Santoyo-Gonzalez and José M. Domínguez-Vera. (2013). A bioinspired hybrid silica–protein material with antimicrobial activity by iron uptake. ***Metallomics*, 5, 193.**

- Carmona, F., Muñoz-Robles, V., Cuesta, R., Gálvez, N., Capdevila, M., Maréchal, J. D., & Dominguez-Vera, J. M. (2014). Monitoring lactoferrin iron levels by fluorescence resonance energy transfer: a combined chemical and computational study. ***Journal of Biological Inorganic Chemistry*, 19, 439-447**.

- Carmona, F., Martín, M., Gálvez, N., & Dominguez-Vera, J. M.. (2014). Bioinspired magneto-optical bacteria. ***Inorganic chemistry, 53(16), 8565-8569.***

ÍNDICE

CAPÍTULO 1.

INTRODUCCIÓN

Salvo raras excepciones, prácticamente todos los organismos estudiados desde el reino *archaea* hasta el ser humano son dependientes del hierro para sobrevivir. A pesar de la ubicua distribución y abundancia de este metal en la biosfera, la vida debe luchar con dos riesgos paradójicos: tanto la deficiencia como el exceso de hierro tienen consecuencias fatales. Los mecanismos homeostáticos que regulan la absorción, transporte, almacén y movilización del hierro celular son por tanto de una importancia crítica en el origen y desarrollo de la vida, existiendo en consecuencia una compleja maquinaria bioquímica que, de manera extraordinaria controla el metabolismo de hierro.

En esta maquinaria, un sinfín de biomoléculas participan en todo un ciclo de procesos químicos que tienen por finalidad el empleo de este metal para llevar a cabo una gran variedad de reacciones redox esenciales para los organismos. Y es que dada la estabilidad termodinámica y el potencial redox de sus dos estados de oxidación más importantes, Fe(II) y Fe(III), el hierro es un elemento vital en buena parte debido a su extraordinaria capacidad para actuar como dador y aceptor de electrones, lo que lo convierte en pieza fundamental en los procesos redox y de transporte de electrones que tienen lugar en el metabolismo de los seres vivos. Estos procesos y reacciones, rigen mecanismos vitales como el transporte de oxígeno, la expresión génica y la fosforilación oxidativa, mecanismo mediante el cual las células eucariotas sintetizan ATP, principal recurso energético de la célula. En cerebro, por ejemplo, el hierro es crucial para el desarrollo neuronal y posee un papel fundamental en el organismo para la funcionalidad de enzimas, síntesis de grupos hemo y clústeres hierro-azufre así como para el transporte electrónico.[1]

Durante la última década, numerosos descubrimientos han dado lugar a una revolución en el entendimiento de eventos moleculares relacionados con el metabolismo del hierro que han desvelado sorprendentes nuevas funciones de proteínas de las que poco o nada se conocía anteriormente, así como el descubrimiento de nuevas proteínas implicadas en la escena del metabolismo del hierro y su control homeostático. Entre éstas, se incluye a las proteínas reguladoras de hierro (IRPs 1 y 2), una variedad de ferrireductasas, transportadores de membrana (DMT1 y ferroportina 1), una ferroxidasa

multicobre involucrada en la exportación de hierro de la célula (hefaestina) y reguladores en el balance mitocondrial de hierro (frataxina).

Los resultados experimentales actuales, haciendo uso de organismos desde la levadura hasta mamíferos, han demostrado su poder para elucidar tanto un mecanismo de hierro normal como sus desórdenes genéticos y sus defectos moleculares subyacentes.

La absorción del hierro, entendida vagamente hasta hace unos años, se ha convertido actualmente en un fructífero campo de investigación bien definido. Recientemente, el ampliamente buscado gen de la hemocromatosis, una enfermedad hereditaria que afecta al metabolismo del hierro provocando un acúmulo excesivo e incorrecto de este metal ha sido descubierto, y una activa investigación se lleva a cabo actualmente para elucidar los mecanismos que subyacen a este descubrimiento.[2]

Uno de los más apasionantes y emergentes campos de investigación en el metabolismo del hierro y sus consecuencias patológicas tiene lugar en el campo de las enfermedades neurodegenerativas. Recientemente, una sorprendente conexión entre el metabolismo del hierro y la ataxia de Friedrich ha sido descubierta[3] y actualmente ha sido ampliamente aceptado que el daño oxidativo en neuronas es una causa primaria de enfermedades degenerativas como la enfermedad de Alzheimer o la enfermedad de Parkinson.[4] Además, como diversos autores han reportado, el Fe(II) libre es capaz de producir este daño oxidativo en neuronas e inducir la agregación de algunas proteínas como el péptido beta amiloideo o la alfa sinucleÍna, claves en el desarrollo de enfermedades neurodegenerativas como Alzheimer y Parkinson, respectivamente.[5,6]

Estos recientes descubrimientos permiten afirmar que el crecimiento en el entendimiento del metabolismo del hierro y sus implicaciones en la salud ha sido abrumador, y que los resultados obtenidos durante los últimos años son probablemente todavía, el prólogo de lo que está por venir.

1.1. Metabolismo y homeostasis del hierro

Al hecho ya mencionado de la necesidad de la vida por el hierro, hay que añadir un conjunto de reacciones que son promovidas por la presencia de Fe(II) libre y que paradójicamente son fatales para la vida. El Fe(II), y otros iones metálicos en menor escala como el Cu(I), generan especies altamente oxidantes, conocidas como especies reactivas del oxígeno (ROS), cuando se encuentran libres (fuera de un metabolismo controlado). El Fe(II) libre en presencia de oxígeno promueve la formación de especies oxidantes a través de la conocida reacción de Fenton[7] (Fig. 1), mediante la cual se generan radicales hidroxilo OH·, especies químicas extremadamente oxidantes, capaces de provocar daño en el DNA, peroxidación en membranas y alterar la función de diversas proteínas, dando lugar a un daño celular irreversible, fallo orgánico e incluso eventualmente la muerte.[8,9,10]

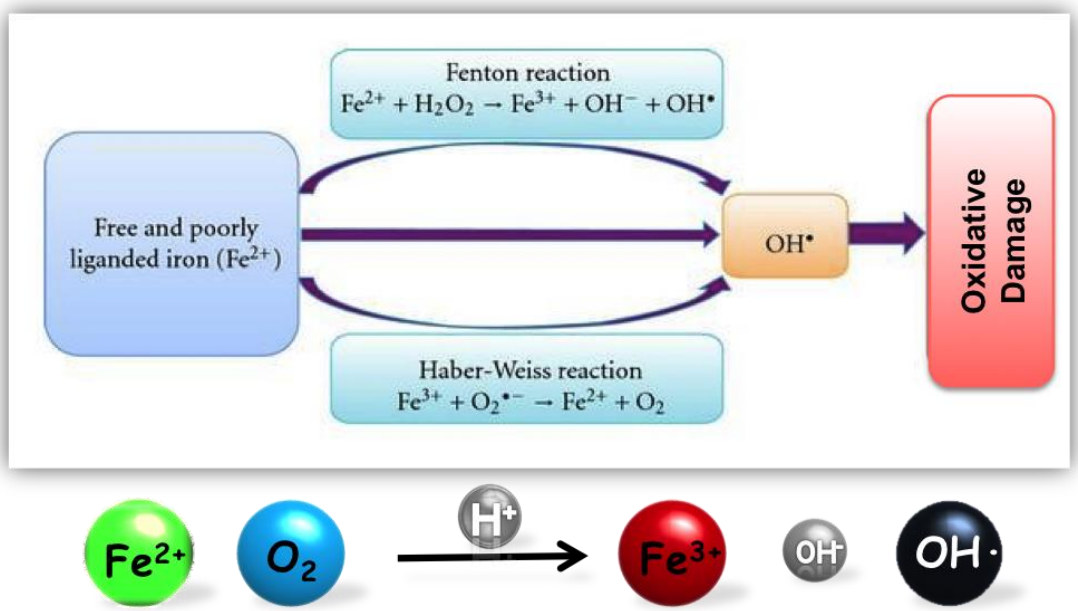

Figura 1. *Reacción de Fenton*

Por otra parte, el hierro es un nutriente esencial para microorganismos patógenos, que requieren este metal para sobrevivir y replicarse. La vida es, en cierta manera, una batalla por el hierro en la que el "host" debe privar de hierro a los huéspedes

indeseados para combatir las infecciones que estos últimos pueden causar. Por todo ello, tanto un exceso como una deficiencia de hierro pueden llegar a ser extremadamente dañinos para el organismo, lo que ha obligado a los seres vivos a desarrollar toda una serie de mecanismos bioquímicos para controlar esta situación. Dichos mecanismos se encuentran estrictamente regulados en todos los organismos a nivel molecular a través de una compleja maquinaria química que comprende una serie de proteínas focalizadas en la absorción, transporte y almacén del hierro, los tres pilares fundamentales que conforman el metabolismo y la homeostasis de este metal (Fig. 2).

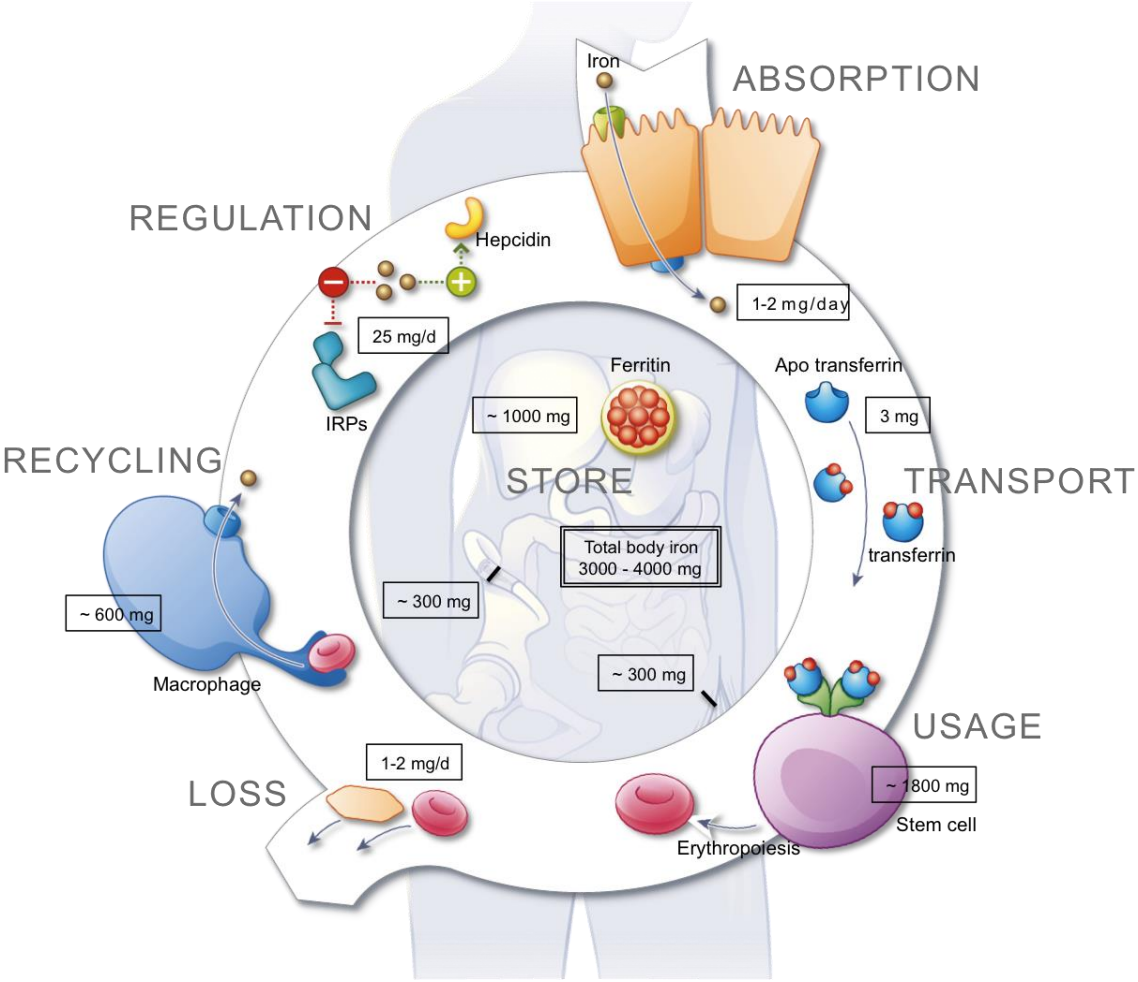

Figura 2. *Metabolismo del hierro*

El requerimiento de hierro en humanos es a nivel traza. Así, el hombre y la mujer adultos presentan valores medios de 55 y 45 mg de hierro por kg de peso respectivamente, que se absorben desde la dieta en torno a cantidades que oscilan entre 1 y 2 mg diarios.[11] Los principales tejidos de almacenamiento de este metal son el hígado, que contiene el 60% del hierro de depósito, y las células del sistema retículo endotelial y el tejido muscular, donde se encuentra el 40% restante. No obstante, este reparto de hierro va cambiando con el paso de los años y la aparición de ciertas patologías, llegándose incluso a situaciones en las que el cerebro puede contener más hierro que el propio hígado.

El hierro que es absorbido a nivel intestinal a través de la dieta es captado y transportado a través del torrente sanguíneo por la *serum* transferrina, una glicoproteína perteneciente a la familia de las transferrinas con gran afinidad por Fe(III).[12] Esta familia de proteínas está compuesta, además de por la ya mencionada *serum* transferrina encargada de distribuir y suministrar hierro a todas las células del organismo, por la lactoferrina, presente en fluidos y secreciones mucosas donde más que desempeñar funciones de transporte como su "hermana" la transferrina, desempeña funciones inmunológicas. El transporte transferrínico de hierro en sangre conlleva una función implícita de "buffer" de hierro en suero, en tanto que mantiene su concentración baja y constante, evitando además que éste quede libre y entre a formar parte de ciclos redox indeseados.

El reconocimiento de la transferrina por parte de la célula tiene lugar a nivel de membrana, donde es reconocida por un receptor específico denominado receptor de transferrina (Tfr) e internalizado por endocitosis mediada por vesículas de clatrina. Una vez en el interior de la célula, el hierro es liberado de la proteína mediante acidificación por el medio químico del endosoma y expulsado al citoplasma por un transportador de hierro denominado DMT1 (Fig. 3). Ya en el citoplasma, es rápidamente incorporado a las diversas enzimas que utilizan este metal como cofactor, principalmente localizadas en la mitocondria, donde desempeña funciones de transporte de electrones, síntesis de clústers [Fe-S] y obtención de energía en proteínas como citocromos y frataxinas.

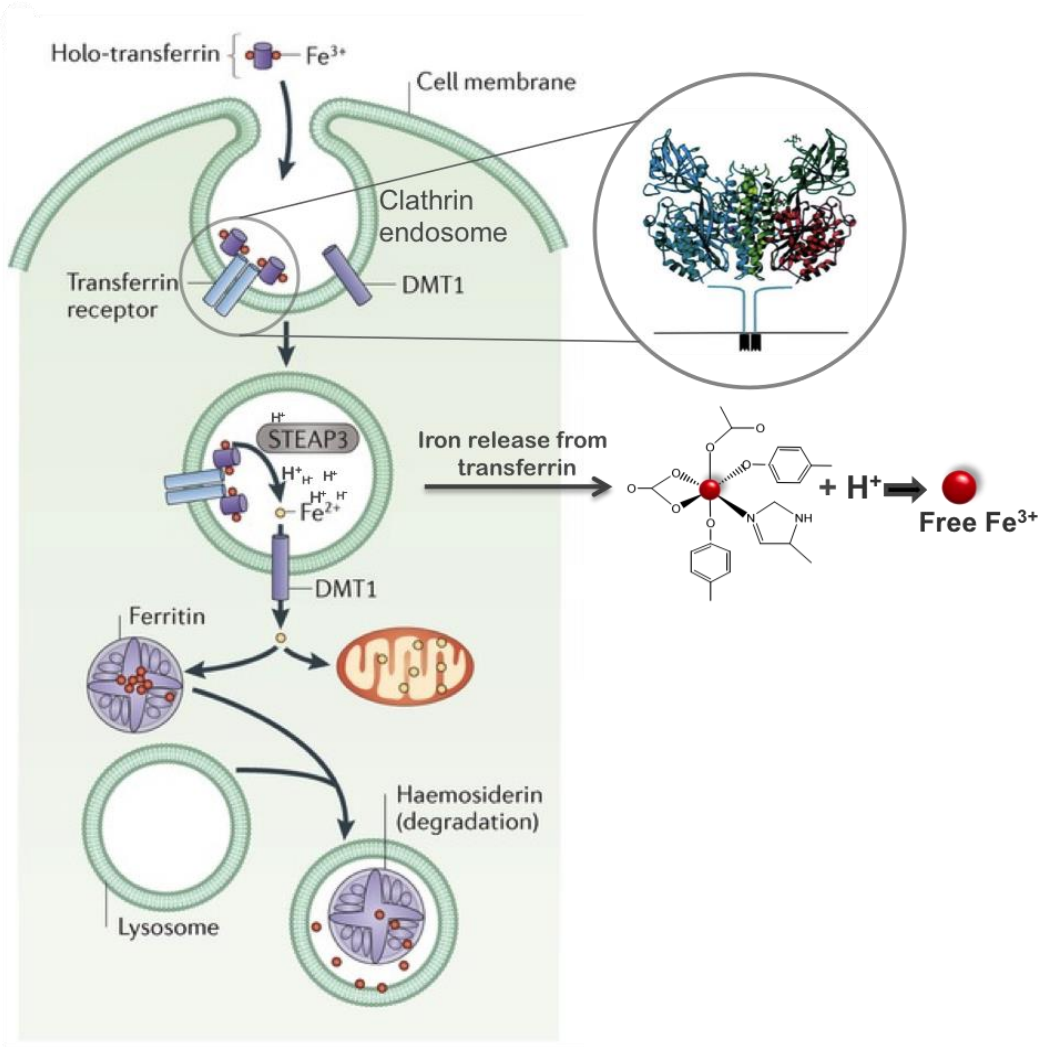

***Figura 3**. Internalización y distribución del hierro en la célula*

El hierro que no es requerido por la célula para fines metabólicos inmediatos no puede quedar libre y debe ser almacenado en una forma que, por otra parte, permita su uso cuando la célula lo requiera. Este almacén de hierro es la ferritina, proteína de almacén de hierro por excelencia en los organismos vivos, capaz de almacenar miles de átomos de hierro en forma de mineral soluble de Fe(III) que queda disponible a expensas de las necesidades metabólicas celulares, protegiendo al mismo tiempo de los efectos dañinos que la presencia de hierro libre puede originar en la célula. El hierro una vez almacenado en la ferritina no es tóxico.

Toda esta maquinaria bioquímica asociada a la homeostasis del hierro intracelular no está exenta de regulación. Por el contrario, existe un mecanismo sutil que modula la capacidad de la célula para captar y almacenar hierro en base a la cantidad intracelular presente del metal a través del control de la síntesis de ferritina (almacén de hierro) y del receptor de transferrina (transporte de hierro). Esta regulación en respuesta a la cantidad de hierro intracelular tiene lugar a nivel post transcripcional por dos proteínas de unión al metal que actúan como factores de traducción del mRNA: IRP1 y IRP2.[13,14] Estas proteínas actúan uniéndose a secuencias específicas del mRNA, llamadas elementos de respuesta a hierro (IREs), localizadas entre las secuencias génicas que codifican la síntesis de ferritina y del receptor de la transferrina, activando o inhibiendo su traducción de manera opuesta. IRP1 e IRP2 modulan su acción sobre el mRNA en función de la presencia o ausencia del metal a través de la formación de clústers [Fe-S] en su estructura, que modulan la acción de estas proteínas en base a una conformación "abierta", carente de clúster [Fe-S] o "cerrada".[15]

En presencia de hierro intracelular, IRP1 sufre un cambio conformacional debido a la formación de clústeres [Fe-S] en su estructura, que impiden su unión al mRNA que codifica la síntesis de ferritina permitiendo su traducción.[16] En otras palabras, cuando hay un nivel elevado de hierro en la célula, el hierro en sí mismo induce a la célula a aumentar su capacidad de almacenamiento, sintetizando ferritina. Cuando por el contrario la cantidad de hierro intracelular es baja, la forma apo de IRP1 adopta una conformación abierta carente de clúster [Fe-S], que se une en el extremo 5' de los elementos de respuesta a hierro (IRE) en el mRNA del receptor de transferrina estabilizándolo y permitiendo su traducción, aumentando en consecuencia la capacidad de la célula para captar más hierro y aumentando por ende la síntesis del receptor de transferrina.[17] Es importante resaltar que esta conformación apo de IRP1, al mismo tiempo que promueve la internalización de hierro transferrínico en la célula inhibe síntesis de ferritina, completando un elegante entramado de regulación que moviliza conjuntamente a toda una serie de proteínas en respuesta a las necesidades de la célula (Fig. 4).

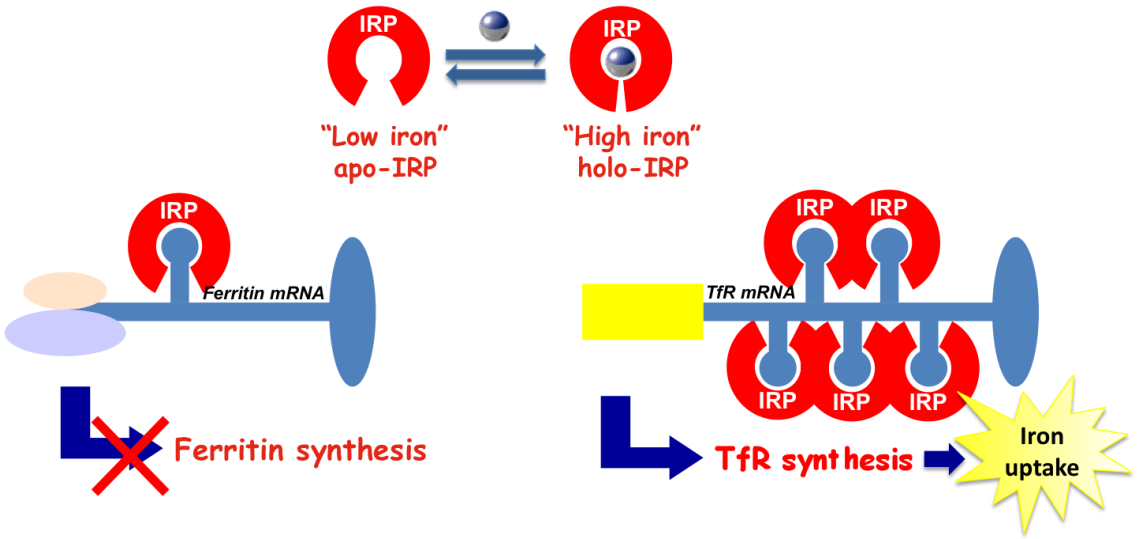

***Fig. 4**: Regulación en respuesta a hierro*

En esta introducción se ha pretendido mostrar que la homeostasis del hierro en los organismos vivos se encuentra estrictamente regulada por una serie de proteínas que actúan de manera cooperativa entre sí y que, en todo momento, el metal se encuentra presente, o bien unido a proteínas y enzimas o almacenado en la ferritina. Un pequeño desajuste en esta maquinaria bioquímica podría dar lugar a alteraciones en el metabolismo del hierro con consecuencias fatales para el organismo, en tanto que permitiría la presencia de hierro libre tóxico capaz de causar muerte celular por estrés oxidativo, así como promover el crecimiento de microorganismos patógenos debido al carácter esencial que este metal supone para su crecimiento.

En este contexto, la presente Tesis Doctoral se enmarca en el estudio de aspectos concretos del metabolismo de hierro, por una parte con un enfoque más clásico que pretende entender mejor la función de metaloproteínas de hierro particulares, como son la ferritina y la lactoferrina y por otra parte, con un enfoque más innovador, intentando recrear escenarios biológicos compuestos de varias metaloproteínas donde poder estudiar cómo la función de una de ellas se ve afectada y controlada por la presencia de otra, y las consecuencias patológicas que de ello podrían derivarse.

Además, pretendemos aprovechar el conocimiento adquirido en estos estudios en el desarrollo de materiales que puedan intervenir directamente en el metabolismo de hierro. Estos materiales, que podemos denominar bioinspirados en el metabolismo del hierro, están diseñados como fruto del estudio de las consecuencias que podría desencadenar una disfunción en algunas de las proteínas que conforman el metabolismo de este metal, y del estudio del papel que adquiere el hierro libre generado como consecuencia de estas disfunciones desde la óptica de su interacción con otras proteínas, metales y de su biodisponibilidad para promover procesos bacterianos infecciosos.

1.2. Lactoferrina: una proteína transportadora de hierro "algo particular"

La lactoferrina es una glicoproteína de 80 kDa perteneciente a la familia de las transferrinas. Aislada por primera vez de leche bovina en 1939,[18] se encuentra presente en humanos en secreciones mucosas como lágrimas, fluido uterino y vaginal, bilis, secreciones nasales, saliva y en calostro y leche materna, donde presenta concentraciones especialmente elevadas (7 mg/mL y 2 mg/mL, respectivamente).[19,20] También puede encontrarse en el plasma sanguíneo, aunque a bajas concentraciones (~1 μg/ml), donde es sintetizada por los neutrófilos.[21]

A pesar de su considerable parecido con su "hermana" la *serum* transferrina, con la que comparte un 60% de homología en su secuencia en humanos,[22] no está totalmente establecido que la lactoferrina actúe realmente como una proteína de transporte de hierro en sangre. Sin embargo, sí han sido reportadas numerosas funciones inmunológicas incluyendo actividades antibacterianas, antivirales y antiparasitarias, entre otras (Fig. 5).[23] De hecho, la lactoferrina es considerada parte del sistema inmune innato debido en gran medida a su extraordinaria afinidad por hierro, ya que priva a los microorganismos patógenos de un metal absolutamente esencial para su viabilidad y en consecuencia, impide su proliferación.

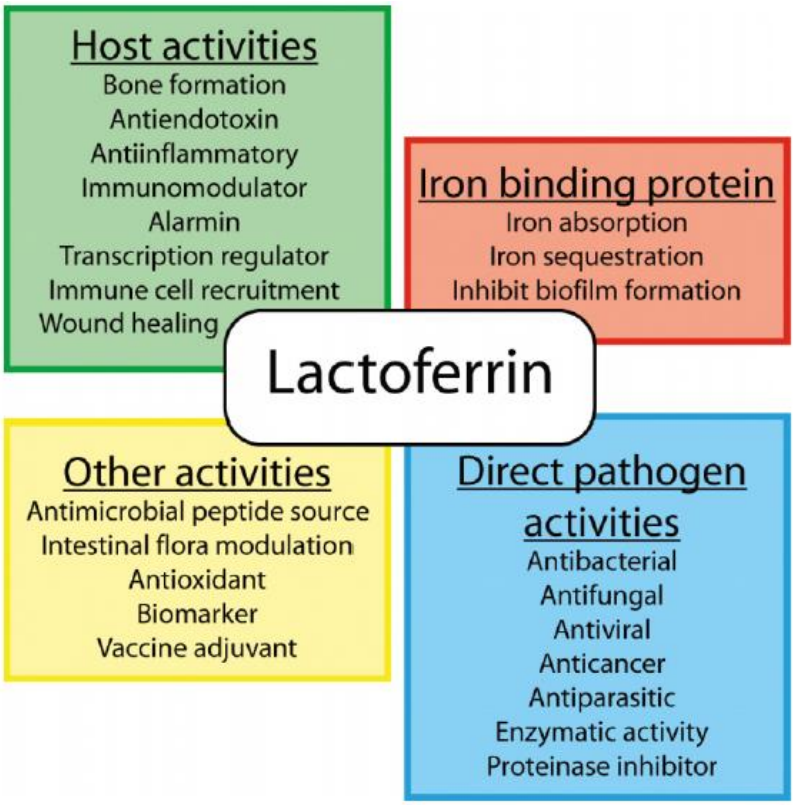

***Fig. 5**: Funciones de la lactoferrina*

Los estudios de difracción de rayos X, disponibles solo para las isoformas apo- y holo- de la lactoferrina, Lf (vacía, 0 Fe/proteína) y $LfFe_2$ (saturada, 2 Fe/proteína), respectivamente, muestran que la estructura de la lactoferrina consiste en una cadena polipeptídica de 703 aminoácidos que conforma dos dominios globulares denominados lóbulos N y C (Fig. 6). El lóbulo N- corresponde a los residuos 1-333, y el lóbulo C- a los residuos 345-692. Los finales de ambos lóbulos se encuentran conectados entre sí por una hélice alfa corta. Estos dos lóbulos homólogos N- y C- están divididos a su vez en dos dominios similares en tamaño conocidos como subdominios N1 y N2 en el lóbulo N- y subdominios C1 y C2 en el lóbulo C-.

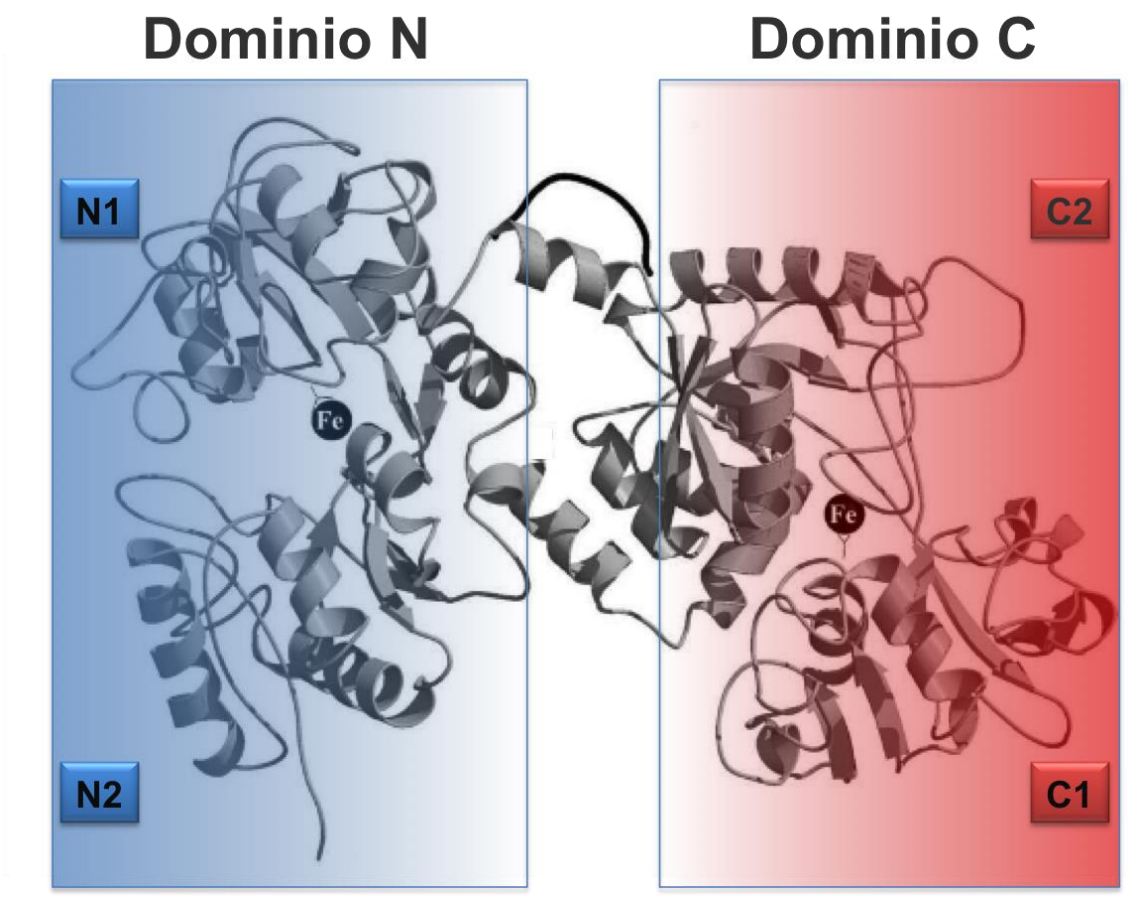

Fig. 6: *Estructura proteica de la lactoferrina en su forma* $LfFe_2$.

La lactoferrina une firmemente ($K_f \approx 10^{22}$ M) pero de manera reversible, dos iones Fe(III).[24,25] Cada centro de unión de hierro se encuentra en la región interespacial de los dominios de cada lóbulo. El entorno químico de ambos sitios de coordinación de Fe(III) es similar, y está constituido por dos oxígenos fenólicos de dos residuos de tirosina, un imidazol de un residuo de histidina y un carboxilato de un residuo de aspártico. La esfera de coordinación del Fe(III) se ve completada, en la forma nativa, con dos átomos de oxígeno de un anión carbonato, estabilizado en la estructura de la metaloproteína por puentes de hidrógeno a las cadenas peptídicas que rodean al centro activo (Fig. 7).

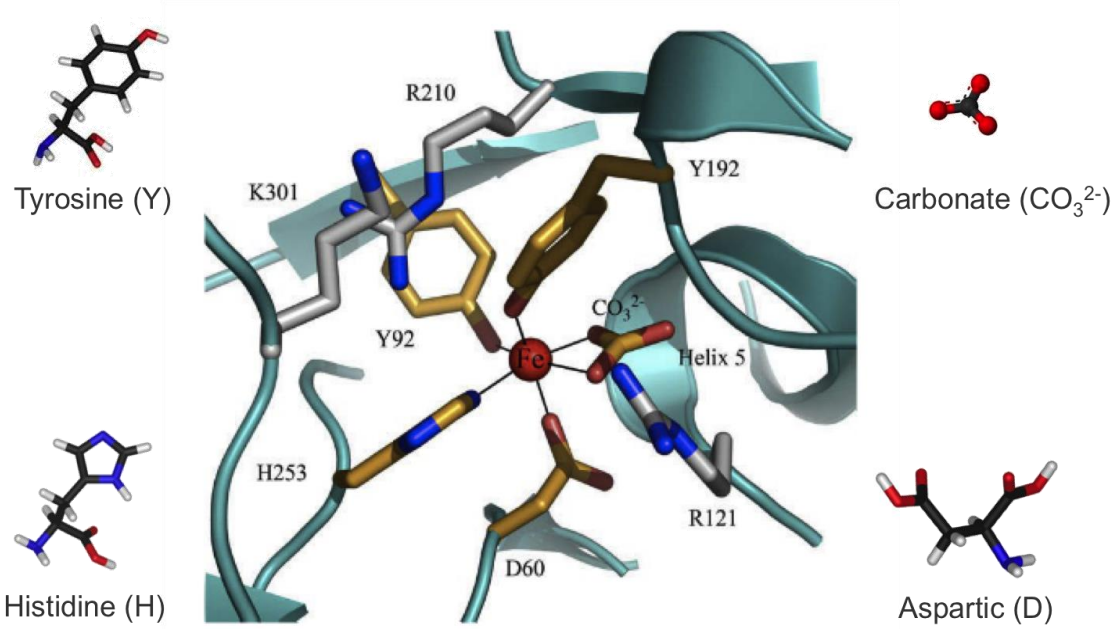

Fig. 7*: Centro activo de la lactoferrina.*

La enorme afinidad por Fe(III) de la lactoferrina, sensiblemente superior a la de la *serum* transferrina a pesar de su homología estructural, viene determinada en buena parte por los cambios conformacionales que tienen lugar cuando incorpora el metal a su estructura. Estos cambios conformacionales se traducen en un movimiento tipo "bisagra" en torno a los centros activos que secuestran firmemente el hierro e impiden su transferencia a otra molécula por competición directa.

La presencia del anión carbonato en la esfera de coordinación de hierro permite un control de la liberación del metal con el pH (Fig. 8). La pérdida de este ligando carbonato al ser protonado es, presumiblemente, el primer paso en la desestabilización de la esfera de coordinación del Fe(III),[26] lo que permite una liberación controlada del ion metálico en un modo que no sería probablemente posible con un set completo de seis ligandos proteicos. Esta liberación del metal tiene lugar en el endosoma, una vez internalizada la metaloproteína en la célula, debido a la consabida bajada de pH que tiene lugar en este tipo de compartimentos celulares.

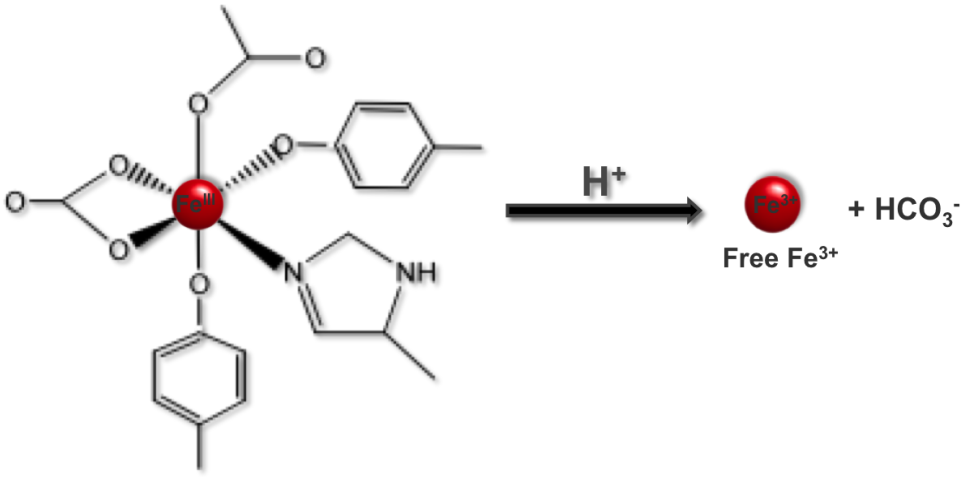

Fig. 8: *Liberación controlada por descenso en el pH del Fe(III) de la lactoferrina.*

La incorporación del primer átomo de hierro en la lactoferrina tiene lugar en el sitio activo del lóbulo C-, originándose entonces un cambio conformacional en la proteína que activa al lóbulo N-, lo que permite la captación de un segundo Fe(III). [27] Este mecanismo de interacción entre ambos lóbulos no está completamente establecido y es actualmente objeto de debate, pero es ampliamente aceptado que la unión del primer átomo del metal da lugar a una serie de desprotonaciones que originan cambios en la conformación de la proteína que afectan al sitio de unión en el lóbulo N-, facilitando entonces la captura del segundo Fe(III).[28] En este contexto, cuando dos átomos del metal son incorporados a la lactoferrina, la conformación del lóbulo C- no cambia significativamente, mientras que el lóbulo N- se cierra como una bisagra para fijar el metal. Esto da como resultado diferentes estructuras terciarias: la forma sin hierro, apolactoferrina (Lf), caracterizada por una conformación abierta del lóbulo N- y una conformación cerrada del lóbulo C-, mientras que ambos lóbulos se encuentran cerrados en la forma saturada en hierro, la hololactoferrina ($LfFe_2$), como se ha demostrado por difracción de rayos X (PDB 1CB6 y 1N76 para Lf y $LfFe_2$, respectivamente).[19,29] Este cambio conformacional explica la afinidad de la lactoferrina por hierro ya que, una vez secuestrados, los átomos de hierro son inaccesibles a otras moléculas por competición directa (Fig. 9).

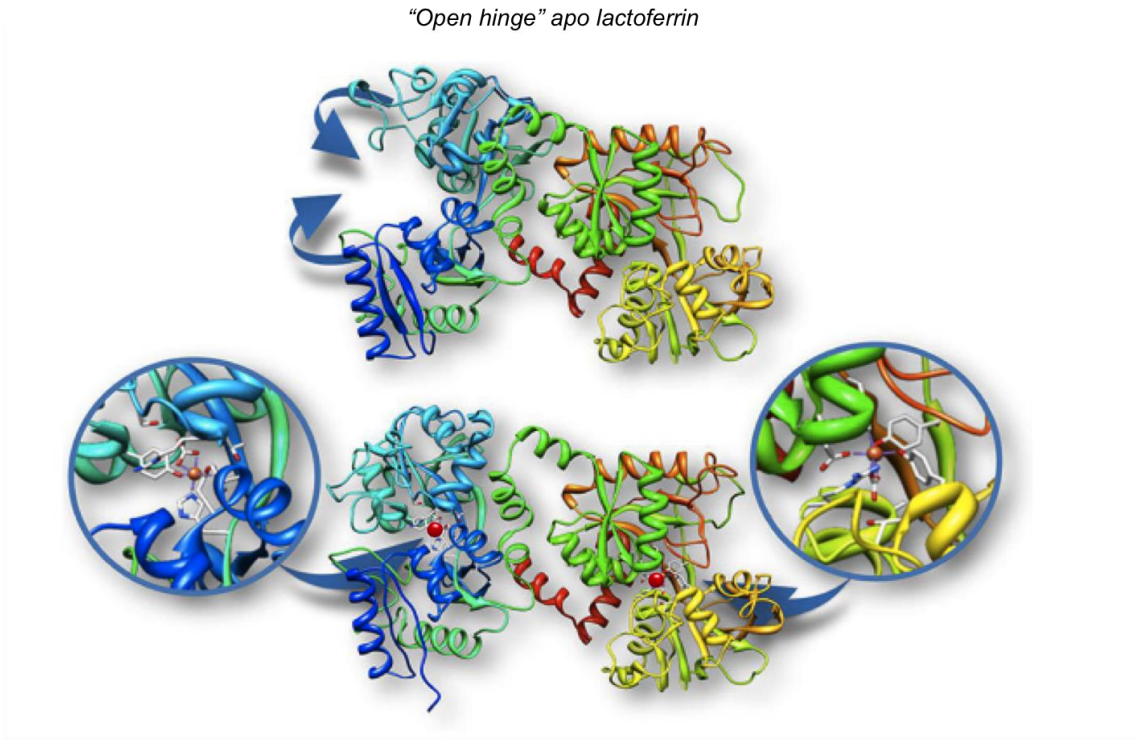

***Fig. 9**: Cambios estructurales en lactoferrina en función de su nivel de hierro.*

Existen múltiples evidencias que demuestran las diversas funciones inmunológicas que presenta la lactoferrina: i) su concentración se incrementa marcadamente en todos los fluidos biológicos durante la mayoría de las reacciones inflamatorias e infecciones virales, muy especialmente en el nido de la inflamación,[30] ii) posee actividades inmunorreguladoras actuando como señal de infección para macrófagos y neutrófilos.[31] Sin embargo, la mayor parte de la actividad inmunológica de la lactoferrina viene determinada por su afinidad por hierro. La evidencia más clara de ello reside en el hecho de que su nivel de saturación de hierro determina su funcionalidad frente al crecimiento de bacterias infecciosas. Las tres formas conocidas de lactoferrina, denominadas: i) apolactoferrina (Lf), ii) la forma mono férrica (LfFe) y iii) la hololactoferrina ($LfFe_2$), difieren en su efecto sobre el crecimiento de microorganismos patógenos. Así, mientras la Lf inhibe el crecimiento de un gran número de bacterias infecciosas, $LfFe_2$ muestra una actividad significativamente menor o nula contra esas mismas bacterias.[32,33,34]

En secreciones mucosas, primera línea de defensa contra microorganismos, la limitación de hierro es imprescindible para inhibir el crecimiento bacteriano. La lactoferrina se encuentra presente en estas mucosas enteramente en su forma libre de hierro (Lf), precisamente para secuestrar todo el hierro posible y privar así de su disponibilidad para microorganismos infecciosos.[35] Su presencia mantiene el nivel de hierro disponible por debajo del requerido para el desarrollo de un microorganismo patógeno[36] e inhibe además la formación del biofilm bacteriano.[37] Esta actividad inmunológica debida a la privación de hierro es meramente bacteriostática en tanto a que el crecimiento bacteriano solamente es retrasado por la privación de hierro, y puede ser completamente restaurado de nuevo tras una suplementación del metal.

A todas estas múltiples funciones de protección de la lactoferrina, hay que añadir otro efecto beneficioso que confiere sobre el organismo en el marco de su cooperación con microorganismos beneficiosos para la salud. La lactoferrina se encuentra presente exclusivamente en mamíferos, lo que sugiere que la aparición de esta proteína a lo largo de la evolución pudo estar relacionada con la nutrición e inmunoprotección infantil. De hecho, en leche materna la concentración de lactoferrina puede llegar a alcanzar los 7 mg/mL[19,20] donde coexiste, en un ambiente óptimo para su proliferación, con numerosas especies de bacterias beneficiosas para el organismo como *Lactobacillus* y *Bifidobacterium*, comúnmente denominadas bacterias probióticas, por el papel clave que ejercen en la nutrición e inmunoprotección infantil así como en adultos.[38,39,40]

La interacción de la lactoferrina con estas especies de bacterias beneficiosas ha sido amplio objeto de estudio desde el punto de vista de la incorporación del hierro por estas bacterias y el papel que la lactoferrina podría desempeñar en la proliferación y viabilidad de éstas. Numerosos estudios han demostrado que la lactoferrina es capaz de promover el crecimiento de bacterias beneficiosas actuando como dadora de hierro,[41,42] y algunos autores han reportado que en medios privados del metal, la presencia de $LfFe_2$ promueve el crecimiento de diferentes cepas de bifidobacterias beneficiosas presentes en leche materna, como *B. breve, B.infantis, B.bifidum, B.longum, B. thermophilum* y *B. adolescentis.*[43,44,45]

No obstante, el mecanismo de transferencia de hierro lactoferrínico a estas bacterias no está del todo establecido y aún requiere mucha investigación para

dilucidar el rol que realmente juega la lactoferrina en la proliferación de estas bacterias beneficiosas para la salud. En este contexto, es oportuno señalar que la lactoferrina ha sido recientemente aprobada por la FDA (Food and Drug Agency) como suplemento natural en productos de alimentación y cosmética para conferirles actividad antimicrobiana.[46] Por todo ello, la investigación sobre la interacción entre lactoferrina y diferentes cepas probióticas presenta un enorme interés para la industria alimentaria de cara a elaborar formulaciones que optimicen la doble función de la lactoferrina: capacidad antimicrobiana y estimulador de proliferación de probióticos.

1.3. Ferritina: más allá de un almacén de hierro

Los organismos han desarrollado un sistema para almacenar hierro constituido por la familia de proteínas de la ferritina. La ferritina es la principal proteína de almacén del hierro en la mayor parte de los organismos vivos en el reino animal, vegetal y microbiano. Su localización es básicamente intracelular y su estructura, altamente conservada, está constituida de una cápside proteica de 450 kDa, la apoferritina, capaz de albergar en su cavidad una enorme cantidad de Fe(III) en forma de nanopartícula de ferrihidrita soluble no tóxica, alcanzando concentraciones alrededor de 10^{16} veces la concentración de Fe(III) en plasma. Una vez almacenado, este hierro ferritínico sigue estando disponible para ser movilizado cuando la célula lo necesite.

La estructura de multitud de ferritinas ha sido determinada mediante difracción de rayos-X en un amplio rango de organismos y tejidos biológicos, siendo evidente que se ha conservado una estructura común a través de la evolución. La ferritina más ampliamente estudiada es la de bazo de caballo, tradicionalmente considerada como el modelo de ferritina en mamíferos. Ésta consiste en una envoltura proteica hueca, la apoferritina, con un peso molecular aproximado de 450 kDa compuesta por 24 subunidades ensambladas en una simetría cúbica que rodea una cavidad de 8 nm de diámetro, capaz de acomodar miles de átomos de hierro como un mineral de Fe(III) tradicionalmente descrito como ferrihidrita [$Fe^{III}_{10}O_{14}(OH)_2$] (Fig. 10).[47]

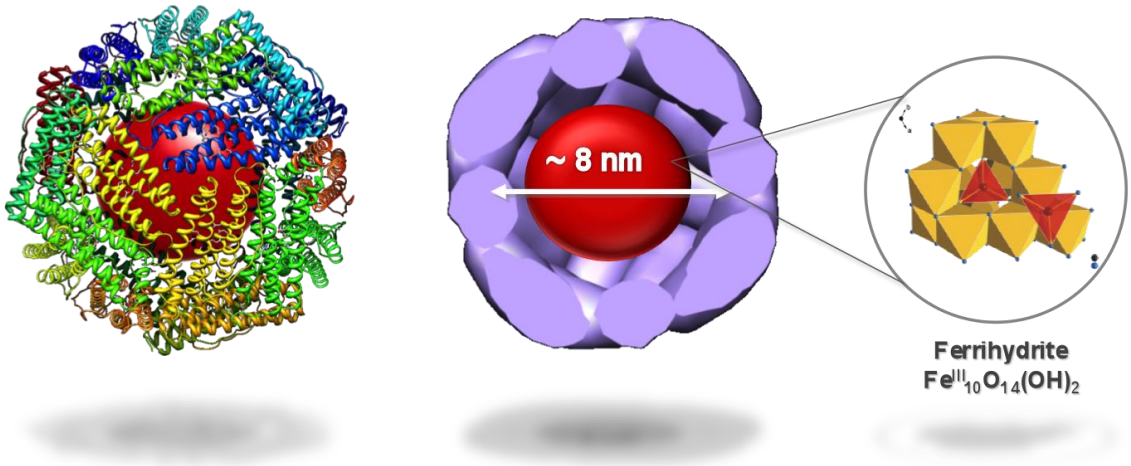

***Fig. 10**: Estructura de la ferritina.*

La envoltura proteica de la ferritina genera dos tipos diferentes de canales, 6 de naturaleza hidrofóbica y 8 de naturaleza hidrofílica, que atraviesan la estructura de la proteína hasta el interior de la cavidad. Los ocho canales hidrófilos poseen aproximadamente 4-5 Å de diámetro con simetría C_3, y son los responsables de la entrada de Fe(II) al interior de la cavidad así como de permitir la entrada y salida de agua, cationes y moléculas hidrofílicas de un tamaño adecuado.

Las 24 cadenas polipeptídicas de la envoltura de proteica pueden ser clasificadas en dos tipos: Las subunidades H (o cadenas pesadas) de 178 aminoácidos y 21 kDa, y las subunidades L (ligeras) con 171 aminoácidos y 19 kDa de peso. Ambos tipos de subunidades están estrechamente relacionadas en términos de estructura primaria (~53% de identidad en la secuencia proteica) y terciaria.[48,49] Sin embargo, estas subunidades tienen diferente funcionalidad. Las subunidades H juegan un papel crucial en la rápida detoxificación del hierro debido a que contienen el centro catalítico ferroxidasa para la rápida oxidación del Fe(II), en cambio, las subunidades L están asociadas con la nucleación, mineralización y almacén del hierro en la cavidad de la ferritina.[50] De acuerdo con esto, el ratio H/L en la cápside proteica de la ferritina varía ampliamente en diferentes tejidos. Así, ferritinas ricas en subunidades L predominan en órganos de almacén de hierro como el hígado y el bazo, mientras que en los órganos en los que se requiere una rápida detoxificación de hierro como el corazón y el cerebro, así como en la leche materna, la ferritina es rica en subunidades H.[51,52] En algunos organismos como bacterias, plantas e invertebrados en general, la cápside proteica se encuentra

exclusivamente compuesta por subunidades H. En vertebrados sin embargo, la ferritina se presenta compuesta principalmente por una combinación de subunidades H y L, como es el caso de la ferritina de bazo de caballo, modelo de ferritina en vertebrados, que contiene aproximadamente un 90% L- y un 10% de subunidades H (Fig. 11).

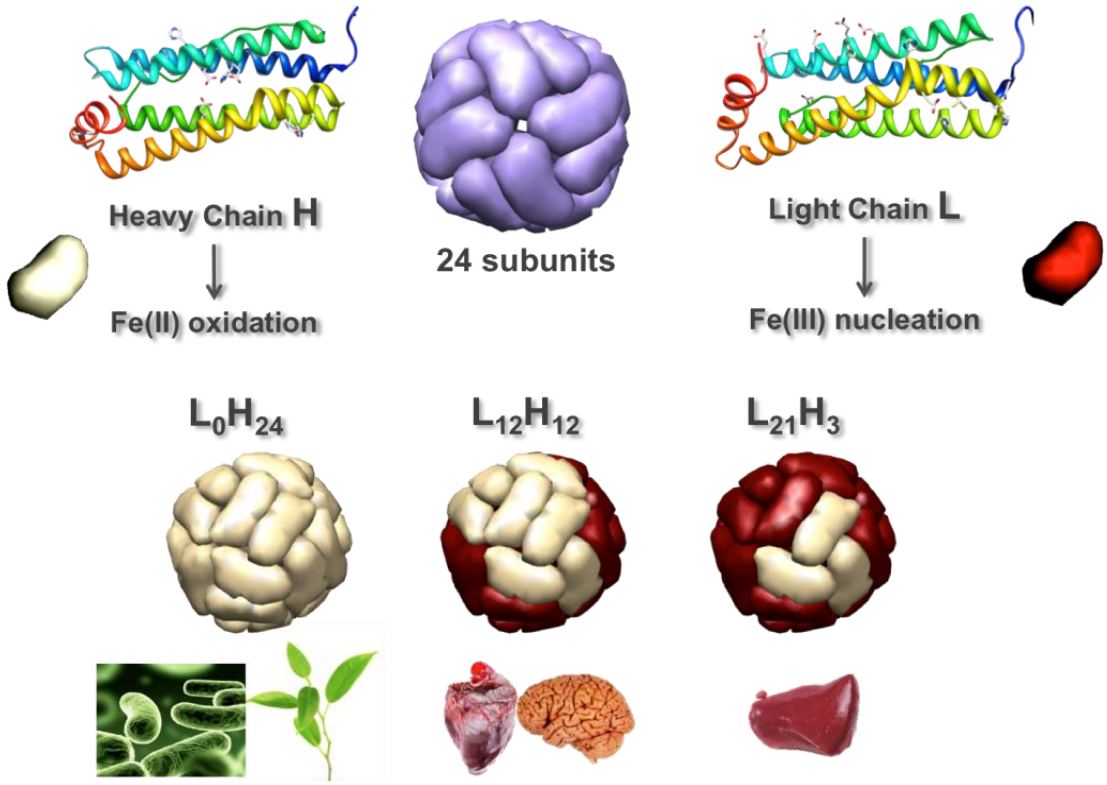

Fig. 11: *Distribución en tejidos de la ferritina según su ratio H/L*

Aunque el núcleo metálico de la ferritina es básicamente ferrihidrita, donde el hierro presenta un estado de oxidación Fe(III), este núcleo se forma a partir de Fe(II) y no de Fe(III). Esto conlleva necesariamente a que, en algún momento de su travesía al interior de la proteína, el Fe(II) sea oxidado a Fe(III), por lo que debe existir un centro ferroxidasa responsable de esta oxidación. No obstante, el mecanismo de la reacción de oxidación de Fe(II) a Fe(III) en el centro ferroxidasa de la ferritina es actualmente objeto de controversia.[50,53,54,55] Durante los últimos años, había sido ampliamente aceptado que el Fe(II) se desplaza a través de los

canales hidrofílicos hasta fijarse en el centro ferroxidasa libre de una subunidad H, donde era catalíticamente oxidado por una reacción con oxígeno molecular hasta formar un complejo peroxo-di-férrico (DFC). Los DFCs formados migrarían espontáneamente del centro ferroxidasa, dejándolo completamente vacante y continuarían su viaje hacia el interior de la cavidad, interaccionando entre ellos para formar entidades multiméricas de Fe(III), que finalmente se fijarían en los puntos de nucleación de la cavidad proteica donde iniciarían el crecimiento del núcleo de hierro.[56,57]

En contraste con esta propuesta, los recientes resultados obtenidos contradicen esta naturaleza "vacía" del centro ferroxidasa, ampliamente aceptada. El modelo propuesto por Hagen et al. propone un mecanismo unificado, tanto en *archaea* como en eucariotas, en el cual dos Fe(II) son oxidados secuencialmente en el centro ferroxidasa.[55] A diferencia con el modelo anterior propuesto, este centro cargado con Fe(III) es considerado un grupo prostético indefinidamente estable hasta la llegada de un nuevo átomo de Fe(II), que dispararía un desplazamiento secuencial de Fe(III) y, en presencia de oxigeno molecular, a la consecuente oxidación catalítica del Fe(II) entrante a Fe(III) (Fig. 12). El Fe(III) desplazado migraría entonces a la cavidad de la ferritina donde formaría el núcleo metálico a través de un mecanismo aún por definir.

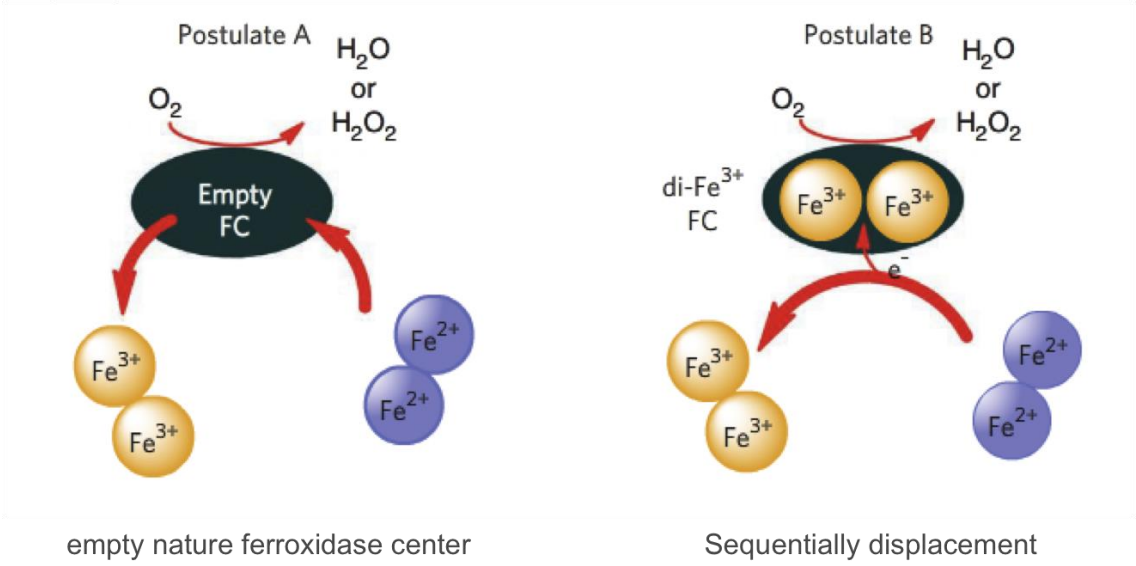

Fig. 12: *Naturaleza del centro ferroxidasa según los dos modelos planteados.*

En este contexto, la existencia permanente de una unidad Fe^{III}-OH-Fe^{III} en el centro ferroxidasa tiene una serie de consecuencias biológicas que sorprendentemente no han sido consideradas.

No pretendemos en esta Tesis aportar datos que avalen una u otra hipótesis. Pretendemos explorar hechos experimentales, ya reportados en trabajos de la década de los 80 que no habían sido explotados en términos de implicaciones biológicas, que van más allá de hipótesis mecanísticas. Como había sido previamente observado, no todo el Fe(III) formado en el centro ferroxidasa en ferritinas constituidas básicamente de cadenas H, termina formando parte del núcleo metálico.[52] Este hecho experimental, que hemos podido medir cuantitativamente en la presente tesis, plantea una serie de cuestiones que no habían sido consideradas anteriormente y que están directamente relacionadas con dos hechos: i) en primer lugar, considerar que las ferritinas H no tienen como única función almacenar hierro sino más bien una función detoxificante de Fe(II), puesto que parte del Fe(III) que generan no es realmente almacenado y ii) las implicaciones biológicas que este Fe(III) no almacenado puede tener en el marco de su posible interacción con otras biomoléculas y metaloproteínas en el escenario biológico donde es generado.

Los desórdenes en las funciones de la ferritina han sido relacionados con enfermedades típicamente relacionadas con el hierro, como la hemocromatosis o la anemia, pero la ferritina está también siendo cada vez más reconocida como una molécula crucial en algunas patologías neurológicas, como la enfermedad de Parkinson o Alzheimer.[6] Por tanto, conocer en detalle los mecanismos de captación y almacenamiento de hierro en función de la composición H/L de la cápside proteica de la ferritina se convierte en un desafío para la comunidad científica, con vistas a entender la etiología de estos síndromes y finalmente alcanzar el diseño de nuevos agentes terapéuticos para estas patologías basados en el metabolismo del hierro.

En este sentido un mal funcionamiento de la ferritina, o lo que es más novedoso, una inadecuada elección por parte de la célula en la composición de la cápside proteica en cuanto a composición de subunidades H/L, puede dar lugar a la existencia de Fe(II) o Fe(III) libre disponibles para generar, respectivamente,

radicales hidroxilo u oxidación de otras biomoléculas que den lugar en definitiva a la aparición de los primeros estadíos de una patología. Estos desarreglos en el metabolismo del hierro son especialmente importantes en células del sistema nervioso.[58]

En particular, en esta Tesis nos hemos centrado en cómo el proceso de almacenamiento de hierro por parte de la ferritina está conjugado con la naturaleza química de una serie de metaloproteínas involucradas en el metabolismo de cobre y cinc, como son las metalotioneínas (MTs). Este tipo de estudio adquiere además especial relevancia desde el punto de vista de la reactividad Fenton que presentan los iones $Cu^{I/II}$ y del papel nocivo que este metal libre, al igual que el hierro, juega en desórdenes neurodegenerativos como la enfermedad de Alzheimer, Parkinson, esclerosis y diferentes encefalopatías.[59,60]

Las metalotioneínas (Fig. 13) son proteínas de bajo peso molecular (6 – 10 kDa) ricas en residuos de cisteína (33%), cuya función biológica no ha sido del todo establecida en la actualidad, aunque es bien conocido que juegan un papel clave en la homeostasis y detoxificación de diferentes metales como cobre y cinc.[61,62]

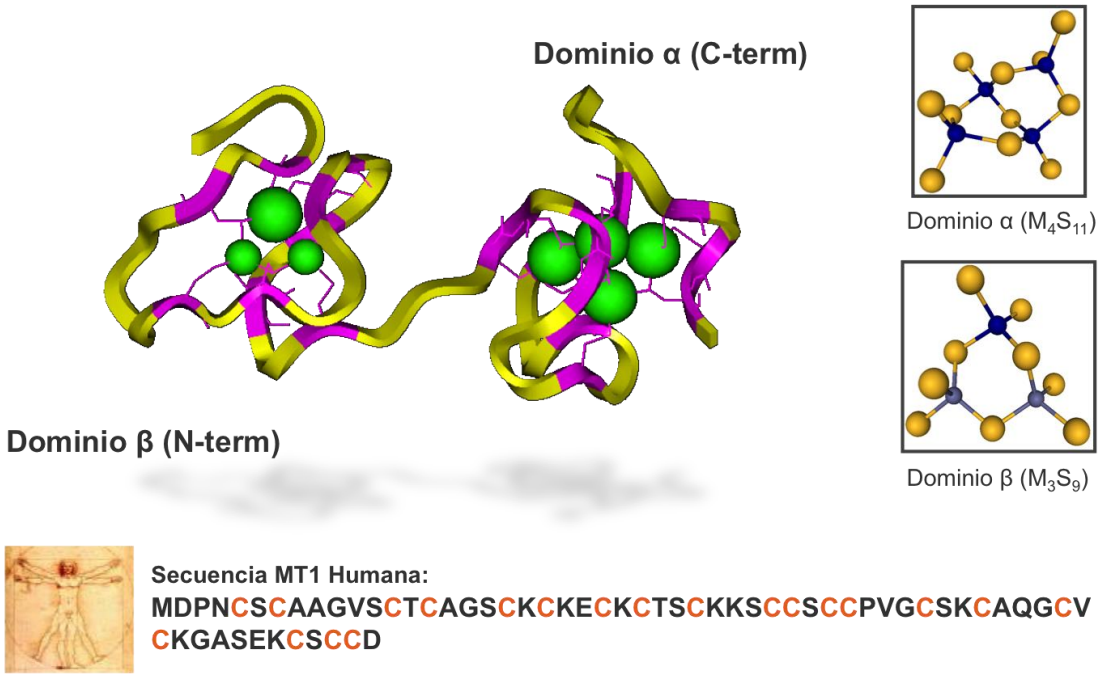

***Fig. 13**: Estructura general de las metalotioneínas de mamífero.*

En mamíferos existen diferentes isoformas de metalotioneína (MT1, MT2, MT3 y MT4) con diferente patrón de expresión en función del tejido en el que se encuentren. Así, mientras MT1 se encuentra distribuida ubicuamente en el organismo, las isoformas MT2 y MT3 son predominantemente sintetizadas en células del sistema nervioso como astrocitos y microglía (MT2) y en neuronas (MT3).[63,64] Esta diferenciación tisular de las metalotioneínas, añadida al hecho de la existencia de isoformas específicas para células concretas del sistema nervioso, permite el estudio "a la carta" de sus interacciones en el proceso de almacenamiento del hierro por las distintas ferritinas presentes en cada una de estas células nerviosas y las posibles consecuencias en el desarrollo de desórdenes neurológicos que dichas interacciones pueden originar.

1.4. Pinceladas sobre el metabolismo de hierro en bacterias.

Como se ha mencionado a lo largo de esta introducción, el hierro es a la vez un nutriente esencial para el crecimiento de microorganismos así como un peligroso metal debido a su capacidad para generar ROS tóxicas.[65,66,67] Debido a esto, las bacterias deben controlar estrictamente la captación y almacén del hierro en su metabolismo. No es de extrañar por tanto que la respuesta a este estrés oxidativo y los mecanismos de control que rigen la homeostasis de hierro en bacterias actúen de manera coordinada (Fig. 14).

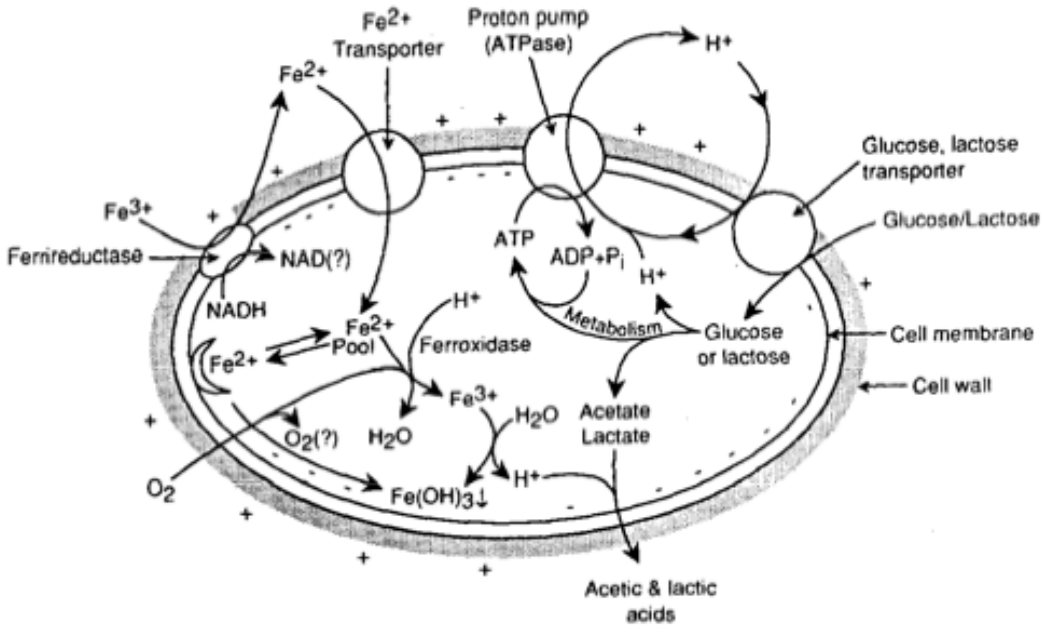

Fig. 14: *Metabolismo del hierro en Bifidobacterias.*

En condiciones aeróbicas y de pH fisiológico, el hierro es un elemento escasamente disponible para los microorganismos debido a su baja solubilidad y a la consecuente precipitación de oxi-hidróxidos de Fe(III).[68] Por esta razón, los microorganismos se encuentran generalmente ante una escasez de hierro biodisponible. Para los patógenos, el problema de la restricción de hierro es más extremo aún, ya que el "host" limita la disponibilidad de hierro, secuestrándolo a nivel extracelular con proteínas de la familia de las transferrinas y a nivel intracelular almacenado o no disponible en proteínas como la ferritina,

hemosiderina y frataxina.[68,69] Es oportuno señalar que a nivel extracelular, el medio habitual de proliferación de bacterias, el "host" secuestra hierro a través de la lactoferrina, que puede llegar a reducir los niveles de hierro libre hasta concentraciones en torno a 10^{-18} M, niveles insuficientes para permitir el crecimiento bacteriano.[70,71]

El mecanismo de captación de hierro en microorganismos es amplio y depende de la especie, pudiendo tener lugar a través de receptores específicos para la entrada de Fe(II), receptores de grupos hemo-Fe o bien la vía mas habitual, consistente en la producción de moléculas extracelulares de alta afinidad por Fe(III), denominados sideróforos.[72,73]

Los sideróforos son moléculas de bajo peso molecular (<1000 Da) que se caracterizan por su alta especificidad por Fe(III) ($K > 10^{30}$).[74] Pueden llegar a encontrarse a en concentraciones extremadamente elevadas (superiores a 200 $mg \cdot L^{-1}$) en el caso de la aerobactina en *E. coli*, como respuesta a la restricción de hierro.[75] En la actualidad han sido caracterizados en torno a 500 sideróforos, los cuales pueden ser clasificados según los grupos funcionales que usan como ligandos de Fe(III). Entre los más estudiados se encuentran la enterobactina (triscatecolatos) y la deferoxamina (trishidroxamatos).[76]

El mecanismo general de captación de hierro mediada por sideróforos en bacterias Gram-positivas y negativas se muestra en la (Fig. 15). Estos sideróforos son demasiado grandes para atravesar la membrana y pared bacterianas por difusión pasiva, por lo que requieren de la presencia de receptores de membrana específicos para su internalización acoplados a sistemas transportadores ABC-permeasa. Una vez en el citoplasma, el ferrisideróforo es degradado por una esterasa o reciclado a través de procesos reductivos que liberan Fe(II) dejando la molécula intacta para reanudar un nuevo ciclo de captación de hierro.[68]

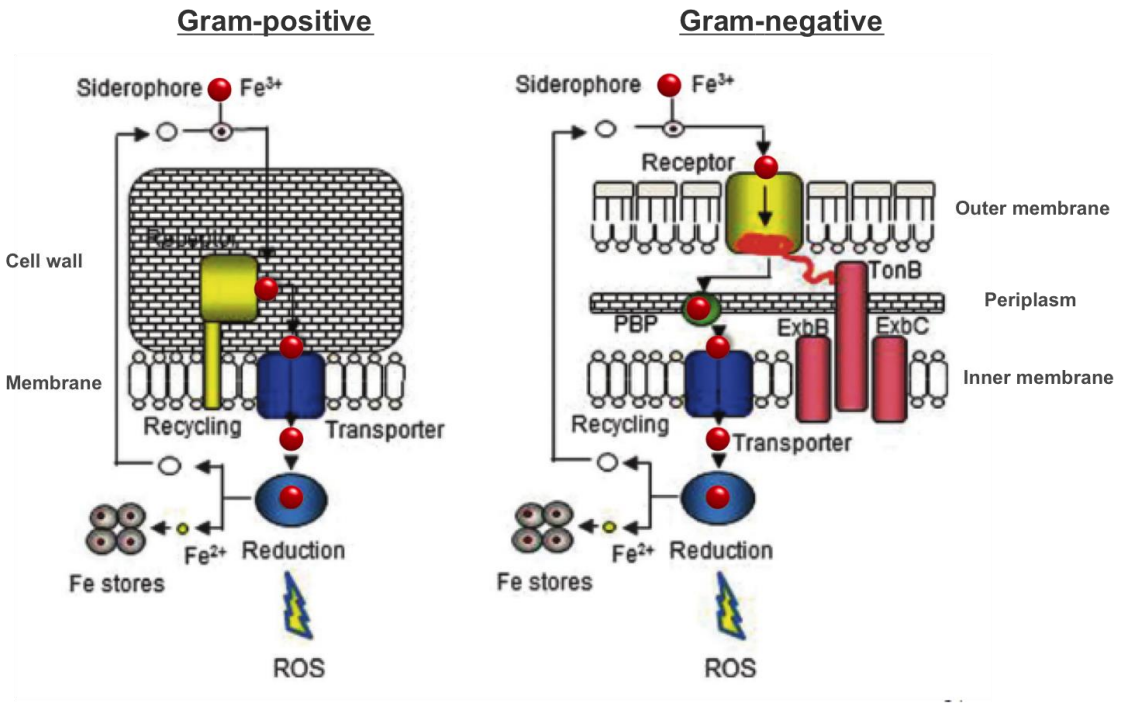

Fig. 15: *Captación de Fe(III) mediada por sideróforo en bacterias.*

Puesto que los problemas que las bacterias deben afrontar para adquirir suficiente hierro de su entorno son especialmente agudos en microorganismos infecciosos debido a que el "host" limita específicamente la disponibilidad de hierro como parte de su defensa innata ante patógenos invasivos, una manera común en los patógenos para adquirir hierro directamente del organismo infectado es precisamente a través de sistemas de transporte mediado por receptores específicos para las proteínas de unión a hierro del "host": los microorganismos tratan de mimetizar las vías usuales de captación de hierro por parte de las células del "host". Estos receptores de membrana liberan el hierro de la lactoferrina y la transferrina, que posteriormente es internalizado a través de un sistema permeasa ABC al interior celular. Este proceso tiene lugar en la superficie exterior de la célula y las formas apo de la proteínas transportadoras de hierro son liberadas extracelularmente en lugar de ser internalizadas y acumuladas (Fig. 16).

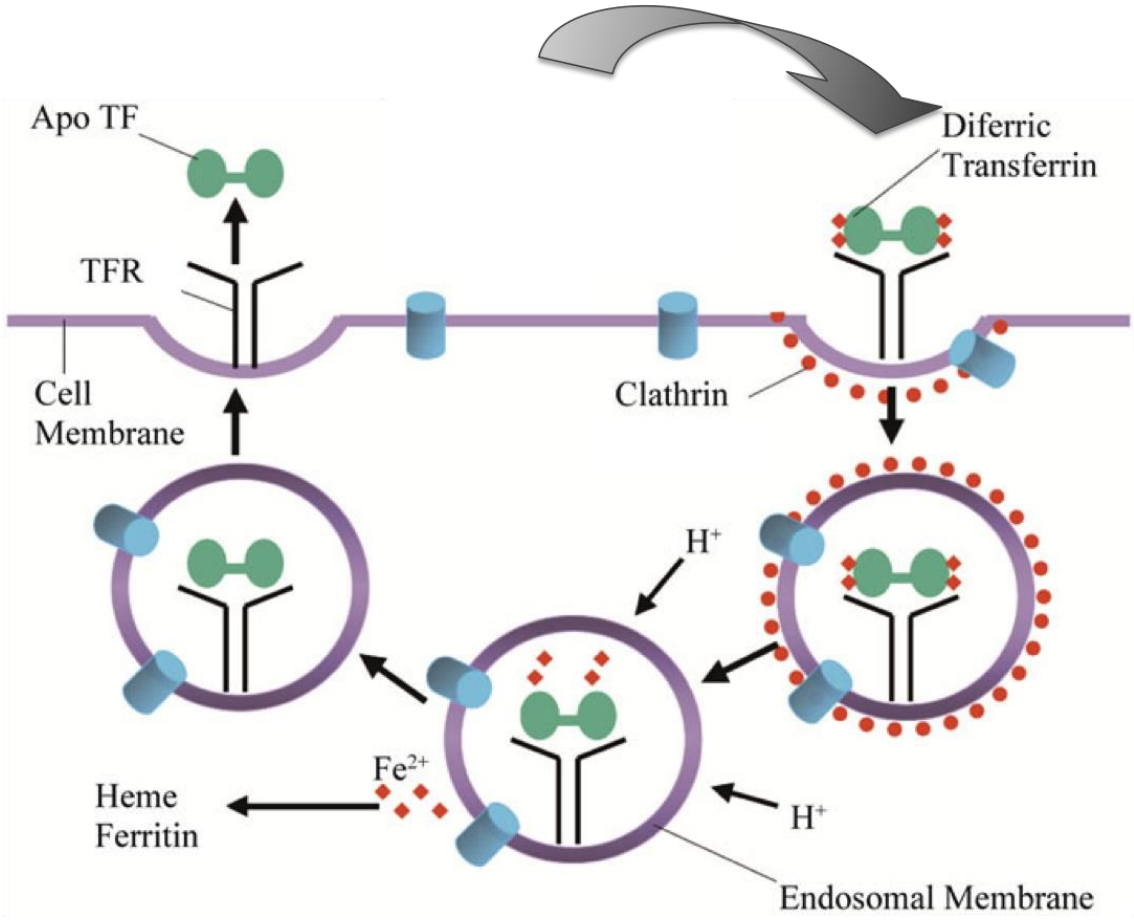

Fig. 16: *Esquema de la captación de hierro mediada por receptor de transferrina en bacterias.*

No obstante, los mecanismos de actuación del "host" frente a las bacterias dependen de la toxicidad de éstas ya que, para el caso de bacterias beneficiosas probióticas como *Bifidobacterium* y L*actobacillus*, promueven su proliferación.

Según la FAO/WHO, los probióticos se definen como "los microorganismos que, cuando son administrados en cantidades adecuadas, confieren efectos beneficiosos para la salud del organismo huésped". Entre otros, estos beneficios incluyen una mayor respuesta inmune, un mejor balance de la microbiota en colon, reducción de enzimas implicadas en el desarrollo del cáncer, control de retrovirus y reducción de los niveles de colesterol en sangre, entre otras.[77]

En esa Tesis nos hemos centrado en cómo este tipo de bacterias probióticas proliferan a expensas del "host" de una forma "voluntaria". En particular, hemos querido profundizar en cómo la lactoferrina, encargada de privar de hierro a microorganismos patógenos es, sin embargo, capaz de transportar hierro a bacterias probióticas haciendo que proliferen en pro del desarrollo adecuado del organismo hospedador.

En este sentido, la presencia conjunta de lactoferrina y apoferritina H en la leche materna es un ejemplo de cómo los mamíferos son capaces de diseñar un "tándem" de proteínas que sirve, tanto para impedir la proliferación de microorganismos patógenos como para, al mismo tiempo, hacer viable la presencia de bacterias probióticas beneficiosas para la salud. Una prueba más de la sutil, elegante y eficiente maquinaria química en pro de un metabolismo de hierro adecuado que los organismos desarrollan para su supervivencia.

1.5. Objetivos

Como se ha puesto de manifiesto en la Introducción, el metabolismo de hierro es esencial para la vida y cualquier desarreglo conlleva la aparición de patologías diversas. Pretendemos en esta Tesis, por un lado, descubrir nuevos desajustes en toda la maquinaria química que define el metabolismo de hierro que den lugar al desarrollo de patologías y en segundo lugar, que el conocimiento adquirido se traduzca en la preparación de materiales que puedan ser útiles conceptualmente para intervenir en dichos desajustes y poder actuar a nivel terapéutico.

El objetivo general de esta Tesis es en cierta forma indagar en aspectos del metabolismo de hierro que generen conocimiento y/o inspiren la creación de un nuevo material que pueda ser aplicado en biomedicina, tanto en terapias variadas relacionadas con un metabolismo de hierro anómalo, como en diagnóstico de enfermedades concretas.

De forma más concreta, los aspectos que pretendemos abordar son los siguientes:

1. Tras un exhaustivo análisis bibliográfico pretendemos demostrar que la proteína ferritina, tradicionalmente considerada como almacén de hierro, no siempre lleva a cabo esta función, o al menos no "únicamente". En particular pretendemos demostrar que la actividad de algunas ferritinas (las denominadas H) están más relacionadas con llevar a cabo una función de detoxificación de Fe(II) que propiamente el almacenamiento del metal.
   Demostrar que estas ferritinas H tienen muy poca capacidad de almacenamiento pero una alta actividad ferroxidasa (oxidación de Fe(II) a Fe(III)) explicaría aspectos nuevos que han pasado desapercibido hasta la actualidad: i) su presencia en algunos fluidos biológicos acompañada del agente quelatante biológico de Fe(III) por excelencia, la lactoferrina y ii) la elección que hace cada célula del tipo de ferritina que en realidad requiere para llevar a cabo su función, como ocurre en algunas células tan particulares como las neuronas.
   Entender el mecanismo de acción de las ferritinas H y su presencia en leche materna, inspira inmediatamente la preparación de materiales que puedan mimetizar funcionalmente este fluido biológico, cuya función primordial en el metabolismo de hierro es precisamente la eliminación del Fe(II) tóxico. Estos materiales podrían ser utilizados como detoxificantes de hierro y por tanto como

antibióticos, puesto que podrían eliminar cualquier forma de hierro libre que sirviera de alimento a un microorganismo patógeno que pudiera dar lugar a una infección.

2. Establecer marcos químicos amplios en los que podamos estudiar la interconexión entre diferentes metaloproteínas relacionadas con la homeostasis de hierro y otros metales, como cobre y zinc. El metabolismo de hierro va ligado al de otros iones metálicos. La homeostasis de iones metálicos es un proceso global que requiere ser estudiado como tal. Para poder abordar la interconexión entre iones metálicos a nivel biológico se requiere un enfoque químico nuevo y complejo dónde poder abordar como la actividad de una metaloproteína se ve afectada por otra. Pretendemos dar un paso en este sentido y diseñar marcos químicos que biomimeticen de una forma más real los procesos de homeóstasis de metales que ocurren en la célula. En particular pretendemos estudiar como interfiere en el proceso de almacenamiento de hierro una familia de metaloproteínas involucradas en el metabolismo de cobre y cinc, como son la metalotioneínas. De los resultados obtenidos podremos deducir el porqué de la elección de cada célula, en función del tejido en el que se encuentre, del par ferritina-metalotioneína adecuado para llevar a cabo sus funciones de forma óptima y lo que es más importante, detectar pares ferritinas-metalotioneínas que podrían generar el inicio de patologías neuronales.

3. El estudio del metabolismo de hierro en bacterias tiene muchos enfoques. Aprender aspectos de dicho metabolismo nos puede permitir: i) diseñar una nueva vía para la aniquilación bacteriana, en relación con la búsqueda de nuevos antibióticos, ii) entender el porqué de la proliferación bacteriana de algunas bacterias beneficiosas para la salud, como son las bacterias probióticas y iii) la preparación de nuevos materiales basados en la actividad bacteriana para producir nanopartículas metálicas, que eventualmente puedan representar una nueva vía de nanomateriales con aplicaciones biomédicas.

1.6. Bibliografía

[1] D. J. Pinero, J. R. Connor, H. R. Lieberman, R. B. Kanarek, C. Prasad (Eds.). *Nutritional Neuroscience, CRC Press*, *Taylor & Francis Group, Boca Raton*, **2005**, p. 235.

[2] T. LaVaute, S. Smith, S. Cooperman, K. Iwai, W. Land, E. Meyron-Holtz, S. K. Drake, G. Miller, M. Abu-Asab, M. Tsokos, R. Switzer III, A. Grinberg, P. Love, N. Tresser, T. A. Rouault. *Nat. Genet*., **2001**, 27, 209–214.

[3] H. Puccio, D. Simon, M. Cossee, P. Criqui-Filipe, F. Tiziano, J. Melki, C. Hindelang, R. Matyas, P. Rustin, M. Koenig. *Nat. Genet*., **2001**, 27, 81–186.

[4] N. B. Cole, D. D. Murphy, J. Lebowitz, L. Di Noto, R.L. Levine, R. L. Nussbaum. *J. Biol. Chem.*, **2005**, 280, 9678.

[5] Q. Q. Pankhursta, D. Hautotb, N. Khanc, J. Dobson. *J. Alzheimers Dis*., **2008**, 13, 49.

[6] D. Berg, G. Beceker, P. Riederer, O. Rieb. *Neurotox. Res*., **2002**, 4, 637.

[7] K. Jomova, M. Valko. *Curr. Pharm. Des*., **2011**, 17, 3460-3473.

[8] H. Heli, S. Mirtorabi, K. Karimian. *Expert Opinion on Therapeutic Patents,* **2011,** 21, 819.

[9] J. A. Imlay, S. M. Chin, S. Linn. *Science*, **1988**, 240, 640–642.

[10] S. Jang, J. A. Imlay. *J. Biol. Chem.*, **2007**, 282, 929–937.

[11] S. Laurent, D. Forge, M. Port, A. Roch, C. Robic, L. Vander Elst, R. N. Muller. *Chem. Rev.,* **2008**, 108, 2064–2110.

[12] K. Gkouvatsos, G. Papanikolaou, K. Pantopoulos. *Biochim. et Biophys. Acta*, **2012**, 1820, 188–202.

[13] R. J. Cherry, A. J. Bjornsen, D. C. Zapien. *Langmuir,* **1998,** 14, 1971.

[14] T. Yoshinobu, J. Suzuki, H. Kurooka, W. C. Moon, H. Iwasaki. *Electrochim. Acta,* **2003**, 48, 3131.

[15] K. Iwai, S. K. Drake, N. B. Wehr, A. M. Weissman, T. LaVaute, N. Minato, R. D. Klausner, R. L. Levine, T. A. Rouault. *Proc. Natl. Acad. Sci. U.S.A.*, **1998,** 95, 4924.

[16] J. Zahringer, B. S. Baliga, H. N. Munro. *Proc. Natl. Acad. Sci. U.S..A,* **1976,** 73, 857.

[17] M. W. Hentze, L. C. Kühn. *Proc. Natl. Acad. Sci. U.S.A.,* **1996***,* 93, 8175–82.

[18] M. Sorensen, S. P. L. Sorensen*. Comptes-rendus des Travaux du Laboratoire Carlsberg*, **1939**, 23, 55–99.

[19] B. F. Anderson, H. M. Baker, G. E. Norris, D. W. Rice, E. N. Baker. *J. Mol. Biol*., **1989**, 209, 711–734.

[20] E. N. Baker, P. F. Lindley. *J. Inorg. Biochem.*, **1992**, 47, 147–160.

[21] R. D. Brown, K. A. Rickard, H. Kronenberg. *Pathology*, **1983**, 15, 27–31.

[22] M. H. Metz-Boutigue, J. Jolles, J. Mazurier, F. Schoentgen, D. Legrand D. G. Spik. *Eur. J. Biochem*., **1984**, 145, 659–676.

[23] E. N. Baker, H. M. Baker. *Biochimie,* **2009**, 91, 3–10.

[24] H. Vogel. *J. Biochem. Cell Biol*., **2012**, 90, 233–244.

[25] E. N. Baker, H. M. Baker. *Cell Mol. Life Sci.,* **2005**, 62, 2531–2539.

[26] R. T. A. MacGillivray, S. A. Moore, J. Chen, B. F. Anderson, H. Baker, Y. Luo Y. *Biochemistry,* **1998,** 37**,** 7919–7928.

[27] R. Pakdaman, M. Petitjean, J. M. El Hage Chahine. *Eur. J. Biochem.*, **1998**, 254, 144–153.

[28] A. F. Bou, J. M. El Hage Chahine. *J. Mol. Biol*., **2000**, 303, 255–266.

[29] J. Kumar, W. Weber, S. Münchau, S. Yadav, S. B. Singh, K. Saravanan, M. Paramasivam, S. Sharma, P. Kaur, A. Bhushan, A. Srinivasan, C. Betzel, T. P. Singh. *Indian J. Biochem. Biophys*., **2003**, 40, 14–21.

[30] H. S. Birgens. *Scand. J. Haematol.*, **1985**, 34, 326–331.

[31] D. Latorre, F. Berlutti, P. Valenti, S. Gessani, P. Puddu. *Biochem. Cell Biol.,* **2012**, *90*, 269–278.

[32] N. Orsi. *Biometals*, **2004**, 17, 189–196.

[33] T. F. Byrd, M. A. Horwitz. *J. Clin. Investig*., **1991**, 88, 351–357.

[34] E. Griffiths, L. Duffy, F. Schanbacher, D. Dryja, A. Leavens, R. Neiswander, H. Qiao, D. DiRienzo, P. Ogra. *Dig. Dis. Sci*., **2003**, 48, 1324–1332.

[35] Y. Makino, S. Nishimura. *J. Chromatogr.*, **1992**, 579, 346–349.

[36] R. A. Finkelstein, C. V. Sciortino, M. A. McIntosh. *Rev. Infect. Dis.*, **1983**, 5, 759–777.

[37] P. K. Singh, M. R. Parsek, E. P. Greenberg, M. J. Welsh MJ. *Nature*, **2002**, 417, 552–555.

[38] N. G. Hord. *Annu. Rev. Nutr.,* **2008**, *28*, 215–231.

[39] H. Gill, J. Prasad. *Advances in experimental medicine and biology*, **2008**, *606*, 423-454.

[40] S. Fijan. *Int. J. Environ. Res. Public Health,* **2014**, *11*, 4745–4767.

[41] C. Liepke, K. Adermann, M. Raida, H. J. Mager, W. G. Forssmann, H. D. Zucht. *Eur. J. Biochem*., **2002**, 269, 712–718.

[42] M. Sherman, S. Bennett, F. Y. Hwang, C. Yu. *Biometals*, **2004**, 17, 285–289.

[43] R. Miller-Catchpole, E. Kot, G. Haloftis, S. Furmanov, A. Bezkorovainy. *Nutr. Res..*, **1997**, 17, 205–213.

[44] M. M. Rahman, W. S. Kim, H. Kumura, K. Shimazaki K. *Int. J. Food Sci. Technol.,* **2010**, 45, 453–458.

[45] H. Saito, H. Miyakawa, N. Ishibashi, T. Yoshitaka, H. Hayasawa, S. Shimamura. *Biosci. Microflora*, **1996**, 15, 1–7.

[46] United States Food and Drug Administration. 2009-11-05. Retrieved 2010-01-23.

[47] N. D. Chasteen, P. M. Harrison. *J. Struct. Biol.*, **1999**, 126, 182.

[48] S. Levi, S. J. Yewdall, P. M. Harrison, P. Santambrogio, A. Cozzi, E. Rovida, A. Albertini, P. Arosio. *Biochem. J.,* **1992***,* 288, 591.

[49] P. D. Hempstead, S. J. Yewdall, A. R. Fernie, D. M. Lawson, P. J. Artymiuk, D. W. Rice, G. C. Ford, P. M. Harrison. *J. Mol. Biol*., **1997**, 268, 424.

[50] E. C. Theil. *Curr. Opin. Struct. Biol*., **2011**, 15, 304.

[51] M. Wagstaff, M. Worwood, A. Jacobs. *Biochem. J.,* **1978**, 173, 969.

[52] P. Arosio, P. A. Ponzone, R. Ferrero, L. Renoldi, S. Levi. *Clin. Chim. acta; Int. J. Clin. Chem.,* **1986**, *161*, 201–208.

[53] X. Liu, E. C. Theil. *Proc. Natl. Acad. Sci. U.S.A.*, **2004**, *101*, 8557–8562.

[54] P. Arosio, R. Ingrassia, P. Cavadini. *Biochim. Biophys. Acta,* **2009,** *1790*, 589–599.

[55] H. K. Ebrahimi, E. Bill, P. L. Hagedoorn, W. R. Hagen. *Nat. Chem. Biol.,* **2012,** *8*, 941–948.

[56] T. Tosha, H-L. Ng, O. Bhattasali, T. Alber, E. C. Theil. *J.Am.Chem.Soc.*, **2010**, 132, 14562.

[57] F. Bou-Abdallah, G. C. Papaefthymiou, D. M. Scheswohl, S. D. Stanga, P. Arosio, N. D. Chasteen. *Biochem. J.*, **2002**, 364, 57.

[58] R. K. Watt, R. J. Hilton, D. M. Graff. *Biochim. Biophys. Acta*, **2010**, 1800, 745.

[59] H. Kozlowski, M. Luczkowski, M. Remelli, D. Valensin. *Coord. Chem. Rev.*, **2012**, 256, 2129.

[60] J. H. Viles. *Coord. Chem. Rev.,* **2012**, 256, 2271.

[61] M. Capdevila, R. Bofill, Ò. Palacios, S. Atrian. *Coord. Chem. Rev.,* **2012**,

256, 46–52.

[62] Ò. Palacios, S. Atrian, M. Capdevila. *J. Biol. Inorg. Chem.,* **2011**, *16*,

991–1009.

[63] J. Hidalgo, R. Chung, M. Penkowa, M. Vasak., *RSC Publishing, Cambridge*, **2009**, 5, 279.

[64] M. Vasak, G. Meloni. *RSC Publishing, Cambridge*, **2009**, 5, 319.

[65] J. A. Imlay, S. M. Chin, S. Linn. *Science*, **1988**, 240, 640–642.

[66] S. Jang, J. A. Imlay. *J. Biol. Chem.*, **2007**, 282, 929–937.

[67] J. A. Imlay, S. Linn. *Science*, **1988**, 240, 1302–1309.

[68] S. C. Andrews, A. K. Robinson, F. Rodriguez-Quinones. *FEMS Microbiol. Rev.*, **2003**, 27, 215–237.

[69] R. A. Finkelstein, C. V. Sciortino, M. A. McIntosh. *Clin. Infect. Dis.*, **1983**, 5, 759–777.

[70] A. G. Oglesby-Sherrouse, M. L. Vasil. *PLoS One*, **2010**, 5, 9930.

[71] A. Nandal, C. C. Huggins, M. R. Woodhall, J. McHugh, F. Rodriguez-Quinones, M. A. Quail, J. R. Guest, S. C. Andrews. *Mol. Microbiol*., **2010**, 75, 637–657.

[72] A. Bagg, J. B. Neilands. *Microbiol. Rev*., **1987**, 51, 509–518.

[73] V. Braun, H. Killmann. *Trends Biochem. Sci*., **1999**, 24, 104–109.

[74] C. Jakopitsch, G. Regelsberger, P. G. Furtmuller, F. Ruker, G. A. Peschek, C. Obinger. *J. Inorg. Biochem*., **2002**, 91, 78–86.

[75] D. Touati. *Arch. Biochem. Biophys*., **2000**, 373, 1–6.

[76] V. Braun, H. Killmann. *Trends Biochem. Sci*., **1999**, 24, 104–109.

[77] J. M. Saavedra. *Am. J. Clin. Nutr*., **2001**, 73, 1147S–1151S.

CAROLVS·RO·IMP·SEMPER·AVG·HISPAN·REX·FUNDATOR·VNIVERSITATIS·GRANATENSIS

CAPÍTULO 2.

FERRITIN IRON UPTAKE AND RELEASE IN THE PRESENCE OF METALS AND METALLOPROTEINS: CHEMICAL IMPLICATIONS IN THE BRAIN

Fernando Carmona[a], Òscar Palacios[b], Natividad Gálvez[a], Rafael Cuesta[c], Sílvia Atrian[d], Mercè Capdevila[b], José M. Domínguez-Vera[a].

[a] *Departamento de Química Inorgánica and Instituto de Biotecnología, Facultad de Ciencias, Universidad de Granada, E-18071 Granada, Spain*

[b] *Departament de Química, Facultat de Ciències, Universitat Autònoma de Barcelona, Cerdanyola del Vallès, E-08193 Barcelona, Spain*

[c] *Departamento de Química, Escuela de Linares, Universidad de Jaén, Jaen, Spain*

[d] *Departament de Genètica, Facultat de Biologia and Institut de Biomedicina, Universitat de Barcelona, Avda. Diagonal 643, E-08028 Barcelona, Spain*

Abstract

Living organisms have developed a chemical machinery based on the ferritin protein for the storage, under a nontoxic form, of the iron that is not required for immediate metabolic purposes. Whereas free iron causes extensive cell damage, ferritin iron is not toxic, yet still available for cell requirements. However, iron storage in ferritin is increasingly being recognized as a crucial process related with some neurodegenerative disorders and therefore, an understanding of the management of iron in the brain, especially the processes of iron uptake and release in ferritin, is compulsory to clarify the role of this metalloprotein in these neuropathologies.

Although knowledge of iron storage and iron release in ferritin is nowadays still limited, even less information is currently available about the influence of free metal ions and other brain metalloproteins in these processes.

In this sense, this review is an excellent opportunity to collect all the information today available about the influence of metals and metalloproteins in ferritin loading and unloading events, which until now are dispersed in the literature. Furthermore, we will focus on the importance of all the above-mentioned interactions in the brain, since the importance of the correct and safe balance of metals in the brain after their well-known implication in neurodegenerative

processes such as the Alzheimer's (AD), Parkinson (PD) and prion protein (PPD) diseases is obvious. In this work, we will not only recall the importance and role of ferritin in the brain but also the putative influence of the interaction between ferritin and some metals and/or metalloproteins and other biomolecules on these neurological dysfunctions. The final part of the review will be devoted to draw some guidelines to where the future prospects point to on the basis of the existing information.

1. Introduction

Iron is essential for life since it is required for the active sites of many metalloproteins that play a key role in crucial biological processes such as oxygen transport, storage and use of oxygen in many oxidation–reduction reactions as well as in electron transfer reactions within the cell [1]. Particularly in the brain, iron is crucial for neuronal development, gene expression, enzyme function, dopamine, heme and iron–sulfur cluster synthesis as well as electron transport [2]. However, excess iron is highly toxic. Iron(II) promotes the formation of highly reactive oxygen species (ROS) via distinct pathways [3]. Among these, the most common one is the Fenton reaction, in which hydroxyl radicals OH• are produced by the reaction of iron(II) and hydrogen peroxide. ROS are extremely powerful oxidizing agents capable of causing irreversible cell damage, organ failure and eventually death [4]. Furthermore, free iron is a key nutrient for pathogenic microorganisms, which require iron to survive and replicate. Life is, in some way, a battle for iron and therefore, hosts must deprive undesirable guests of iron in order to combat the infections they cause. Therefore, both excess and deficiency of iron are harmful, and organisms have been forced to develop mechanisms to manage this situation. To do so, they store the iron that is not required for immediate metabolic needs in a non-toxic form. This stored iron is neither available for producing damaging radicals nor for allowing the viability of pathogen microorganisms. Once required, iron can be recovered from the store to participate in cell metabolism.

Ferritin is the primary iron storing protein in most living organisms throughout the animal, plant and microbial kingdoms. The structure of many ferritins isolated

from a wide range of organisms and biological tissues have been determined, and it becomes evident that a common structure has been conserved throughout evolution. The most extensively studied ferritin is that of horse spleen, traditionally considered as the model of mammalian ferritin. It consists of a hollow protein shell (Mr about 450 kDa) composed of 24 subunits arranged in cubic symmetry, that surrounds an aqueous cavity of 8 nm in diameter, capable o accommodating thousands of iron atoms as an iron(III) mineral, traditionally described as ferrihydrite [$Fe^{III}_{10}O_{14}(OH)_2$] [5]. Ferrihydrite is consistent with a single hexagonal phase ($P6_3$ mc; a = ~5.95 Å, c = ~9.06 Å). In its ideal form, this structure contains 20% tetrahedrally and 80% octahedrally coordinated iron(III) [6].

However, it is important to note that the nature of the ferritin core is not completely accepted. In fact, recent studies have pointed out that a polyphasic model, including ferrihydrite and magnetite (or other iron(II)-containing phases) would describe in a more realistic manner the ferritin core, especially once the protein has undergone some chemical disorder [7]. In any case, ferrihydrite is certainly a labile mineral and it is therefore the ideal choice to allow an adequate turn over of iron from the ferritin store to the cell.

Ferritin is remarkably stable to temperature and pH changes, as demonstrated by its stability up to 70 ºC and over extreme pH values of 3–10. At pH < 3 the 24 subunits dissociate but reversibly reassemble at pH > 3 [8]. The 24-polypeptide chains of the apoferritin shell can be classified into two types: the H (or heavy) subunits of 178 amino acids and 21 kDa, and the L (or light) subunits with 171 amino acids and 19 kDa, Fig. 1. The two types of ferritin subunits are closely related both in terms of primary (~53% protein sequence identity) and tertiary structure [9,10]. However they have different functionality. Thus, whereas the H subunit plays a key role in the rapid detoxification of iron, since it contains a catalytic ferroxidase center for rapid iron(II) oxidation, the L subunit is associated with iron nucleation, mineralization and long-term iron storage in the ferritin cavity [11]. In agreement with this, the H/L ratio in a ferritin shell varies widely in different tissues. L-subunit-rich ferritins predominate in iron storage organs such as the liver and spleen, while organs that require iron detoxification properties such as the heart and brain contain H-rich ferritins [12]

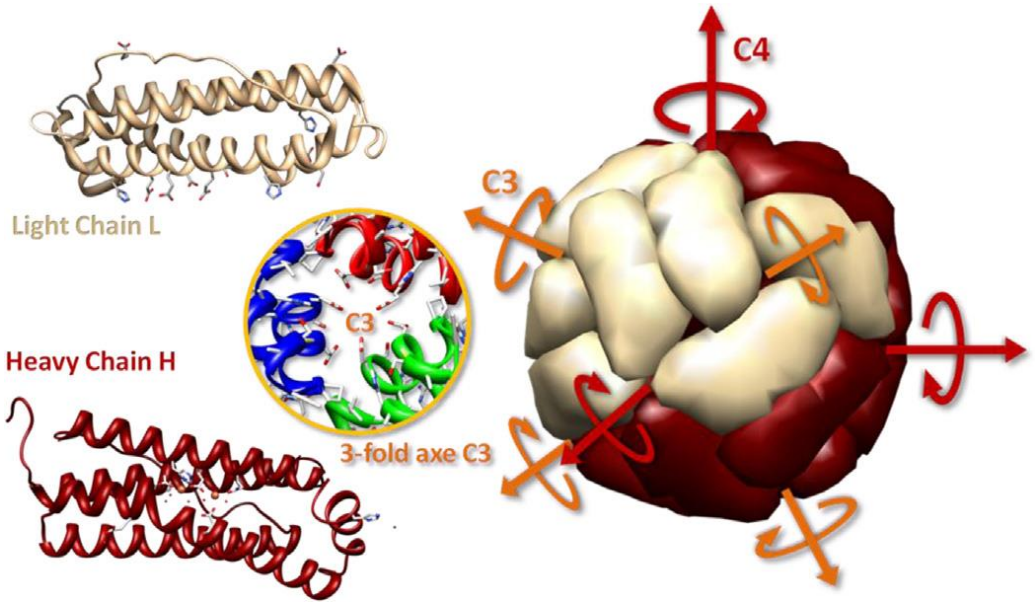

Fig. 1. Horse spleen ferritin structure: a 24-subunit oligomer with a combination of heavy (H) and light (L) polypeptide subunits that form a spherical hollow molecule.

It is interesting to note that ferritins in bacteria, plants and invertebrates are exclusively made by H-like subunits, i.e. they are pure H-like ferritins. Ferritins with a combination of H and L subunits are found only in vertebrates, and they have thoroughly been characterized in mammals. As an example, the traditionally considered model of mammalian ferritin, horse spleen ferritin, usually contains 90% L- and 10% H- subunits.

The multimeric construction of the ferritin shell allows the generation of different types of channels leading to the polymer cavity. Eight hydrophilic channels of ~4–5 Å in diameter and with C3 symmetry (Fig. 1) allow the transfer of water, metal cations and hydrophilic molecules of the appropriate size from the external solution to the cavity or vice versa.

Synthesis of the ferritin H and L monomers is mainly regulated at translation level in response to labile iron concentrations by two mRNA-binding proteins: IRP1 and IRP2 (iron-regulator protein). When cytoplasmic iron is high, IRP1 forms a Fe-S protein that acts as the aconitase enzyme. When iron is low, IRP1 adopts an open

conformation, devoid of the Fe-S cluster that binds to the 5' iron responsive elements (IRE) of the ferritin mRNA, this repressing its translation [13]. Conversely, IRP2 presence in the cell is regulated by degradation, quickly induced by iron overload [14]. These systems function in close coordination with an antithesis control of the transferrin receptor (TfR) synthesis, because the union of IRP1 to the 3' loops of TfR mRNA in low iron conditions stabilizes this messenger, increasing the synthesis rate of TfR, and therefore provoking an enhanced transferrin uptake. However, besides this smart control mechanism exerted by iron levels, at least ferritin H synthesis is also transcriptionally regulated by classical promoter elements and transcription factors that act in inflammatory scenarios [15], which would account for the H-rich ferritin shells usually associated with this kind of processes.

Disorders in ferritin functions have been related with typical iron-related diseases, such as hemochromatosis or anemia, but ferritin is also increasingly being recognized as a crucial molecule in some neurological pathologies, as Parkinson (PD) or Alzheimer's (AD) diseases [16]. Therefore, knowing the ferritin iron uptake, storage, and release mechanisms in detail becomes a challenge for the scientific community in order to understand the etiology of these syndromes and eventually to approach the design of new therapeutic agents based on iron metabolism.

The ferritin core forms from iron(II), and not iron(III). As it will be discussed in the next sections, iron(II) is oxidized and stored mainly as an iron(III) mineral. Likewise, when the cell requires iron from ferritin this is removed as iron(II). If the ferritin protein is purely viewed as an iron store, there are two processes that have to operate properly: a fast and efficient iron storage, and a controlled release of iron. In a biological scenario, when ferritin loses its iron storing ability, free iron(II) remains in the cytoplasm. Equally, when ferritin releases iron in an uncontrolled manner, iron(II) is produced and dumped into the cytoplasm. In other words, a dysfunction of ferritin always gives rise to the existence of free iron(II), with independence of the reason of its malfunction. As mentioned above, free iron(II) promotes ROS that produces oxidative damage. Interestingly, oxidative damage in neurons is a primary cause of degenerative diseases such as AD [17]. Furthermore, as recently reviewed by Kozlowski et al. [18], Fernández et

al. [19], Hureau and Dorlet [20] and Viles [21], free iron(II) and other metals might contribute to some neurological diseases by inducing aggregation of some proteins, as it is the case of ß-amyloid, α-synuclein or the prion protein that respectively accumulate in patients of AD, PD and prion protein disease (PPD).

The reasons for the malfunctioning of ferritin, either at iron uptake, storage or iron release, are still not clear, but data are increasingly supporting two lines of evidence. First, the existence of an excess of a chemical reductant interacting with ferritin has been postulated [22]. Second, genetic mutations affecting either the structure of the ferritin polypeptide [23], or the H [24] or L [25] ferritin mRNA IRE regions this leading to undesirable H/L ratios in the ferritin shells have been recently reported. Both mentioned pathways of ferritin dysfunctions have been intensively studied, related to neurological disorders and reviewed [26].

Ferritin can bind or accommodate metal ions other than Fe in several types of binding sites [27,28]. More importantly, the disruption of the ferritin function in iron uptake or iron release is influenced by the presence of some metals [29], some metalloproteins [30,31], and some other types of biomolecule. Zinc(II), for example, binds to specific ferritin sites and inhibits ferritin iron core formation [32–39]. Copper(II) also binds tightly to ferritin but has an opposite effect to zinc(II), since it has a positive catalytic effect on the uptake of iron by ferritin [40]. Otherwise, some metalloproteins such as ceruloplasmin [41] or metallothioneins [42] are capable to respectively promote the uptake or the removal of iron from ferritin, the latter giving rise not only to the existence to free toxic iron(II) but also to putatively damaging free copper(I) or zinc(II) ions that were initially bound to it. Other biomolecules such as glutathione (GSH), xanthine oxidase and superoxide dismutase (SOD) have also been reported to interact with ferritin (cf. last paragraph of Section 7).

However, the study and analysis of the interactions between ferritins and all these biomolecules and metal ions, as well as their biological significance, has remained until now dispersed in the literature. In this sense, this review aims at collecting all the information now available about the influence of metals and biomolecules, basically metalloproteins, in ferritin iron uptake and iron release. It is our belief that this will provide a solid basis of knowledge from where to extract comprehensive conclusions and to build future prospects. In fact the scenario we

try to draw does not center exclusively in iron in ferritin but in the "ferritin + metal or biomolecule" system, a landscape much more complex than the former, but probably more realistic in terms of physiological significance. Finally, we will try to focus on the importance and consequences of all the above-mentioned interactions in the brain. The uncontrolled release of iron, but also of other metal ions such as zinc or copper, all of them essential but of well established toxicity when in excess, has been revealed to have important consequences in the brain, mainly in neurodegenerative pathologies. Consequently, we are confident that the review and synthesis of all the current available data on this subject will shed light on the possible interpretation of the underlying mechanisms triggering these diseases as well as provide clues to succeed in the design of strategies for their amelioration.

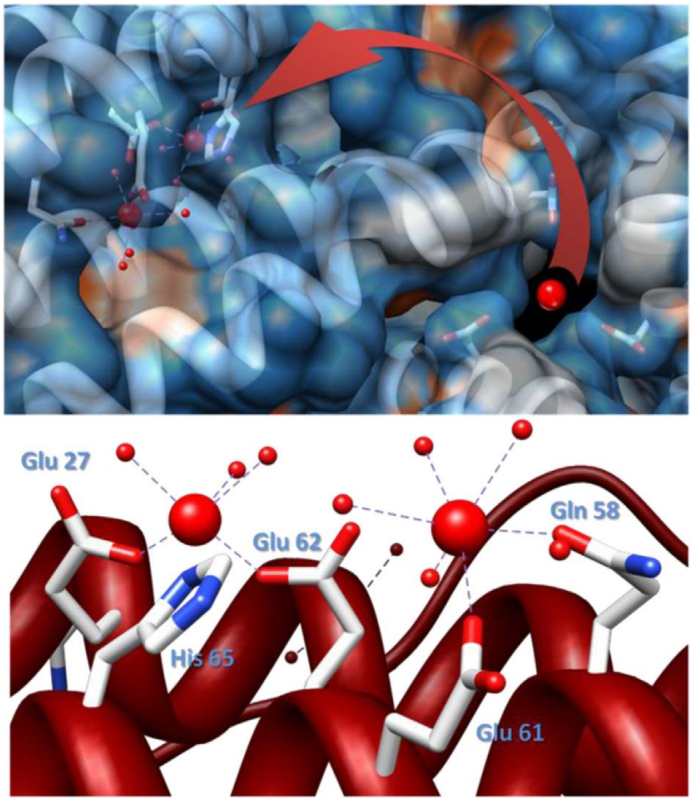

Fig. 2. The trip of iron(II) through the hydrophilic channel to reach the ferroxidase center (top). The two iron coordination sites at the ferroxidase center (bottom).

2. Ferritin iron uptake

The process of iron uptake by ferritin has been extensively studied and reviewed [43]. Our purpose here is to briefly describe the chemistry of iron during its travel across the ferritin channels to the cavity, allowing the reader to envisage how the different steps that comprise the global ferritin iron uptake process can be affected by the presence of metals and metallobiomolecules.

The iron concentration in the cytosol is sensibly higher than that of any other transition metal. The reductive ambient of cytosol clearly favors the presence of iron(II) over iron(III), which leads to respective average values of 10^{-7} and 10^{-18} M [44].

Iron(II)-citrate and iron(II)-thiol-containing biomolecules such as cysteine and glutathione seem to be the major components of the cytosolic iron pool [45]. The high concentration of glutathione in the cytosol (ranging between 2 and 8 mM) enables iron(III) reduction at physiologic pH. Iron(II) is then taken up by apoferritin, which is mainly located in the cytoplasm.

Iron(II) and other metal ions trafficking from the surrounding exterior to the ferritin cavity has been proposed to occur through the 3-fold channels [46]. Calculations of the electrostatic surface potential of ferritin identified a funnel of negative charge that would attract the iron(II), and other metal cations, toward the ferritin hollow [47]. In the most widely accepted model, iron(II) moves through the hydrophilic channels until observation a ferroxidase center of an H-subunit (Fig. 2) where it is catalytically oxidized by reaction with cellular oxygen [48] to form a diferric peroxo complex (DFC) [49,50], where iron atoms occupy two specific coordination sites (A and B).

Most of the structural information about the ferroxidase center has been inferred by a combination of kinetics and site-directed mutagenesis [51]. In the recombinant human H-ferritin, the necessary amino acids include Glu27, Glu62 and His65 at site A, and Glu107, Gln141 and Ala144 at site B. The participation of some of these amino acids has been confirmed in the X-ray structure of the zinc(II) complex of the same recombinant ferritin (Fig. 2) [38].

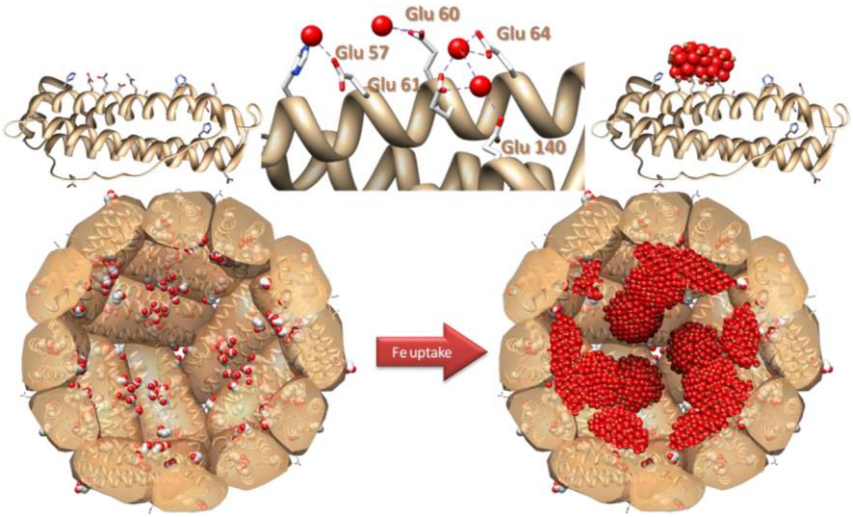

Fig. 3. Nucleation sites (top) and schematic representation of the formation of the first iron clusters. Ferritin core growth (bottom): from the nucleation sites to the final iron oxide nanoparticle

The structure of the ferroxidase center of ferritin from the hyper-thermophilic archaeal anaerobe *Pyrococcus furiosus* under aerobic conditions reported by Hagen et al. exhibits three iron atoms [52]: an iron site A appears to be the strongest affinity site since it is found occupied in the isolated protein, while sites B and C are found only occupied after soaking apobacterionferritin crystals in iron(II) solutions under aerobic conditions. The iron–iron distances between sites A and B vary between 2.6 and 3.6 Å in the different subunits.

In another X-ray absorption spectroscopy study on eukaryotic ferritin, Theil et al. [53] described three different states that were trapped by rapid freeze quench of iron(II) ferritin reacting with O_2 : an initial diiron(II) high-spin state, which is described with iron being in an average six-coordinate environment with a Fe–Fe distance of 3.44 Å, and a peroxodiron(III) intermediate with the very short Fe–Fe distance of 2.53 Å, which finally evolves toward a μ-oxo/hydroxo diiron(III) species with a Fe–Fe distance of 3.00 Å.

An X-ray structure was reported for *Escherichia coli* bacterioferritin by Le Brun et al. [54]. The diiron species obtained by soaking under aerobic conditions, followed by flash freezing, was proposed to be in the reduced state. The iron coordination

environment is contributed by one His and one Glu residue per iron and two bridging Glu residues. The iron–iron distance was 3.7 Å. Longer soaking times provided an iron center proposed to be a μ-oxo/hydroxo diiron(III) species, with an intact coordination sphere and an iron–iron distance of 3.6 Å.

Recently, Bertini et al. reported the first X-ray picture of iron(III) products at the ferroxidase site in higher eukaryote ferritins [55] by flash freezing crystals of frog ferritin soaked during two different times in iron(II) solutions under aerobic conditions. The structure for long soaking times resulted in the observation of invariant diiron(III) sites with a Fe–Fe distance of about 3.1 Å, suggesting the presence of a μ-oxo/hydroxo bridge between iron atoms. The electronic absorption spectra is typical of iron(III) ferritin in solution. The structure for short soaking times was investigated by using copper(II) instead of iron(II) to avoid oxidation. Two different copper(II) ions were found at sites A and B of the ferroxidase center with a Cu–Cu distance of about 4.3 Å. While the coordination environment of copper at site A was similar to that of iron(III) in the structure for long soaking times, copper at site B also contains a bridging carboxylate but differs from that of site A because of the absence of bridging water/hydroxo and the additional coordination to the protein residue His54. Interestingly, His54 binding to metal ion had been observed in the cobalt(II) ferritin structure [46]. The authors hypothesized that the coordination of iron(II) at the ferroxidase center is similar to that of copper(II) and concluded that oxidation at the ferroxidase center requires changes in the coordination environment of iron(II) at site B and a parallel reduction in the metal–metal distance.

The path from the ferroxidase center to the cavity has been analyzed on the basis of a paramagnetic-NMR study [56]. Theil, Bertini et al. have proposed that the DFCs continue their travel to the cavity through the channels. In this journey, the DFC species interact between them to form multimeric iron(III) entities, which ultimately are fixed at the nucleation sites of the cavity and that initiate the growth of the iron core (Fig. 3).

In contrast to this model, Hagen et al. assume that core formation starts directly after formation of the ferroxidase center without occurrence of small clusters en route to core formation. Studies of this group on the *P. furiosus* ferritin suggest that the ferroxidase center, i.e. the invariant metallic motive constituted by iron atoms

bridged by a peroxo group, which are permanently bound to specific amino acids of the protein, is a stable prosthetic group and that after formation of a stable diiron center, iron(II) is oxidized on its way to the core by the iron(III) in the ferroxidase center, and electrons are transferred to O_2 [57]. EPR [58] and kinetic studies [59] support this assumption.

On the other hand, studies by Le Brun et al. on the mechanism of iron deposition in mammalian ferritins suggest an additional pathway based on a reaction on the mineral surface that would allow simultaneously the iron oxidation and nucleation steps [60,61]. Thus iron(II) could migrate through the 3-fold channels and be directly oxidized to iron(III) on the surface of the mineral core.

Likewise, it has been traditionally considered that some oxo anions, in particular phosphate, increase the rate of iron core formation [62]. Ferritins from different origins contain phosphate that is associated with the iron core. In bacterial ferritin, the phosphate/iron ratio can be as high as close to unity [63], whereas a ratio of approximately 0.1 has been found in mammalian ferritins [64]. Recently, Watt et al. showed that phosphate inhibited iron loading into L ferritin, due to the lack of the ferroxidase center, whereas iron loading into H ferritin showed identical iron loading pattern in the presence or absence of phosphate [65].

In any case, analyzing all the literature data, it appears that although the ferritin uptake process has been extensively addressed, there is a limited knowledge of the mechanism of growth of the iron core at the ferritin cavity, and still much needs to be learned about how the iron core grows at the nucleation sites to yield the final nanoparticle.

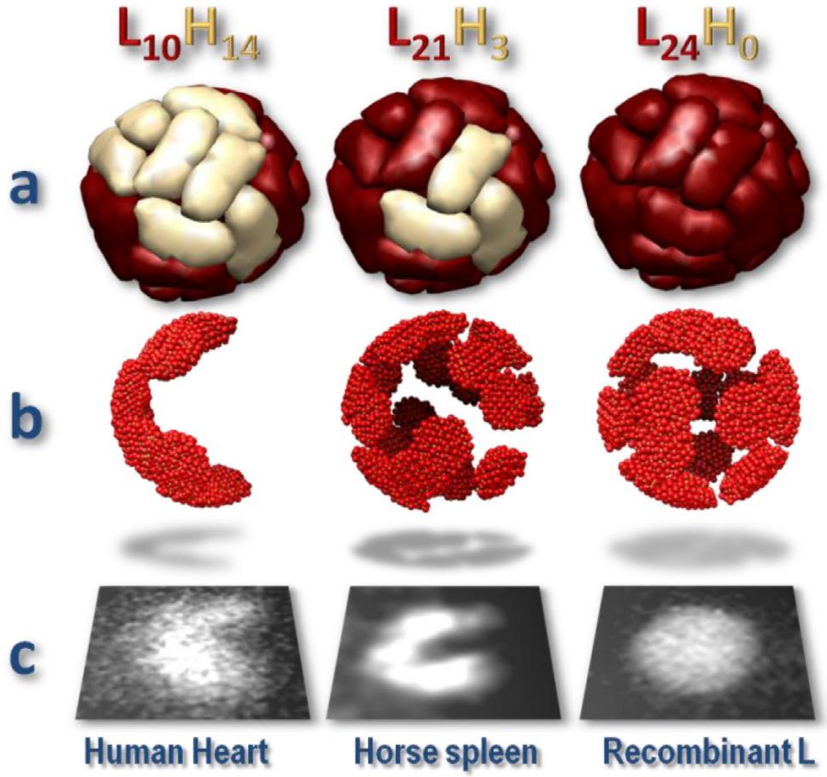

Fig. 4. (a) Structure of human heart, horse spleen and recombinant L ferritin. L subunits are in red and H in cream. (b) Modeled morphology of the iron core and its projection taking into account only L nucleating subunits. (c) Experimental transmission electron microscopy HAADF-STEM images every ferritin, exhibiting expected morphologies after the 24-n model.

In this context, and after a transmission electron microscopy study of horse spleen, heart and recombinant H and L ferritins, we have recently proposed a new model for the ferritin iron core growth based on 24-n nucleation sites (where n is the number of H subunits) [66]. This implies that only L subunits participate in the mineral growth with a nucleation center per subunit. The iron atoms nucleate at these 24-n sites, grow and connect to produce the final iron particle. The subtraction of some nucleation sites to the initial 24 subunits breaks the original cubic morphology and leads to the capability of reproducing other complex morphologies found in ferritins containing distinct combinations of H and L subunits (Fig. 4).

From these studies, it is evident that the iron storing ability of a ferritin is mainly related to the number of its L subunits. This is in line with previous evidence that L-chain rich ferritins form iron particles of greater average size, crystallinity and magnetic order.

Bearing in mind the different stages that iron atoms wander from the entry into the ferritin capsid until reaching its cavity, it is reasonable to consider that the presence of some other metal cations than those of iron or some biomolecules could affect and/or alter the global process of ferritin iron uptake. In particular, three mechanisms could be envisaged: (i) some metal cations blocking the ferroxidase center, this avoiding the required iron(II) oxidation, (ii) some metal cations blocking the nucleation centers, this inhibiting the necessary nucleation of the multimeric iron(III) species to start the growth of the mineral core, and (iii) some biomolecules promoting the iron(II) oxidation, this facilitating the ferritin iron reconstitution. Specific literature examples of each of these three possible mechanisms of ferritin iron uptake alteration will be discussed in detail in the following sections. What is necessary to emphasize here is that the process of iron storage can be, and indeed is, affected by parallel metal metabolisms, either increasing or decreasing the iron uptake of ferritin. Therefore, the iron storage process must definitively be analyzed in a broader and more realistic scenario where metal trafficking – not only iron – should be analyzed as a whole. As an example of this approach, we have recently found out that an excessive proportion of H subunits in the ferritin capsid results in a significant decrease of the amount of stored iron with the consequent existence of free iron(III), which is not fixed in the nucleation sites and that in turn is capable to oxidize some metalloproteins, ultimately leading to the liberation of other metals such as copper(I) or zinc(II) [67]. This kind of processes, where different free metal ions are generated and released by a cascade process starting in a non-appropriate iron storage of ferritin are especially significant in the brain, where improper iron uptake by ferritin has been suggested to result in the progression of neurological diseases. Hence, Dobson and co-workers proposed that AD patients could have a dysfunction in the brain iron storage that occurs as a consequence of disrupted ferritin H and L chain synthesis [68].

3. Ferritin iron release

A detailed knowledge of the iron release process from ferritin is also crucial to understand how iron can be made available when it is required by the cell and because of the possible role of free iron(II) in oxidative stress and in the progression of neurodegenerative diseases.

At physiological conditions, iron is released by ferritin when the iron concentration in the cytosol decreases, either because it has been taken for cell metabolism or because the overexpression of ferroportin, which acts as an iron export pump. The in vivo mechanism of iron release from ferritin is still undetermined. However it has already been made patently clear that the ferroxidase centers of the H-subunits, which are central to the mechanism of ferritin iron uptake as stated in the previous section, are not involved in iron release. Therefore, the ferritin iron uptake and the ferritin iron release processes utilize distinct pathways [69].

Four global models have been proposed to account for the ferritin iron release: (i) the existence of an equilibrium between the iron stored in ferritin and the iron in cytoplasm, (ii) the ferritin capsid degradation, (iii) the participation of a chaperone that would dock with ferritin and directly remove iron(III), and (iv) the existence on an electron donor biomolecule that would dock with ferritin to reduce the iron(III) of the ferrihydrite mineral and facilitate iron(II) mobilization, which would be chelated by a chaperone molecule outside the ferritin molecule (Fig. 5).

Although there is a lack of definitive evidence to support the reduction-chelation model (option iv above), this mechanism is thought to be the one that operates in vivo since some data seem to support this hypothesis more strongly than others. On the one hand, the well-known reducing nature of the intracellular environment provides molecules such as flavins, glutathione and ascorbic acid, which are capable of reducing the iron from the ferritin core [70]. Furthermore, in vitro studies show that the most efficient method to remove iron from ferritin is by reduction-chelation (Fig. 5) [71]. In fact, this is the strategy commonly used in the laboratory to produce apoferritin from ferritin, emptying the ferritin capsid of iron, frequently by using thioglycolic acid (TGA) as reducing agent and 2,2'-bipyridyl (bipy) or ferrozine (fz) as iron(II) chelators.

Direct chelation and mobilization of iron(III) from ferritin by iron biochelators

(option iii above), as transferrin is, has been described to be too slow to take place in a physiologically relevant time scale [72]. Furthermore, ferritin is essentially an intracellular protein and does not seem reasonable to envisage a mechanism of iron release from ferritin by a plasmatic protein. Likewise, a genuine large hexadentate iron chelator such as desferrioxamine, a well known siderophore and a drug for iron chelatotherapy, extracts iron from ferritin albeit at a slow rate [73], probably because of the difficulties that this large molecule finds to pass through the narrow 3-fold ferritin channels. Only by using smaller and, in fact non-biologically available iron(III) chelators, such as the aceto- and benzo-hydroxamate molecules, and in the presence of physiological concentrations of urea (reported as an agent able to open the ferritin pores [74]), complete removal of iron from ferritin can be achieved in 1 h at pH 7.4 [75].

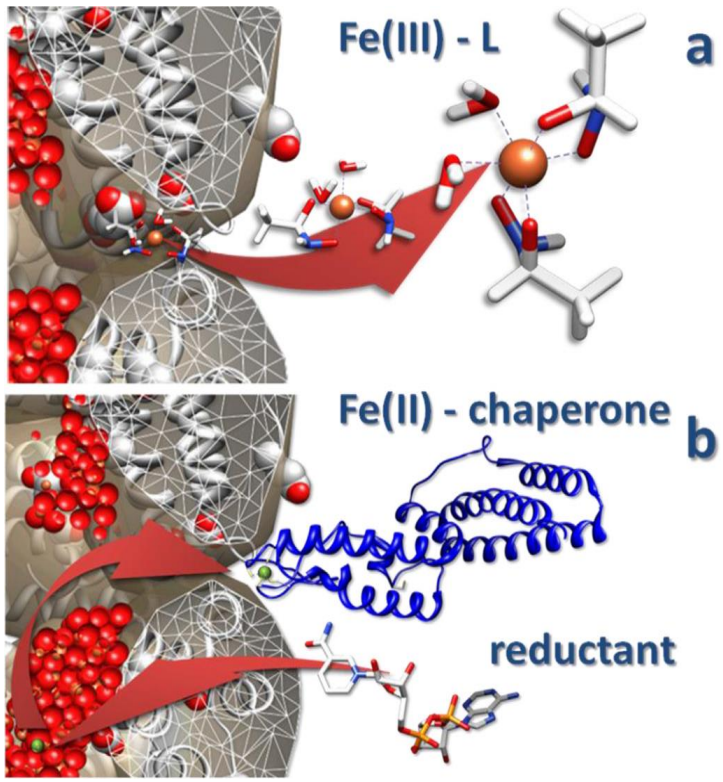

Fig. 5. Schematic representation of the two main mechanisms proposed for ferritin iron release. Top: direct chelation (model iii). A molecule (L) directly chelates iron(III) at the hydrophilic channels. Bottom: reduction-chelation (model iv). A reductant reduces iron(III) to iron(II), which leaves the ferritin and it is taken up by a chaperone.

A route recently proposed by Bou-Abdallah et al., involving the release of iron from ferritin iron by triazine chelates, which are capable of rapidly mobilizing iron from ferritin, must be also considered. This way of iron release is catalyzed by oxygen and involves reduction of the iron core by the superoxide anion. The reduced iron diffuses out of the ferritin shell and forms iron(III) complexes with the concomitant production of superoxide anions [76].

Going deeper into the reduction-chelation mechanism, two general scenarios have been conceived depending on the size of the reductant. For biomolecules small enough to traverse the ferritin channels, the reaction would take place in the ferritin cavity, giving rise to iron(II) and the oxidized biomolecule. This route has been shown to occur when catechol and 6-hydroxydopamine (6-OHDA) react with ferritin [77,78]. Interestingly, the interaction of 6-OHDA and ferritin triggers a cycle of reactions that could sustain PD [79]. In this disease, the neuromelanin in the substantia nigra contains high iron levels, part of which could produce OH• radicals via Fenton reaction. These can readily oxidize the neurotransmitter dopamine to the neurotoxic 6-OHDA, which is a strong reducing agent, and therefore is, in turn, able to release iron(II) from ferritin [79]. This cycle of events could well explain the development of PD due to continuous neuron damage.

For biomolecules significantly larger than the ferritin channels, it has been considered that the reduction of iron(III) to iron(II) could occur by electron tunneling, without direct physical interaction between the biomolecule and the ferritin iron core. In this sense, it must be noted that electron transfer proteins are capable of reducing the iron core of some ferritins, suggesting the existence of both a docking site and an electron transfer pathway through the protein shell of ferritin [80]. In some cases, this docking site has been discovered, as it occurs when ferredoxin specifically binds to the heme group of bacterial ferritin and opens electron transfer through the protein shell [81]. Likewise, a combination of computational modeling methods allowed showing how flavin molecules bind to the ferritin protein surface and transfer electrons across the protein shell reaching the iron core [82]. We also recently demonstrated that some metallothioneins can promote iron release from ferritin by pumping electrons through the shell that reduce iron(III) to iron(II), which diffuses into the intracellular milieu [42].

In any case, either if the reductant biomolecule traverses and contacts the ferritin

core or if an electron tunneling process takes place, both options lead to the mobilization of iron(II), which finally diffuses through the ferritin channels into the cell cytoplasm, where it is able to participate in free radical-producing processes. Therefore, when cells require iron from ferritin, more than a reductive biomolecule is needed because, in order to prevent the formation of ROS from free iron(II), a metallochaperone or an iron(II) chelator is also necessary to rapidly bind and sequester the liberated iron(II) [83].

If we do accept that the ferritin iron release takes place in the cell through a controlled reduction–chelation mechanism, it is also reasonable to consider that it could be affected and/or altered by the excess, or default, of some biomolecules. In particular, two possibilities could be envisaged: (i) the excess of the reductant, which would give rise to an uncontrolled reduction of iron(III), and consequently to an uncontrolled iron(II) delivery, and (ii) the absence or default of the chaperone, necessary to capture the released iron(II), and prevent ROS formation. The implications and consequences of these two possibilities of ferritin iron release alterations will be extensively discussed in the following sections.

4. Iron and ferritin in the brain

As it has been previously stated, iron is essential for life, and in the brain is important for neuronal development, gene expression, enzyme function, dopamine, heme and iron–sulfur cluster synthesis as well as in electron transport [84–86].

More rigorous and definitive data are still needed to know the exact map of the distribution of iron and ferritin within the brain. The huge amount of data that can be found in the literature are often contradictory [87]. However, it is now accepted that the iron amounts in substantia nigra, a small nervous structure of about 500 mg located bilaterally in mesencephalon, which produces the dopamine neurotransmitter, and hippocampus would be close to 200 ng/mg and 50 ng/mg, respectively. It is accepted that PD is caused by a progressive degeneration of nervous cells located in substantia nigra, whereas AD is provoked by the death of nervous cells in hippocampus. The reason for the degeneration of neurons in substantia nigra in PD remains unknown at present, although it is noteworthy that

large concentrations of iron, comparable to those in the liver, are found in this brain compartment of PD patients. In fact, Youdim et al. formulated the hypothesis that PD is a progressive siderosis of substantia nigra, which enhances the oxidative stress [88]. Controversy of about one order of magnitude in the iron levels measured in neurological disorders and controls have been excellently reviewed by Galazka-Friedman and Friedman [87]. However, as stated by the authors, it is still possible that iron is involved in the pathogenesis of neurological disorders, as even minor changes in the amount and form of iron may initiate the processes leading to cell death. In any case, it is striking that the iron level in human brain increases linearly with age, reaching a plateau in substantia nigra at forty, because it is precisely at this age when neurological episodes begin. Furthermore, the local excess of iron occurs at the site where neurodegeneration develops and where specific protein aggregation occurs. This evidence suggests that an increased concentration of iron, even subtle, in the tissues contributes to generate oxidative stress.

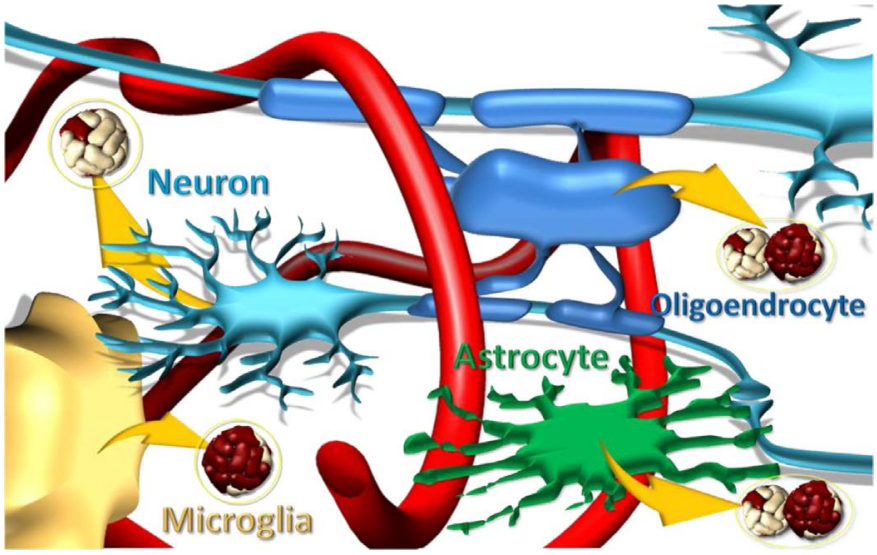

Fig. 6. Predominant ferritin type (H- or L-rich) in neuron and glia

Nevertheless, it is also true that the question whether iron accumulation might be an initiating factor of these diseases or whether it occurs as a consequence of

impaired metabolic processes has not found an answer yet. Similarly, the question where the excess of iron comes from is also unsolved. However, whatever the origin would be, high levels of free iron are toxic owing to the formation of ROS that finally lead to neuronal death [89]. Also, the pathologic aggregation of proteins seems to be modulated by iron [90–92].

Both total brain and substantia nigra iron is stored in ferritin [93–95]. Ferritin is also highly synthesized within the glial compartment, predominantly in oligodendrocytes, microglia and astrocytes [96] (Fig. 6). Under normal conditions, most of the iron in the brain is safely stored, and there is no need for a substantial increase of the total amount of iron(II) to provoke an increase of the amount of free radicals. Therefore, a minimal ferritin disorder could justify a degeneration of the nervous cells.

As it occurs in the distribution of H- and L- ferritin content throughout the body, the H/L ferritin ratio varies in the different regions of brain in agreement with the requirements of every cell type to detoxify or store iron [97]. H-rich ferritin is found mainly in neurons whereas L-rich ferritin is more abundant in microglia [98]. Both, H- and L- ferritin subunits are synthesized in oligodendrocytes and astrocytes [99] (Fig. 6). Furthermore, the concentrations of H- and L-ferritins in the substantia nigra increase during life, probably a protective response to the increase of iron with age. The distribution of types of ferritin within substantia nigra, especially the presence of H-rich ferritin in neurons and L-rich ferritin in glia agree with the protection role of H-ferritin against the cytotoxic effect of iron(II) and the storage capability of L-ferritin.

Hippocampus is a part of the temporal lobe cortex, which plays a crucial role in memory. Its atrophy with the decline in the number of nervous cells is the starting point of AD. The cause of this neurodegenerative disorder also remains unidentified, although it seems that iron mediated oxidative stress may play a role.

Galazka-Friedman [100] reported that the Mössbauer spectroscopic pattern of hippocampus samples and that of ferritin were highly coincident, as it happened with that of substantia nigra. The only difference in these spectra was the intensity of signals, which reflects different iron concentrations in the two brain areas. The average size of iron cores of ferritin in the hippocampus measured by electron

microscopy was about 3.1 nm. In agreement with previous studies reported by our group [66], which correlate size and morphology of the ferritin core with shell composition, this small size should correspond to a high content of H subunits, in agreement with ELISA studies that revealed a higher average concentration of H ferritin (150 ± 30 ng/mg) than L ferritin (20 ± 10 ng/mg) on the same type of samples [100].

The complex distribution of ferritin in the brain and the subtle balance in the appropriate composition of H and L chains show that ferritin can be a key component in brain function.

5. Copper, zinc and related biomolecules in the brain

Since iron uptake and release by ferritin shells is likely to be influenced, when non disrupted, by excess of other significant metal ions in brain cells or their subcellular compartments, it is worth catching a glimpse into the incidence of Zn(II) and Cu(I)/(II) in mammalian organisms, and precisely, in mammalian brain cells. Zn(II) is present in the brain at large amounts (10 μg/g) [101]. Most of this zinc accumulates inside cells, where it can reach cytosolic concentrations up to 150 μM, as in neurons [102,103] (Fig. 7), in contrast with the 0.15 μM Zn(II) typical of central nervous system (CNS) extracellular fluid and serum [102]. Despite these impressive amounts, free Zn(II) is a minimal percentage of total Zn(II), hardly reaching levels above 1 nM [104,105]. This implies that, in physiological conditions, most of the brain Zn(II) is coordinated to some biomolecule, mainly proteins and other smaller compounds [106–108]. Most of the pool brain Zn is highly role-specific, being related to neuronal intracellular signaling and neurotransmission [109]. Noteworthy, the so-called zinc-enriched neurons (ZEN) accumulate 10–15% of the total brain Zn(II) confined in their presynaptic vesicles (Fig. 7) [110]. Pathologies that lead to abnormally increased synapsis rate (ischemia, epilepsy) supposes an excessive postsynaptic uptake of Zn(II) followed by a massive accumulation of intracellular free Zn(II) that, at the end, directly provokes neuronal death or takes part in other undesirable

processes by interacting with biomolecules such as ferritin. When Zn(II) reaches levels that would compromise cell functionality and viability [111,112], it is

translocated into specific cell compartments (mitochondria in neurons), or sequestered by buffering peptides in the cytosol, mainly metallothioneins (MT) [113]. MTs are small (6–10 kDa), cysteine rich (33%) metalloproteins that bind a wide spectrum of heavy metal ions. They are major players in the homeostasis of physiological Zn(II) and/or Cu(I), as well as in metal detoxification processes. The mammalian MT system includes four highly similar MT isoforms (MT1–MT4, the latter not present in the brain), which are 60- to 68-amino acid peptides with fully conserved Cys motif distribution. The tissular expression pattern of the four MTs shows substantial differentiation. Hence, MT1 and MT2 are ubiquitous, highly inducible isoforms that respond to a considerable number of factors mainly metal overload and oxidative stress. In CNS, MT1/2 are predominantly synthesized in astrocytes and microglia, both in gray and white matter [114], and have been widely associated with the prevention and healing of CNS inflammation and injuries, being greatly induced under these conditions. MT3, the brain-specific isoform, first identified as a growth inhibitory factor (GIF) [115], is constitutive in neurons (prominently hippocampal neurons), some glial cells and in the extracellular brain space [116], and it appears mainly involved in neuronal growth and survival regulation, and, significantly, in processes localized in axon and dendrite interfaces, as the same synaptic transmission. A recent review of protein interactions in which MT is involved highlights the role of the different MT isoforms in the brain Zn(II) secretion and recirculation events [117]. Although Zn(II) is a redox-inactive ion, the zinc- thionein/thionein cycle, besides preventing deleterious free Zn(II) concentrations, provides an indirect pathway of redox buffering mechanism through the thiol/disulfide equilibrium of their abundant cysteine residues [118]. Finally, it is worth noting that the tripeptide glutathione (GSH) has also been shown to thwart the toxicity caused by excess zinc, most probably by direct chelation, so that in emergency situations, a considerable amount of Zn–GSH complexes is likely to be present in brain cells [119].

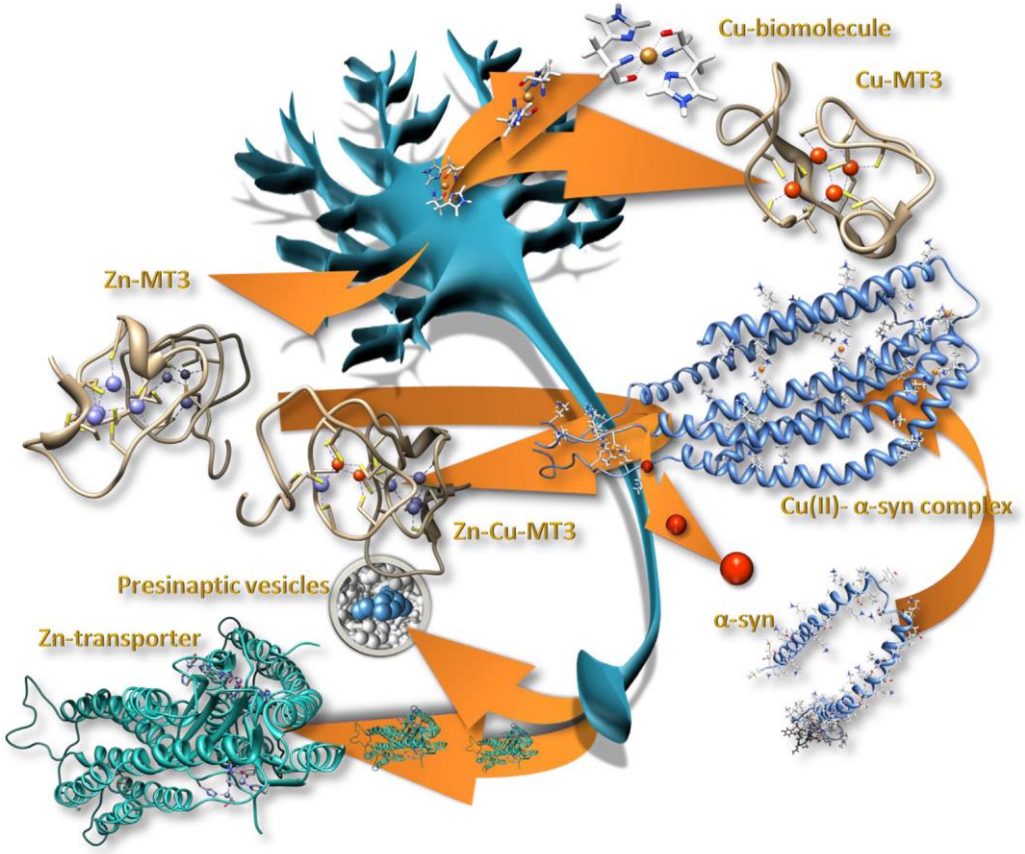

Fig. 7. Zinc- and copper-containing biomolecules in neurons. In the absence of 3D structures of the distinct metal-MT3 species, the drawings included in this figure just represent the presence of these complexes in neurons and do not have any structural value.

In contrast with zinc, and despite the fact that copper is also a catalytic cofactor in crucial enzymes, its content per adult body is less than 110 mg (cf. 3 g for Zn(II)), and in the brain it does not exceed 9–10 mg approximately [120]. Free Cu, being redox active, is extremely dangerous for cells, and therefore cells avoid deleterious effects by maintaining the levels of free Cu^{2+} lower tan 10^{-18} mM [121]. Cu is far from being equally distributed in the brain, and e.g. substantia nigra accumulates twice as much Cu as the surrounding brain regions (Fig. 7) [122]. Copper in the brain is mainly associated with holoenzymes, transporters and chaperones, and homeostatic proteins [123]. Cu-containing enzymes are mainly involved in cell respiration, iron metabolism, ROS defense mechanisms, and significantly, the synthesis of neurotransmitters (dopamine [124]) and neuron myelinization [122].

Copper is mainly transported in blood bound to ceruloplasmin (CP), although minor amounts are also coordinated to albumin. In the frame of this review attention has to be drawn to the membrane anchored CP reported in astrocytes [125], due to its ferroxidase activity. Brain cells, and especially neurons, avoid excessive intracellular copper by pumping it out to the cell membranes or supposedly by sequestering it into MT complexes, although the knowledge on brain Cu-MT and their behavior is far more limited than that of Zn-MT. It is obvious that direct deleterious effects of Cu in the brain by ROS generation (Fenton reaction) derived from its redox nature are effectively avoided by MT coordination. But the most fascinating aspect of Cu ions in the brain concerns the increased evidence about their involvement in the onset and progression of neurodegenerative disorders as AD, PD, amyotrophic lateral sclerosis (ALS), and transmissible spongiform encephalopathies (TSEs) (for excellent recent reviews, see [18,21]). All these disorders are triggered by the aggregation of misfolded monomers and subsequent formation of insoluble deposits that accumulate in the brain, of the respectively associated proteins: the Aß-peptide, α-synuclein, SOD and the prion proteins. In all these cases, interaction of Zn(II)-MT3 with the aggregation-prone Cu-loaded peptides seems to preclude their harmful effects. Precisely, it has been shown that the interaction of Zn7 -MT3 and Cu(II)-Aß-peptides or Cu(II)-α-synuclein triggers a metal swap reaction which eliminates Cu(I) from the brain peptides and generates Zn,Cu-MT3 species with four Cu(I) ions bound to a partially oxidized MT3 domain, and the four Zn(II) ions remaining in the domain [126,127]. Therefore MT3 in brain metal homeostasis appears far from acting just as a mere reservoir of metal ions, becoming instead a key controller of redox reactions and, indirectly, of metal-induced protein damage, misfolding and aggregation.

6. Interaction of ferritin with metal ions

Iron-, zinc- and copper-handling proteins, as well as the metabolism and homeostasis of these physiological metal ions, are intimately related in all organisms. As an example, mutations in the genes controlling the multi-copper ceruloplasmin protein have been associated with iron overload diseases in humans [128]. People with low levels of ceruloplasmin have been shown to have increased

iron deposits in various tissues [129]. Therefore, it seems reasonable to assume that in the framework of the interaction between iron, copper and zinc metabolisms, the ferritin protein could play a central role.

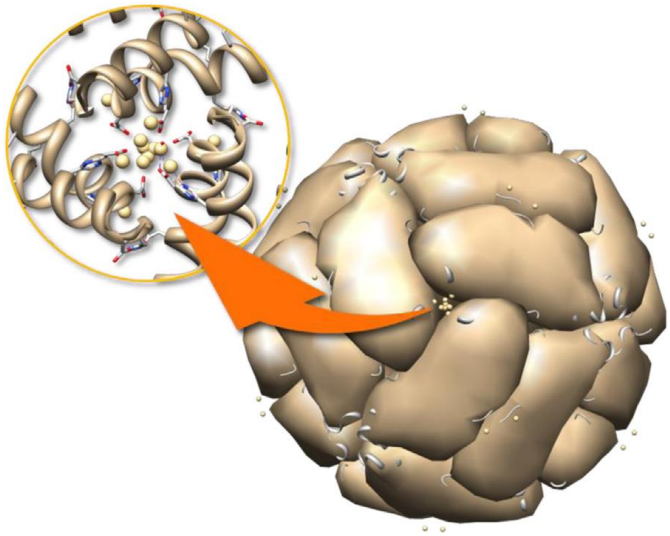

Fig. 8. Structure of the cadmium(II) apoferritin (Protein Data Bank file: 1AEW) [10]. Cadmium(II) concentrates preferentially around the entry of the C3 channels.

This statement could have sense when taking into consideration the higher iron levels, in most tissues, with respect to those of copper and zinc, but also because of the huge number of iron atoms confined inside ferritin, a situation that does not occur in the case of copper or zinc, this multiplying the consequences of any dysfunction taking place in ferritin owing to the amount of free and toxic iron that can be released.

The interaction of ferritin with metal ions has been extensively studied in order to gain a better understanding of the interactions and/or interferences that the later can cause in ferritin function, either in the iron uptake or iron release processes. Different studies provide evidence that metal cations are bound by ferritin [28] usually in two separate types of sites of very different binding constants. These two classes of binding sites are localized either within the cavity or at the external shell [28]. Interestingly, the largest number of binding sites is for divalent metal

cations, although some of them are functional and others are nonspecific and do not play any decisive role in the genuine properties of ferritin.

Among the metals studied in the literature, we have considered here those that have a well-described role on the ferritin function as well as a biological relevance, especially at brain level, i.e. cadmium(II), zinc(II) and copper(II). Zinc(II) and cadmium(II) cause inhibition of iron uptake by ferritin [130]. Before any iron fills a ferritin capsid, all metals compete for the iron binding sites during iron reconstitution. Once the iron core starts formation, metal ions alter the ferritin function by a different mechanism, some of them inhibiting, other promoting the iron core growth.

Cadmium(II) binding is diminished by the presence of a ferritin core, clearly pointing out that cadmium(II) compete with iron(II) for the same sites inside the ferritin shell. In fact, when the ferritin cavity is empty, up to 24 Cd(II) can be bound to its inner surface, one per subunit [28]. However, the mechanism by which cadmium(II) affects the ferritin iron reconstitution is not only based on the competition for iron binding at the cavity level, but also lies in the fact that cadmium(II) strongly binds other nonspecific sites, especially at the external shell surface. There, cadmium(II) has probably the greatest affinity for these sites, and is able to exclude almost all other metals from binding. It should be noted that cadmium binds sites localized around the entry of the hydrophilic channels (Fig. 8), and that it may even hinder the entry of other metals, including iron, and therefore block the ferritin iron reconstitution. Based on the interaction with the ferritin shell and on the effect that this interaction provokes in the solubility of the ferritin protein, cadmium(II) is commonly used as a precipitant agent of ferritin [131] and in fact, most commercial ferritins contain significant amounts of cadmium coming from the preparation process.

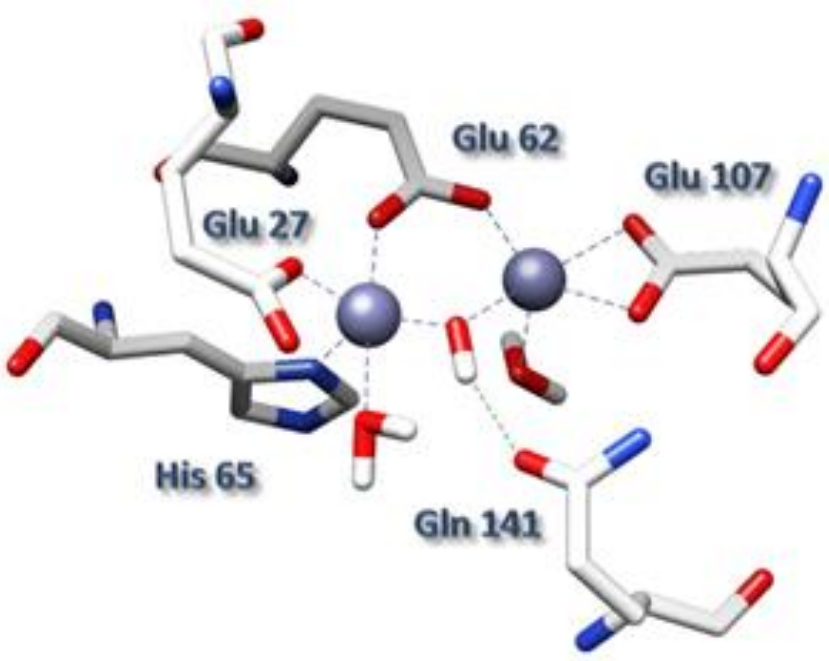

Fig. 9. Modeled dizinc ferroxidase complex based on crystallographic data [132].

As stated throughout the review, iron uptake by ferritin involves the oxidation of two iron(II) located at the highly conserved ferroxidase centers of the individual H-subunits. The role of these centers therefore appears to be essential for the iron(II) oxidation catalysis and the subsequent ferritin core formation by nucleation at the L-subunits. Studies on iron oxidation by mammalian, bacterial, and archaeal ferritins have indicated that different mechanisms can be operative in the zinc(II) inhibition of the iron core formation, taking into account that H-ferritin ferroxidase activity is inhibited by zinc(II) [128].

In human H-chain ferritin, two main types of Zn(II) binding sites have been described: at the entrance of the eight C3 channels and at the ferroxidase site of the protein. The kinetics and binding data indicate that the binding of zinc(II) in the three-fold channels, which is the main pathway of iron(II) entry in ferritin, blocks the access of most of the iron to the internal ferroxidase sites, which accounts for the inhibition by these metal ions of the oxidative deposition of iron in ferritin.

Zinc(II) has been assumed to be the best iron(II) substitute for structural determination purposes because it is redox stable, and because both ions are similar in size and are moderate Lewis acids. Hence, the structure of recombinant

human H dizinc(II) ferroxidase complex has been solved by X-ray crystallography (Protein Data Bank file 2CEI) [38]. A perspective view of this is displayed in Fig. 9. The zinc at site A is coordinated to a nitrogen atom from His65 and three oxygen atoms, two from Glu27, Glu62 and the third one presumed to be from a water molecule. The zinc at site B is coordinated by both carboxylate oxygen atoms of Glu107 and Glu62, which bridge the two metal sites. Furthermore, a computational study identified a hydroxide bridge between sites A and B, and another water molecule at site B and showed that no other ligand or peripheral molecules are present in the experimental dizinc ferroxidase center [132]. Finally, and according to these authors, the modeled structures of the diiron and dizinc complexes are close, suggesting that the dizinc ferroxidase is an accurate model of the native diiron complex.

Although the empty ferroxidase site accommodates two zinc(II) ions, the binding of just one zinc(II) is enough to abolish the iron(II) oxidation capability of the ferroxidase center [57]. It is interesting to note here that zinc(II) binds relatively tightly to horse spleen apoferritin, displacing iron(II) under anaerobic conditions but however, once the ferroxidase center is filled with two iron(III), zinc(II) is no longer able to bind there, nor does it inhibit the iron core formation. A similar situation has been described for cadmium(II). Therefore, the existence of a competition between metals for different apoferritin binding sites takes place but once the ferritin biomineralization process is triggered neither cadmium or zinc are able to affect the ferritin machinery.

Interestingly, in the case of the recombinant human H-ferritin, the structure of the distinct complexes with zinc(II) reveal a surprising similarity between them, indicating that the dinuclear site in this recombinant ferritin is quite a rigid site for this metal ion. Surprisingly, this is not the case when iron occupies these same binding sites. As previously described, coordination of iron at the ferroxidase center undergoes changes during oxidation with the subsequent iron-iron distance shortening [55].

The rigidity of the zinc(II) coordination at the ferroxidase site with respect to the flexibility found for iron is probably a consequence of the non-redox chemistry of zinc(II), which has a definitive importance in how zinc(II) affects the ferritin iron uptake. This is more evident when the coordination of copper to the ferroxidase

center and its effect to the ferritin function is analyzed (see below).

The lack of ferroxidase activity in ferritin due to the presence of zinc(II) is extremely relevant in neurons, where the concentration of zinc(II) becomes very significant (Section 5) and the ferritin is predominantly H-rich (Section 4). A minimum amount of free zinc(II) could inhibit the appropriate iron(II) oxidation by ferritin, giving rise to a cascade radical process that would conclude with neuronal death.

Furthermore, the interaction of zinc(II) with ferritin can be extrapolated to other neurological scenarios. For instance, AD is complicated by prooxidant intraneuronal free iron(II) and, interestingly, by zinc(II) overloading within amyloid plaque. Interestingly, the AD β-amyloid protein precursor has been described to exhibit ferroxidase activity due to the existence of what Bush et al. denominate a H-ferritin-like active site, which is captivatingly also inhibited by zinc(II) [133]. However, it must be taken into account that the ferroxidase activity of the AD β-amyloid protein precursor has been recently called into question and asked for its revaluation [134].

The interaction of copper with ferritin has also been investigated. Copper(II), as in the case of zinc(II), was shown to bind relatively tightly to horse spleen ferritin. Once bound, copper(II) has a catalytic effect on the aerobic oxidative uptake of iron(III) by ferritin, which means that it induces an opposite effect to that of zinc(II). The difference between the effect of zinc(II) and copper(II) has been explained by Moore et al. in terms of the capability of copper(II) to take part in redox reactions [40]. In the absence of any other metal ions, two iron(II) bind at this site, are oxidized by O_2 and form the DFC. Now, returning to the opposite effects of zinc(II) and copper(II) in horse spleen ferritin, it is plausible to consider that if these two ions are bound in a way that they occupy just one end of the site, an incoming iron(II) occupying the other end might be oxidized by copper(II) but not by zinc(II). The iron(III) produced could then migrate from the site to allow another iron(II) to take its place alongside the produced copper(I). At this point a two-electron reduction of O_2 would generate copper(II) and iron(III) and, with the migration of iron(III) away from the site, the cycle could be reinitiated [40]. Unfortunately, only crystal data of ferritin–copper(II) and not copper(I) complex are yet available to confirm this hypothesis, but it should be highlighted that, as

stated before, both the distances and bond angles found for the zinc(II) complexes of ferritin point out to an extreme rigidity of the site that would justify a zinc inhibitory role of the ferroxidase activity, but a promoting role for copper.

The loss of the ferroxidase activity of ferritin in the brain becomes a transcendent problem when pathological iron(II) accumulates and neurodegenerative processes are triggered. It is quite intriguing to realize that the presence of free, and toxic iron(II), can be generated either by an excess of zinc that inhibits the ferroxidase activity of ferritin, or by a deficiency of copper. In fact, when copper lacks, there is also a malfunction of the multicopper ferroxidase ceruloplasmin protein and a development of the aceruloplasminemia disease, which leads to glial iron accumulation and dementia.

7. Interaction of ferritin with metalloproteins and other biomolecules

Two metalloproteins, specifically Cu- or Zn-containing proteins, have been reported in literature to somehow interact with ferritin: ceruloplasmin, a blue multicopper oxidase with ferroxidase activity [135], and metallothioneins (see Section 5).

The oldest studies, carried out before the 2000 decade, called into question the mechanism of ferritin iron uptake described before in this review, and which is nowadays universally accepted. Aust and coworkers defended, at the end of the 90s, the docking between ceruloplasmin and ferritin [41]. This research group was defending that the ferroxidase activity of the H-subunits was leading to iron loaded ferritins with properties notably differing from those of native ferritins. In parallel, they reported that the enzymatic load of apoferritin with iron by using intact human ceruloplasmin rendered iron loaded ferritins with nearly identical properties to those of native ferritins [136]. Therefore, to accomplish the iron(II) to iron(III) oxidation by ceruloplasmin, a protein–protein complex formation was hypothesized, and the existence of a specific recognition site for the interaction of both proteins and the stimulation of its ferroxidase activity was suggested. In fact, the symptoms of iron overload as well as of excessive deposition of insoluble iron found in patients diagnosed with aceruloplasminemia (low concentrations of active ceruloplasmin) or Menkes disease (a disorder that affects copper levels in

the body, leading to copper deficiency) supported the proposed interaction. Unfortunately, this research line was stopped and no further data giving continuity to this hypothesis have ever been reported.

Much more recently, our groups reported an intriguing interaction between metallothionein and ferritin. Two proteins apparently designed by nature to protect cells, and organisms, from free transition metal ions, and to respectively maintain the homeostatic levels of Zn and Cu, and Fe generated deleterious effects when observation each other. This serendipitous discovery occurred during the search for a biomolecule able to capture the released iron(II) from ferritin and thus capable to prevent ROS formation (Section 3 of this work). For this study, the Zn-complexes of the mammalian metallothionein isoforms found in the brain, MT1, MT2 and MT3 (Section 5), and the model horse spleen ferritin where chosen. The obtained results were astonishing (respectively 55.6, 23.9, and 59.5% of iron release) and they correlated well with the Zn/Cu-thionein character of the assayed MTs [137]. Further experiments carried out either with Cu-loaded or Zn,Cu-heteronuclear complexes of these MTs confirmed parallel behaviors and suggested that not only iron(II) and zinc(II), but also copper(I) can be liberated to the media if ferritins and metallothioneins meet in the cell [authors' unpublished results]. Interestingly, neither binding between the two participant proteins nor a disruption of the ferritin structure was detected during the interaction. However, iron and zinc liberation from their respective metalloproteins was reported to be the consequence of the oxidation of the cysteinic residues of the MTs. Therefore, a proposal of a tentative redox reaction between the two biomolecules by electron transfer through the ferritin shell was proposed owing to the size of the Zn-MT complexes, which impairs them reaching the mineral by traversing the protein shell through the ferritin channels (Fig. 10). Recent theoretical studies [82] and experimental observations [138] commented above give nowadays further support to this proposal.

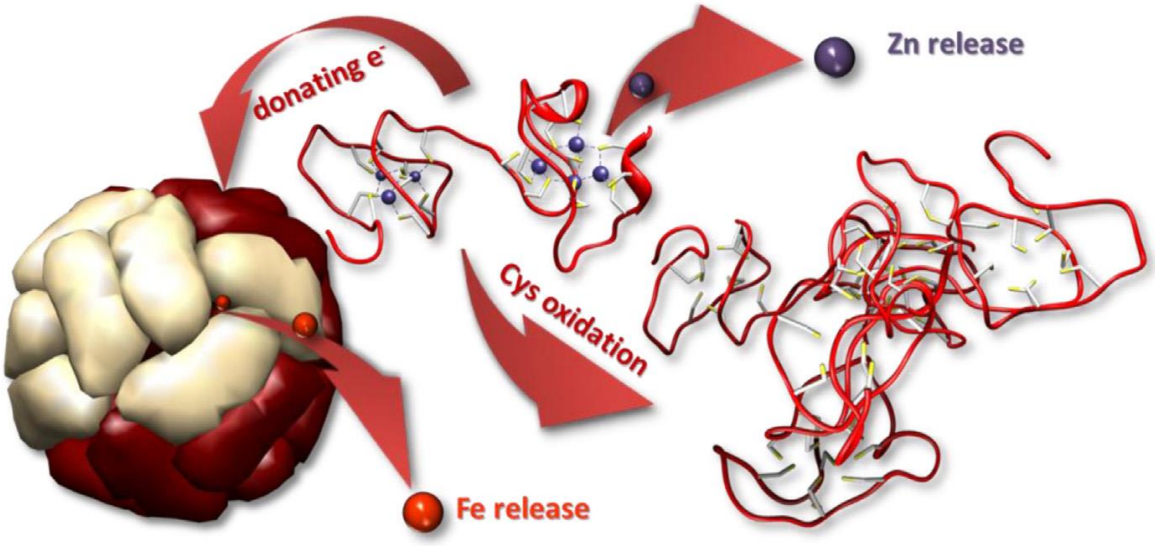

Fig. 10. Iron removal from horse spleen ferritin by mammalian Zn-MTx (x = 1, 2 or 3) takes place with simultaneous liberation of iron(II) and zinc(II).

The interaction of ferritin with multiple biomolecules, not strictly metalloproteins, has also been reported in the literature. Two groups can be differentiated depending on the result of these interactions: those that are thought to retrieve ferritin form circulation, and those that are proposed to serve the upload or release process of iron into or from ferritin. Here we will concentrate only in biomolecules that are present in the brain. The first group includes a variety of ferritin-binding proteins identified in mammals: H-kininogen, alpha-2-macroglobulin, fibrinogen, and apolipoprotein B (ApoB) [139,140]. All these proteins are present in the brain and have been proposed to form complexes with ferritin to most likely remove it from circulation. High-molecular-weight kininogen (KNG) is a central constituent of the contact-kinin system, which represents an interface between thrombotic and inflammatory circuits and is critically involved in stroke development [141]. Alpha2-macroglobulin (alpha(2)M) is an abundant plasma protein similar in structure and function to the so called alpha2-macroglobulin, which is also produced in the brain where it binds multiple extracellular ligands, being then internalized by neurons and astrocytes. In the brain of AD patients, alpha(2)M has been localized to diffuse amyloid plaques [142]. The blood protein fibrinogen, which leaks into the CNS immediately after blood-brain barrier disruption or vascular damage, serves as an early signal for the

induction of glial scar formation via the TGF- /Smad signaling pathway [143]. At least two mechanisms of interaction between these proteins and ferritin have been proposed [140]: one is direct binding, such as that proposed for H-kininogen, and fibrinogen; the other is an indirect binding through heme on the surface of the ferritin molecule, such as that described for the heme-binding protein, ApoB. In this case, some distinctions should be made: those biomolecules supposed to contribute to the uptake process and those involved in the release of iron from ferritin. Some fatty acids appear to achieve the first goal, while, SOD and xanthine oxidase and cytochrome P-450 seem to fulfill the second purpose. Arachidonic acid (ARA) is one of the most abundant fatty acids in the brain and its disturbed metabolism may be associated with neurological disorders such as AD and bipolar disorder [144]. Interestingly, Bu et al. [145] recently reported a 60 μM affinity specific binding site of ferritin for ARA. Also, they described that its binding enhances iron mineralization and decreases iron release at the same time that protects the fatty acid from oxidation. This binding site was proposed to be located in the 2-fold intersubunit pocket, allowing the ARA tail to project well into the ferrihydrite mineralization site on the L-ferritin subunit, while shorter saturated fatty acids as caprylate were described not to have significant effects on mineralization.

As stated in previous sections, iron(II) can be released from ferritin by reductants small enough to reach the mineral core by using the ferritin channels, and this is the case of $O_2^{\bullet-}$. Interestingly, two distinct research groups reported diverging results with respect to the capability of $O_2^{\bullet-}$ to affect the release of iron(II) from ferritin and this implied the participation of two other biomolecules: SOD and xanthine oxidase. Both, the research groups of Biemond et al. [146] and of Thomas et al. [147] found that iron was mobilized from ferritin by xanthine oxidase. However, after observation that iron release could be completely inhibited by SOD, Thomas et al. concluded that $O_2^{\bullet-}$ was the active iron-mobilizing species. Similar conclusions can be drawn from the studies between the interaction of ferritin with cytochrome P-450 [148] or with the intracellularly ocurring Cu(I)-glutathione complex $Cu(GSH)_2$ [149]. Oppositely, the observation that SOD had no blocking effect on the release of iron from ferritin by xanthine oxidase, led to Biemond et al. to suggest that probably electrons were transferred from the enzyme-substrate

complex to ferritin via an unknown mechanism. Finally, Bolann and Ulvik reported that in hypoxic tissues xanthine oxidase can release iron from ferritin by an $O_2^{\bullet -}$ independent process [150].

8. Concluding remarks

Over millions of years, living organisms have produced ferritin for a crucial function: iron storage. Ferritin is at the center of iron metabolism, providing protection by scavenging free iron and storing iron when needed. Dysfunction in ferritin, either at iron uptake or iron release leads to the existence of free iron(II), which can be the beginning of a range of neurological pathologies.

The enormous progress made in understanding the mechanism of action of ferritin, nevertheless, revealed a number of transcendent issues that still remain to be solved such as: (i) the influence of the H- or L-nature of its subunits in the formation of the iron core, (ii) the identification of the putative ferritin-binding biomolecules that can promote iron release or (iii) the role and interference of metals and metalloproteins in ferritin iron uptake and iron release. This review has been mainly focused in the last issue. However, much more data collecting information from realistic scenarios where other free metal ions different than iron, and other metalloproteins interact with ferritin are still needed. It is our belief that this review will provide a basis of knowledge from where to extract comprehensive conclusions and to build future prospects.

We have reviewed different situations in which the interaction of ferritin with a metal ion or a metalloprotein gives rise to the existence of free toxic metals, iron or iron plus other metals. For example, it is true that zinc(II) can be found at high concentrations in neurons but fortunately it is mainly complexed or compartimentalized. However, any anomalous zinc(II) metabolism provoking the appearance of free zinc(II) in neuron would cause an inhibition of the ferroxidase activity of ferritin and the subsequent existence of not stored free iron(II). Then, the free zinc(II) and iron(II) would result in causing neuron death. Interestingly, the presence of the multicopper ceruloplasmine could overcome this problem as this protein promotes iron(II) oxidation and also ferritin reconstitution. This is a genuine example to show how the metabolism of these three metals is interrelated

and how its study in depth requires a full approach where interactions between free and protein-containing metals must be considered.

In another scenario, an excessive proportion of H-subunits in ferritin can result in an increase of iron(II) oxidation level but a in significant decrease of the amount of iron stored in the mineral core of ferritin, with the consequent existence of free iron(III), which is capable to oxidize some metalloproteins, such as metallothioneins, ultimately leading to the liberation of metal ions like copper(I) or zinc(II). Likewise, the iron(III) stored in the mineral core of ferritin can also oxidize the metal-MT complexes causing the liberation of iron(II) and of the metal ions bound to metallothioneins.

Although we are aware of the evident difficulties associated with the study of more integrative systems, it is our conviction that the future goals for the elucidation of the iron uptake and release processes in ferritin should aim at considering not only the presence of distinct metals but also that of other metalloproteins, which coexist with ferritin in the different tissues and cell compartments. It is our belief that only with this approach, a realistic view of the chemical implications of their interactions can be achieved. This is especially important in the brain when trying to shed light into the neuropathologies associated with the dysfunction of metalloproteins that give rise to an uncontrolled release of metals, a fact that probably underlines the origin of some of the most dramatic neurological diseases affecting nowadays the worldwide population.

Acknowledgments

This work was supported by the “Spanish Ministerio de Ciencia e Innovación,” MICINN and FEDER (grants BIO2012-39682-C02-01 and BIO2012-39682-C02-02 respectively to S.A. and M.C., and CTQ2012-32236 to J.M.D.-V.). Authors from Barcelona Universities are members of the 2009SGR-1457 “Grup de Recerca de la Generalitat de Catalunya.” Authors from the Universidad de Granada and Jaen are members of the FQM-368 “Grupo de Investigacion de la Junta de Andalucia.”

References

[1] R. Crichton, Inorganic Biochemistry of Iron Metabolism: from Molecular Mechanisms to Clinical Consequences, John Wiley & Sons, England, 2001.

[2] D.J. Pinero, J.R. Connor, in: H.R. Lieberman, R.B. Kanarek, C. Prasad (Eds.), Nutritional Neuroscience, CRC Press, Taylor & Francis Group, Boca Raton, 2005, p. 235.

[3] K. Jomova, M. Valko, Curr. Pharm. Des. 17 (2011) 3460.

[4] H. Heli, S. Mirtorabi, K. Karimian, Expert Opinion on Therapeutic Patents 21(2011) 819.

[5] N.D. Chasteen, P.M. Harrison, J. Struct. Biol. 126 (1999) 182.

[6] F.M. Michel, L. Ehm, S.M. Antao, P.L. Lee, P.J. Chupas, G. Liu, D.R. Strongin, M.A.A. Schoonen, B.L. Phillips, J.B. Parise, Science 316 (2007) 1726.

[7] N. Gálvez, B. Fernández, P. Sánchez, R. Cuesta, M. Ceolín, M. Clemente, S. Trasobares, M. López-Haro, J.J. Calvino, O. Stéphan, J.M. Domínguez-Vera, J. Am. Chem. Soc. 130 (2008) 8062.

[8] S.P. Martsev, A.P. Vlasov, P. Arosio, Protein Eng. 11 (1998) 377.

[9] S. Levi, S.J. Yewdall, P.M. Harrison, P. Santambrogio, A. Cozzi, E. Rovida, A. Albertini, P. Arosio, Biochem. J. 288 (1992) 591.

[10] P.D. Hempstead, S.J. Yewdall, A.R. Fernie, D.M. Lawson, P.J. Artymiuk, D.W. Rice, G.C. Ford, P.M. Harrison, J. Mol. Biol. 268 (1997) 424. [11] E.C. Theil, Curr. Opin. Struct. Biol. 15 (2011) 304.

[12] M. Wagstaff, M. Worwood, A. Jacobs, Biochem. J. 173 (1978) 969.

[13] J. Zähringer, B.S. Baliga, H.N. Munro, Proc. Natl. Acad. Sci. U.S.A. 73 (1976) 857.

[14] K. Iwai, S.K. Drake, N.B. Wehr, A.M. Weissman, T. LaVaute, N. Minato, R.D. Klausner, R.L. Levine, T.A. Rouault, Proc. Natl. Acad. Sci. U.S.A. 95 (1998) 4924.

[15] S.V. Torti, E.L. Kwak, S.C. Miller, L.L. Miller, G.M. Ringold, K.B. Myambo, A.P. Young, F.M. Torti, J. Biol. Chem. 263 (1988) 12638.

[16] D. Berg, G. Beceker, P. Riederer, O. Rieb, Neurotox. Res. 4 (2002) 637.

[17] B. Uttara, A.V. Singh, P. Zamboni, R.T. Mahajan, Curr. Neuropharmacol. 7 (2009) 65.

[18] H. Kozlowski, M. Luczkowski, M. Remelli, D. Valensin, Coord. Chem. Rev. 256 (2012) 2129.

[19] A. Binolfi, L. Quintanar, C.W. Bertoncini, C. Griesinger, C.O. Fernández, Coord.

Chem. Rev. 256 (2012) 2188.

[20] C. Hureau, P. Dorlet, Chem. Rev. 256 (2012) 2175. [21] J.H. Viles, Coord. Chem. Rev. 256 (2012) 2271.

[22] J.M. Domínguez-Vera, B. Fernández, N. Galvez, Future Med. Chem. 2 (2010)

609.

[23] A.R.J. Curtis, C. Fey, C.M. Morris, L.A. Bindoff, P.G. Ince, P.F. Chinnery, A.

Coulthard, M.J. Jackson, A.P. Jackson, D.P. McHale, D. Hay, W.A. Barker, A.F. Markham, D. Bates, A. Curtis, J. Burn, Nat. Genet. 28 (2001) 350.

[24] J. Kato, K. Fujikawa, M. Kanda, N. Fukuda, K. Sasaki, T. Takayama, M. Kobune, K. Takada, R. Takimoto, H. Hamada, T. Ikeda, Y. Niitsu, Am. J. Hum. Genet. 69 (2001) 191.

[25] M.E. Martin, S. Fargion, P. Brissot, B. Pellat, C. Beaumont, Blood 91 (1998) 319. [26] R.K. Watt, R.J. Hilton, D.M. Graff, Biochim. Biophys. Acta 1800 (2010) 745. [27] J.G. Joshi, A. Zimmerman, Toxicology 48 (1988) 21.

[28] S. Pead, E. Durrant, B. Webb, C. Larsen, D. Heaton, J. Johnson, G.D. Watt, J. Inorg. Biochem. 59 (1995) 15.

[29] I.G. Macara, T.G. Hoy, P.M. Harrison, Biochem. J. 135 (1973) 785.

[30] A. Mazur, S. Green, A. Saha, A. Carleton, J. Clin. Invest. 37 (1985) 18097. [31] S.-H. Juan, J.-H. Guo, S.D. Aust, Arch. Biochem. Biophys. 341 (1997) 280.

[32] G.R. Bakker, R.F. Boyer, J. Biol. Chem. 261 (1986) 13182.

[33] N.E. Le Brun, A.M. Keech, M.R. Mauk, A.G. Mauk, S.C. Andrews, A.J. Thomson, G.R. Moore, FEBS Lett. 397 (1996) 159.

[34] A. Treffry, P.M. Harrison, J. Inorg. Biochem. 21 (1984) 9.

[35] X. Yang, N.E. Le Brun, A.J. Thomson, G.R. Moore, N.D. Chasteen, Biochemistry 39 (2000) 4915.

[36] T.J. Stillman, P.D. Hempstead, P.J. Artymiuk, S.C. Andrews, A.J. Hudson, A. Treffry, J.R. Guest, P.M. Harrison, J. Mol. Biol. 307 (2001) 587.

[37] F. Bou-Abdallah, P. Arosio, S. Levi, C. Janus-Chandler, N.D. Chasteen, J. Biol. Inorg. Chem. 8 (2003) 489.

[38] L. Toussaint, L. Bertrand, L. Hue, R.R. Crichton, J.P. Declercq, J. Mol. Biol. 365 (2007) 440.

[39] M.J. Yablonski, E.C. Theil, Biochemistry 31 (1992) 9680.

[40] J. McKnight, N. White, G.R. Moore, J. Chem. Soc. Dalton Trans. (1997) 4043. [41] C.A. Reilly, M. Sorlie, S.D. Aust, Arch. Biochem. Biophys. 354 (1998) 165, and references therein.

[42] R. Orihuela, B. Fernández, O. Palacios, E. Valero, S. Atrian, R.K. Watt, J.M. Domínguez-Vera, M. Capdevila, Chem. Commun. 47 (2011) 12155. [43] P.M. Proulx-Curry, N.D. Chasteen, Coord. Chem. Rev. 144 (1995) 347. [44] R.C. Hider, X. Kong, Dalton Trans. 42 (2013) 3220.

[45] P.M. Harrison, P. Arosio, Biochim. Biophys. Acta 1275 (1996) 161.

[46] E.C. Theil, R.K. Behera, T. Tosha, Coord. Chem. Rev. 257 (2013) 579, and references therein.

[47] T. Douglas, D.R. Ripoll, Protein Sci. 7 (1998) 1083. [48] X. Liu, E.C. Theil, Acc. Chem. Res. 38 (2005) 167.

[49] T. Tosha, H-L. Ng, O. Bhattasali, T. Alber, E.C. Theil, J. Am. Chem. Soc. 132 (2010) 14562.

[50] F. Bou-Abdallah, G.C. Papaefthymiou, D.M. Scheswohl, S.D. Stanga, P. Arosio, N.D. Chasteen, Biochem. J. 364 (2002) 57.

[51] X. Liu, E.C. Theil, Proc. Natl. Acad. Sci. U.S.A. 101 (2004) 8557.

[52] J. Tatur, W.R. Hagen, P.M. Matias, J. Biol. Inorg. Chem. 12 (2007) 615.

[53] J. Hwang, C. Krebs, B.H. Huynh, D.E. Edmondson, E.C. Theil, J.E. Penner-Hahn, Science 287 (2000) 122.

[54] A. Crow, T.L. Lawson, A. Lewin, G.R. Moore, N.E. Le Brun, J. Am. Chem. Soc. 131 (2009) 6808.

[55] I. Bertini, D. Lalli, S. Mangani, C. Pozzi, C. Rosa, E.C. Theil, P. Turano, J. Am.

Chem. Soc. 134 (2012) 6169.

[56] P. Turano, D. Lalli, I.C. Felli, E.C. Theil, I. Bertini, Proc. Natl. Acad. Sci. U.S.A. 107 (2010) 545.

[57] K.H. Ebrahimi, P.-L. Hagedoorn, W.R. Hagen, J. Biol. Inorg. Chem. 15 (2010)

1243.

[58] J. Tatur, W.R. Hagen, FEBS Lett. 579 (2005) 4729.

[59] K.H. Ebrahimi, P.L. Hagedoorn, J.A. Jangejon, W.R. Hagen, J. Biol. Inorg. Chem.

14 (2009) 1265.

[60] N.E. Le Brun, A. Crow, M.E.P. Murphy, A.G. Mauk, G.R. Moore, Biochim. Biophys. Acta 1800 (2010) 732.

[61] A. Lewin, G.R. Moore, N.E. Le Brun, Dalton Trans. (2005) 3597.

[62] J.L. Johnson, M. Cannon, R.K. Watt, R.B. Frankel, G.D. Watt, Biochemistry 38 (1999) 6706.

[63] J.S. Rohrer, Q.T. Islam, G.D. Watt, D.E. Sayes, E.C. Theil, Biochemistry 29 (1990) 259.

[64] A. Treffry, P.M. Harrison, Biochem. J. 171 (1978) 313. [65] R.J. Hilton, A. David, R.K. Watt, Biometals 25 (2012) 259.

[66] J.D. López-Castro, J.J. Delgado, J.A. Perez-Omil, N. Galvez, R. Cuesta, R.K. Watt, J.M. Domínguez-Vera, Dalton Trans. 41 (2012) 1320.

[67] F. Carmona, O. Palacios, S. Atrian, J.M. Dominguez-Vera, M. Capdevila, under review.

[68] Q.Q. Pankhursta, D. Hautotb, N. Khanc, J. Dobson, J. Alzheimers Dis. 13 (2008)

49.

[69] S. Yasmin, S.C. Andrews, G.R. Moore, N.E. Le Brun, J. Biol. Chem. 286 (2011) 3473.

[70] S. Sirivech, E. Frieden, S. Osaki, Biochem. J. 143 (1974) 311.

[71] M.S. Joo, G. Tourillon, D.E. Sayers, E.C. Theil, Biol. Met. 3 (1990) 171. [72] D.C. Harris, Biochemistry 17 (1978) 3071.

[73] J. Johnson, J. Kenealey, R.J. Hilton, D. Brosnahan, R.K. Watt, G.D. Watt, J. Inorg. Biochem. 105 (2011) 202.

[74] X. Liu, W. Jin, E.C. Theil, Proc. Natl. Acad. Sci. U.S.A. 100 (2003) 3653.

[75] N. Gálvez, B. Ruiz, R. Cuesta, E. Colacio, J.M. Domínguez-Vera, Inorg. Chem. 44 (2005) 2706.

[76] F. Bou-Abdallah, J. McNally, X.X. Liub, A. Melman, Chem. Commun. 47 (2011) 731.

[77] P. Sánchez, N. Gálvez, E. Colacio, E. Min˜ ones, J.M. Domínguez-Vera, Dalton

Trans. (2005) 811.

[78] W. Linert, G.N.L. Jameson, J. Inorg. Biochem. 79 (2000) 319.

[79] G.N.L. Jameson, W. Linert, in: G. Poli, E. Cadenas, L. Packer (Eds.), Free Radicals in Brain Pathophysiology, Marcel-Decker, New York, 2000, p. 247.

[80] G.D. Watt, D. Jacobs, R.B. Frankel, Proc. Natl. Acad. Sci. U.S.A. 85 (1988) 7457. [81] S.K. Weeratunga, C.E. Gee, S. Lovell, Y. Zeng, C.L. Woodin, M. Rivera, Biochemistry 48 (2009) 7420.

[82] V. Subramanian, D.G. Evans, J. Phys. Chem. B 116 (2012) 9287.

[83] H. Shi, K.Z. Bencze, T.L. Stemmler, C.C. Philpott, Science 320 (2008) 1207. [84] D.H. Boldt, Am. J. Med. Sci. 318 (1999) 207.

[85] J. Connor, in: J. Connor (Ed.), Metals and Oxidative Damage in Neurological

Disorders, Plenum Press, New York, 1997, p. 23.

[86] J.R. Connor, S.A. Benkovic, Ann. Neurol. 32 (1992) S51.

[87] J. Galazka-Friedman, A. Friedman, Acta Neurobiol. Exp. 57 (1997) 217.

[88] M.B.H. Youdim, D. Ben-Shachar, P. Riederer, Acta Neurol. Scand. 126 (1989) 47.

[89] R.A. Cherny, C.S. Atwood, M.E. Xilinas, D.N. Gray, W.D. Jones, C.A. McLean, K.J. Barnham, I. Volitakis, F.W. Fraser, Y. Kim, X. Huang, L.E. Goldstein, R.D. Moir, J.T. Lim, K. Beyreuther, H. Zheng, R.E. Tanzi, C.L. Masters, A.I. Bush, Neuron 30 (2001) 665.

[90] M. Perez, J.M. Valpuesta, E.M. De Garcini, C. Quintana, M. Arrasate, J.L. Lopez-Carrascosa, A. Rabano, J.G. De Yebenes, J. Avila, Am. J. Pathol. 152 (1998) 1531.

[91] A. Takeda, M. Hashimoto, M. Mallory, M. Sundsumo, L. Hansen, A. Sisk, E. Masliah, Lab. Invest. 78 (1998) 1169.

[92] M. Hashimoto, E. Masliah, Brain Pathol. 9 (1999) 707.

[93] D.T. Dexter, C.J. Carter, F.R. Wells, F. Javoy-Agid, Y. Agid, A. Lees, P. Jenner, C.D. Marsden, Brain 114 (1991) 1953.

[94] B. Hallgren, P. Sourander, J. Neurochem. 3 (1958) 41.

[95] J. Sian-Huelsmann, S. Mandel, M.B.H. Youdim, P. Riederer, J. Neurochem. 118 (2011) 939.

[96] J.R. Connor, K.L. Boeshore, S.A. Benkovic, S.L. Menzies, J. Neurosci. Res. 37 (1994) 461.

[97] J.R. Connor, B.S. Snyder, P. Arosio, D.A. Loefer, P. Le Witt, J. Neurochem. 65 (1995) 717.

[98] P. Ponka, C. Beaumont, D. Richardson, Semin. Hematol. 35 (1998) 35.

[99] L. Zecca, M.B. Youdim, P. Riederer, J.R. Connor, R.R. Crichton, Nat. Rev. Neurosci. 5 (2004) 863.

[100] J. Galazka-Friedman, Hyperfine Interact. 182 (2008) 31. [101] C.J. Frederickson, Int. Rev. Neurobiol. 31 (1989) 145. [102] A. Takeda, Brain Res. 34 (2000) 137.

[103] R.A. Colvin, Am. J. Physiol. Cell Physiol. 282 (2002) 317. [104] C.E. Outten, T.V. O'Halloran, Science 292 (2001) 2488. [105] L.A. Finney, T.V. O'Halloran, Science 300 (2003) 931.

[106] I. Bertini, L. Decaria, A. Rosato, J. Biol. Inorg. Chem. 15 (2010) 1071. [107] L. Decaria, I. Bertini, R.J.P. Williams, Metallomics 2 (2010) 706. [108] W. Maret, Y. Li, Chem. Rev. 109 (2009) 4682.

[109] A. Takeda, Biometals 14 (2001) 343.

[110] C.J. Frederickson, J.Y. Koh, A.I. Bush, Nat. Rev. Neurosci. 6 (2005) 449. [111] D.W. Choi, M. Yokoyama, J.K. Koh, Neuroscience 24 (1988) 67.

[112] G.J. Lees, A. Lehmann, M. Sandberg, A. Hamberger, Neurosci. Lett. 120 (1990) 155.

[113] M. Capdevila, R. Bofill, O. Palacios, S. Atrian, Coord. Chem. Rev. 256 (2012) 46.

[114] J. Hidalgo, R. Chung, M. Penkowa, M. Vasak, in: A. Sigel, H. Sigel, R.K.O. Sigel (Eds.), Metallothioneins and Related Chelators, Metal Ions in Life Sciences, vol. 5, RSC Publishing, Cambridge, 2009, p. 279.

[115] Y. Uchida, Biol. Signals 3 (1994) 211.

[116] M. Vasak, G. Meloni, in: A. Sigel, H. Sigel, R.K.O. Sigel (Eds.), Metallothioneins and Related Chelators, Metal Ions in Life Sciences, vol. 5, RSC Publishing, Cambridge, 2009, p. 319.

[117] S. Atrian, M. Capdevila, Biomolecular Concepts (2013), http://dx.doi.org/10.1515/bmc-2012-0049.

[118] W. Maret, A. Krezel, Mol. Med. 13 (2007) 371. [119] C.-J. Chen, S.-L. Liao, J. Neurochem. 85 (2003) 443.

[120] E. Gaggelli, H. Kozlowski, D. Valensin, G. Valensin, Chem. Rev. 106 (2006) 1995.

[121] T.D. Rae, P.J. Schmidt, R.A. Pufahl, V.C. Culotta, T.V. O'Halloran, Science 284 (1999) 805.

[122] K.M. Davies, D.J. Hare, V. Cottam, N. Chen, L. Hilgers, G. Halliday, J.F.B. Mercer, K.L. Double, Metallomics 5 (2013) 43.

[123] L. Decaria, I. Bertini, R.J.P. Williams, Metallomics 3 (2011) 56.

[124] T.C. Steveson, G.D. Ciccotosto, X.M. Ma, G.P. Mueller, R.E. Mains, B.A. Eipper, Endocrynology 144 (2003) 188.

[125] L.W.J. Klomp, Z.S. Farhangrazi, L.L. Dugan, J.D. Gitlin, J. Clin. Invest. 98 (1996) 207.

[126] G. Meloni, V. Sonois, T. Delaine, L. Guilloreau, A. Gillet, J. Teissie, P. Faller, M.

Vasak, Nat. Chem. Biol. 4 (2008) 366.

[127] G. Meloni, M. Vasak, Free Radic. Biol. Med. 50 (2011) 1471.

[128] K. Yoshida, K. Furihata, S. Takeda, A. Nakamura, K. Yamamoto, H. Morita, S. Hiyamuta, S. Ikeda, N. Shimizu, N. Yanagisawa, Nat. Genet. 9 (1995)

267.

[129] Z.L. Harris, Y. Takahashi, H. Miyajima, M. Serizawa, R.T.A. MacGillivray, J.D.

Gitlin, Proc. Natl. Acad. Sci. U.S.A. 92 (1995) 2539.

[130] N.D. Chasteen, S. Sun, S. Levi, P. Arosio, in: C. Hershko (Ed.), Progress in Iron

Research, Plenum, New York, 1994, p. 23.

[131] P.J. Artymiuk, E.R. Bauminger, P.M. Harrison, D.M. Lawson, I. Nowik, A. Treffry, S.J. Yewdall, in: R.B. Frankel, R.P. Blakemore (Eds.), Iron Biominerals, Plenum Press, New York, 1991, p. 269.

[132] D.E. Bacelo, R.C. Binning Jr., Chem. Phys. Lett. 507 (2011) 174.

[133] J.A. Duce, A. Tsatsanis, M.A. Cater, S.A. James, E. Robb, K. Wikhe, S.L. Leong, K. Perez, T. Johanssen, M.A. Greenough, H.-H. Cho, D. Galatis, R.D. Moir, C.L. Masters, C. McLean, R.E. Tanzi, R. Cappai, K.J. Barnham, G.D. Ciccotosto, J.T. Rogers, A.I. Bush, Cell 142 (2010) 857.

[134] K.H. Ebrahimi, P.-L. Hagedoorn, W.R. Hagen, PLoS One 7 (2012) e40287.
[135] N.E. Hellman, J.D. Gitlin, Annu. Rev. Nutr. 22 (2002) 439.

[136] M.E. Van Eden, S.D. Aust, Arch. Biochem. Biophys. 381 (2000) 119, and enclosed references.

[137] O. Palacios, S. Atrian, M. Capdevila, J. Biol. Inorg. Chem. 16 (2011) 991.

[138] H. Yao, Y. Wang, S. Lovell, R. Kumar, A.M. Ruvinsky, K.P. Battaile, I.A. Vakser, M. Rivera, J. Am. Chem. Soc. 134 (2012) 13470.

[139] M. Hashimoto, Y. Nambo, T. Kondo, K. Watanabe, K. Orino, J. Equine Sci. 22 (2011) 1, and references therein.

[140] A. Usami, M. Tanaka, Y. Yoshikawa, K. Watanabe, H. Ohtsuka, K. Orino, Biometals 24 (2011) 1217, and references therein.

[141] F. Langhauser, E. Göb, P. Kraft, C. Geis, J. Schmitt, M. Brede, K. Göbel, X. Helluy, M. Pham, M. Bendszus, P. Jakob, G. Stoll, S.G. Meuth, B. Nieswandt, K.R. McCrae, C. Kleinschnitz, Blood 120 (2012) 4082.

[142] D.M. Kovacs, Exp. Gerontol. 35 (2000) 473.

[143] C. Schachtrup, J.K. Ryu, M.J. Helmrick, E. Vagena, D.K. Galanakis, J.L. Degen, R.U. Margolis, K. Akassoglou, J. Neurosci. 30 (2010) 5843.

[144] S.I. Rapoport, J. Nutr. 138 (2008) 2515.

[145] W. Bu, R. Liu, J.C. Cheung-Lau, I.J. Dmochowski, P.J. Loll, R.G. Eckenhoff, FASEB J. 26 (2012) 2394.

[146] P. Biemond, H.G. van Eijk, A.J.G. Swaak, J.F. Koster, J. Clin. Invest. 73 (1984)

1576.

[147] C.E. Thomas, L.A. Morehouse, S.D. Aust, J. Biol. Chem. 260 (1985) 3275. [148] S. Puntarulo, A.I. Cederbaum, Biochim. Biophys. Acta 1289 (1996) 238.

[149] M.E. Aliaga, C. Carrasco-Pozo, C. López-Alarcón, C. Olea-Azar, H. Speisky, Bioorg. Med. Chem. 19 (2011) 534.

[150] B.J. Bolann, R.J. Ulvik, Biochem. J. 243 (1987) 55.

RESULTADOS/CONCLUSIONES DEL CAPITULO 2 QUE MOTIVARON EL CAPITULO 3.

En este artículo previo se han puesto de manifiesto las discrepancias sobre los mecanismos de actuación del centro ferroxidasa de la ferritina, haciendo hincapié en cómo la propia función de la ferritina viene regulada por la composición de su cápside proteíca, concretamente en la relación entre subunidades H y L, y se ha pretendido adelantar las implicaciones biológicas que una síntesis "inadecuada" por parte de la célula a la hora de elegir esta combinación de subunidades H y L para la formación de una ferritina funcional podría tener, especialmente a nivel cerebral.

El capítulo 3 pretende ir más allá de la controversia existente entre los diferentes mecanismos de actuación del centro ferroxidasa de la ferritina y hemos querido poner de manifiesto, por primera vez, que la alta actividad ferroxidasa y baja capacidad de almacenamiento de hierro de las ferritinas ricas en subunidades H, tiene implicaciones biológicas en un contexto más amplio que engloba a otras metaloproteínas presentes en la célula. Este enfoque novedoso se ha llevado a cabo estudiando la actividad ferroxidasa y la capacidad de almacenamiento de diferentes ferritinas (con diferente relación H/L) en presencia de metalotioneínas, proteínas de especial interés a nivel neurológico por encargarse de la homeóstasis de otros metales, como cobre y cinc.

Este siguiente capítulo trata en definitiva de abrir un debate sobre las consecuencias de los diferentes mecanismos de actuación de la ferritina en presencia de otras metaloproteínas existentes en su entorno como las metalotioneínas, recreando así un escenario biológico más real y preciso.

UNIVERSITATIS·GRANATENSIS·FUNDATOR·REX·HISPAN·CATHOLICVS·CAROLVS·RO·IMP·SEMPER·AVG

CAPÍTULO 3.

CHEMICALLY AND BIOLOGICALLY HARMLESS VS. HARMFUL FERRITIN/COPPER-METALLOTHIONEIN COUPLES

Fernando Carmona, Daniela Mendoza, Scheghajegh Kord, Michela Asperti, Paolo Arosio, Sílvia Atrian, Mercè Capdevila, Jose M. Dominguez-Vera

Abstract: The simultaneous measurement of the decrease of available Fe^{II} and the increase of available Fe^{III} allowed the analysis of the ferroxidase activity of two distinct apoferritins. Although recombinant human apoferritin (HuFtH) rapidly oxidizes Fe^{II} to Fe^{III}, this is not properly stored in the ferritin cavity, as occurs in horse spleen H/L-apoferritin (HsFt). Fe storage in these apoferritins was also studied in the presence of two Cu-loaded mammalian metallothioneins (MT2 and MT3), a scenario occurring in different brain cell types. For HuFtH, unstored Fe^{III} triggers the oxidation of Cu-MT2 with concomitant Cu^{I} release. In contrast, for HsFt, there is no reaction with Cu-MT2. Similarly, Cu-MT3 does not react during either HuFtH or HsFt Fe reconstitution. Significantly, the combination of ferritin and metallothionein isoforms reported in glia and neuronal cells are precisely those that avoid a harmful release of Fe^{II} and Cu^{I} ions.

Iron is an essential element for organisms but it is highly toxic in excess. It is well known that free Fe^{II} promotes the formation of highly reactive oxygen species capable of causing irreversible cell damage.[1] Organisms have developed chemical machinery based on the ferritin family of proteins to manage the availability of vital, but potentially toxic, free Fe^{II}.[2-4] Thus, every type of tissue must contain an appropriate type of ferritin (Ft) that scavenges for and stores any Fe which is not required for immediate metabolic purposes. Therefore the Fe is rendered non-toxic and yet still available for when it is required by the cell. The structures of many Ft proteins isolated from a wide range of organisms and biological tissues have been determined. The most extensively studied ferritin is that found in horse spleen, traditionally used as a model for mammalian Ft. It consists of a hollow protein shell composed of 24 subunits arranged in cubic symmetry and has a Mr of about 450 kDa. The shell encapsulates an aqueous cavity of 8 nm in diameter, capable of accommodating

thousands of Fe atoms as an Fe^{III} mineral, often described as ferrihydrite, $[Fe^{III}_{10}O_{14}(OH)_2]$. [5]

There are two different types of monomer included in the 24 subunits which compose the Ft shell: the heavy (H) subunits, 178 amino acids and 21 kDa, and the light (L) subunits, 171 aminoacids and 19 kDa, and each have different functionality. Thus, whereas the H monomers play a key role in rapid Fe detoxification, because they contain a catalytic ferroxidase center for Fe^{II} oxidation, the L subunits seem to be associated with Fe nucleation, mineralization and long-term Fe storage in the ferritin cavity.[2] In accordance with this, the H/L ratio in a ferritin shell varies widely in different organisms and different tissues, but it is worth noting that Ft proteins with a combination of H and L subunits are only found in vertebrates. In this subphylum, L-subunit-rich ferritins predominate in Fe storage organs such as the liver and spleen, whereas organs that require Fe detoxification, such as the heart and most brain cells, contain mostly H-rich ferritins. As an example, horse spleen Ft contains about 90% L- and 10% H- subunits. In bacteria, plants and invertebrates, ferritins are exclusively composed of H-like subunits.

To load apoferritin (apoFt), a Ft molecule that does not contain Fe, requires Fe^{II} and not, Fe^{III} as the substrate. In broad terms, it is accepted that Fe^{II} moves through the hydrophilic channels until it finds the ferroxidase center of an H-subunit, here it is catalytically oxidized to Fe^{III} by reaction with cellular O_2. It then moves to the cavity where it is finally stored as a ferrihydrite nanoparticle.[6] The mechanism of the ferroxidase oxidation of Fe^{II} to Fe^{III}, as well as the path of Fe^{III} from the ferroxidase center to the cavity, are currently a point of controversy.[2,6-10] In any case, if any Fe^{III} remains at the ferroxidase center, somehow close to the surface of ferritin, some biomolecules could be able to scavenge it. In fact, Hagen et al. have shown that transferrin, a large protein (80 kDa) that is unable to enter the Ft cavity, scavenges the two Fe^{III} ions of the ferroxidase center.[10] However, in these experiments transferrin just served as an Fe^{III} sensor to confirm the nature of the ferroxidase center and the results have little biological relevance because Ft is basically intracellular, whereas transferrin is the plasma Fe^{III} transport protein.

Considering this background, and with the aims of, (a) gaining further insight

into the biological consequences of ferroxidase center function, and (b) correlating the apoferritin composition resulting Fe^{III} unavailable, we decided to study how Fe^{II} is oxidized by two apoFts with different H/L ratios: recombinant human H-apoFt (HuFtH), a homopolymer of 24 identical H- subunits each with a ferroxidase center, and the commonly studied horse spleen apoFt (HsFt), a heteropolymer formed of approximately 3 H- and 21 L-subunits (L-subunits lack the ferroxidase center). The Fe^{II} to Fe^{III} oxidation activities of HuFtH and HsFt, and their capacities to make the formed Fe^{III} unavailable, were studied by following a very simple protocol. This was based on monitoring the decrease of available Fe^{II}, and the increase of available Fe^{III}, in a batch of 15 fresh samples initially containing Fe^{II} and the respective apoFts in catalytic proportions (approx. 200 Fe^{II}/apoFt). The addition, at different reaction times, of an excess of ferrozine (fz) or apolactoferrin (Lf) serves as an indicator, via measurement of the respective UV-vis absorbances at 562 nm ($[Fe^{II}(fz)_3]^{2+}$) or 464 nm (Fe^{III}-Lf), of the concentration of available Fe^{II} or Fe^{III} at every step of the Ft reconstitution process. The combination of Fe^{II} decrease and Fe^{III} increase availability patterns provides a dynamic picture of the overall Fe uptake process carried out by Ft. Hence, monitoring ($[Fe^{II}(fz)_3]^{2+}$) concentration, i.e., recording the time dependence of A^{562nm} allows evaluation of the capability of each apoFt to oxidize Fe^{II} because the faster is the Fe^{II} oxidation process, the faster is the decrease of the UV-vis absorbance at 562 nm. As shown in Figure 1, the free Fe^{II} concentration decreases in the presence of HsFt (L-rich) to reach a plateau corresponding to a remaining 40% of the initial Fe^{II}, while the decrease of free Fe^{II} in the presence of HuFtH (entirely H-subunits) is significantly higher, so that within a few minutes almost all the initial Fe^{II} is no longer available to react with fz. These results corroborate the idea that the ferroxidase activity of apoFt increases with its H/L ratio, as activity is clearly higher for HuFtH than for HsFt.

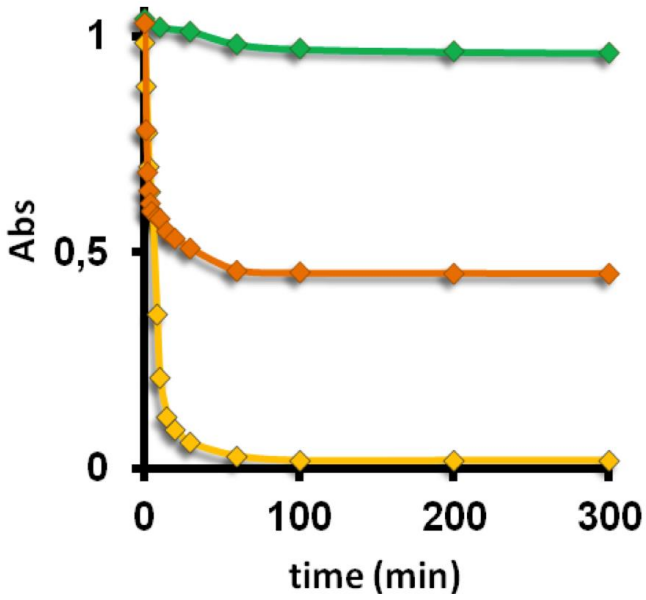

Figure 1. *Fe(II) availability in the presence of two different apoFts: Absorbance at 562 nm, i.e.* $[Fe^{II}(fz)_3]^{2+}$ *concentration, after addition, at different times, of ferrozine to the mixtures HsFt +* Fe^{II} *(orange) and HuFtH +* Fe^{II} *(yellow). Green data correspond to the control (absence of protein). As shown in the control, under our experimental conditions,* Fe^{II} *remains stable in solution at least 300 minutes.*

An analogous batch of experiments was performed but Lf in the presence of bicarbonate was added instead of fz, (see Experimental). Monitoring the UV-vis absorbance of the Fe^{III}-Lf complex at 464 nm provides information about the concentration of available Fe^{III} produced by the Ft reconstitution process. As can be seen in Figure 2, HsFt does not yield any peaks at this wavelength, suggestive of the low availability of Fe^{III} formed by this apoFt, whereas HuFtH gives rise to the development of the UV-vis band at 464 nm typical of Fe^{III}-Lf, and which is independent of the allowed Fe^{II}-HuFtH reaction time. This absorbance correlates with a permanent concentration of 0.16 mM of free Fe^{III}, which corresponds to almost 50% of the Fe^{II} that was allowed to react with HuFtH.

According to previous reports on this subject, we cannot rule out the possibility of a small fraction of the initial Fe^{II} being stabilized in the ferritin cavity and therefore unavailable for fz complexation.[11] However, the rapid increase of

A^{464nm} due to the formation of Fe^{III}-Lf in the presence of HuFtH confirms that for this protein, Fe^{II} is not available for fz complexation because a large proportion of the initial Fe^{II} is actually oxidized to Fe^{III} rather than stabilized within the protein as Fe^{II}. In either case, the presence or absence of a small fraction of stabilized Fe^{II} within the ferritin cavity is neither the focus of this work nor is it crucial for the conclusions which wewill draw, our focus is on the presence/absence of available Fe^{III} during the Ft mineralization process. In this context, our results clearly demonstrate that once Fe^{II} is oxidized by HsFt, the resulting Fe^{III} is in an inaccessible form, probably because these Fe^{III} ions are stored inside the protein cavity and Lf is too large to pass through the Ft channels to bind Fe^{III}. However, although HuFtH oxidizes practically all of the initial Fe^{II}, half of the formed Fe^{III} is available to large biomolecules such as Lf. Furthermore, according to our results and contrasting them with those reported by Hagen et al.,[10] the amount of Fe^{III} complexed by Lf during the Fe reconstitution process of HuFtH is almost double than that corresponding to the number of Fe atoms at the ferroxidase centers (24 x 2 per protein). Here, the protein is present in catalytic quantities, and therefore a large excess of Fe^{II} has been added (a situation that is probably closer to the actual *in vivo* scenario) and so we can conclude that the target of Lf is probably not only the Fe^{III} ions fixed at the ferroxidase centers but also the Fe^{III} cations formed at such centers and which are not really stored by HuFtH within the protein cavity. This protein, therefore, conclusively exhibits high ferroxidase activity but a low Fe storage capacity.

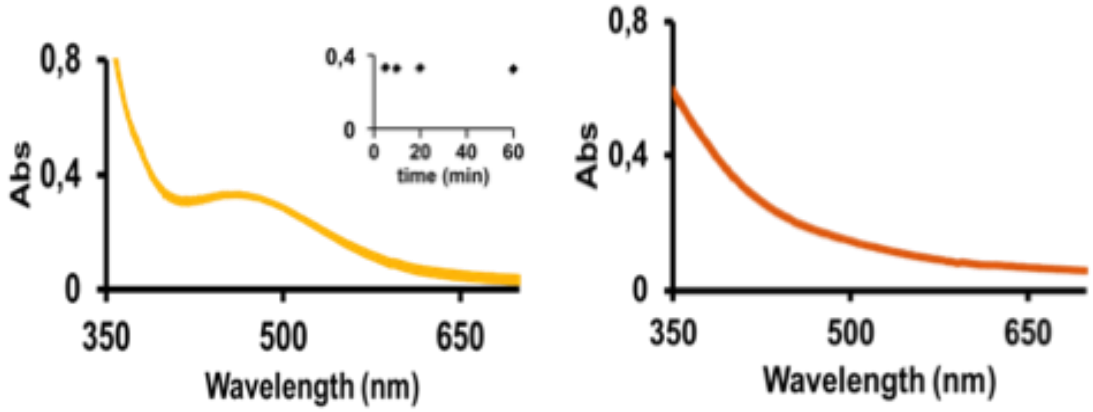

***Figure 2**. Fe^{III} availability after oxidation of Fe^{II} by two different apoFt proteins: UV-vis spectra after addition, at different times, of lactoferrin to the mixtures HuFtH + Fe^{II} (left) and HsFt + Fe^{II} (right). The inset corresponds to the time dependence of the absorbance at 464 nm, i.e. [Fe^{III}-Lf] concentration.*

In contrast, HsFt exhibits low ferroxidase activity but with a high Fe^{III} storage capacity since we did not observe Fe with Lf, thus indicating that although relatively little Fe^{III} is formed, it is genuinely stored within the ferritin cavity (i.e., it is not available for a chelating agent). More interestingly, and in a second stage of this work, we focused on the biological relevance of our results by investigating some of the chemical consequences of the observed Fe^{III} availability during reconstitution of Ft. We tried to go one step further beyond the demonstration that once Fe^{II} has been oxidized at the ferroxidase center of Ft, some Fe^{III} ions can then be scavenged by an Fe^{III} chelator. If, according to the present results and those of Hagen et al.,[10] Fe^{III} produced in the Ft ferroxidase center is available for complexation by a large molecule such as transferrin, it should also be able to act as an oxidant against metallothioneins (MTs).[12] This possibility takes special relevance in view of the Fenton reactivity of $Cu^{I/II}$ ions and the widely assumed presence of Cu-containing MTs in brain cells. Bearing this in mind, we studied the Fe reconstitution of the two different ferritins from our study (HuFtH and HsFt) in the presence of the Cu-loaded forms of two mammalian MT isoforms (MT2 and MT3). MTs are small (6 - 10 kDa) and cysteine rich (33%) metaloproteins. They are naturally found bound to either Zn^{II} and/or Cu^{I} but their biological function is still a matter of debate although they are accepted as

major players in the homeostasis of physiological Zn and Cu.[13,14] We paid particular attention to MT2 and MT3 because the former is predominantly synthesized in astrocytes and microglia, where ferritin is mainly found in the L-rich form, while the latter is a brain-specific isoform constitutively expressed in neurons, where H-rich ferritins are predominant.[15,16] Therefore, the coexistence of certain combinations of Ft and MT (i.e., MT2 with L-rich or MT3 with H-rich ferritins) can be considered to be a direct reflection of the situation encountered in different types of brain cells. In accordance with the Zn-thionein character of MT2[17] and the partial Cu-thionein character of MT3,[18,19] they would constitute mixed Zn, Cu-MT complexes (instead of homonuclear Cu-MT species) when synthesized in the brain, even in the presence of physiologically high Cu concentrations. For this reason we used the metal-MT2 and metal-MT3 preparations that result from the recombinant synthesis of MT2 and MT3 in Cu-supplemented *E. coli* cultures grown under regular aeration,[20] which is the closest approximation to mammalian cell conditions. They yielded a mixture of Zn_1Cu_{10}- and Zn_2Cu_{10}- as major species for MT2[17] and a mixture of Zn_4Cu_6- and Cu_{10}- complexes for MT3[18], which from now on and for the sake of simplicity we shall refer to as the Cu-MT2 and Cu-MT3 complexes.

For these experiments, we prepared a batch of Fe^{II}-apoFt mixtures with HsFt and with HuFtH, and allowed them to react aerobically for 15 minutes. These reaction mixtures were then degassed and saturated with argon prior to the addition of the Cu-loaded forms of MT2 or MT3 with the appropriate chelating agent, either BTA or fz. The Cu^{I} released or the Fe^{II} formed as a result of the oxidation of the Cu-MTs by Fe^{II} could be respectively determined by monitoring the UV-vis absorbance at either 480 nm (Cu^{I}-BTA) or 562 nm ($[Fe^{II}(fz)_3]^{2+}$) with time.

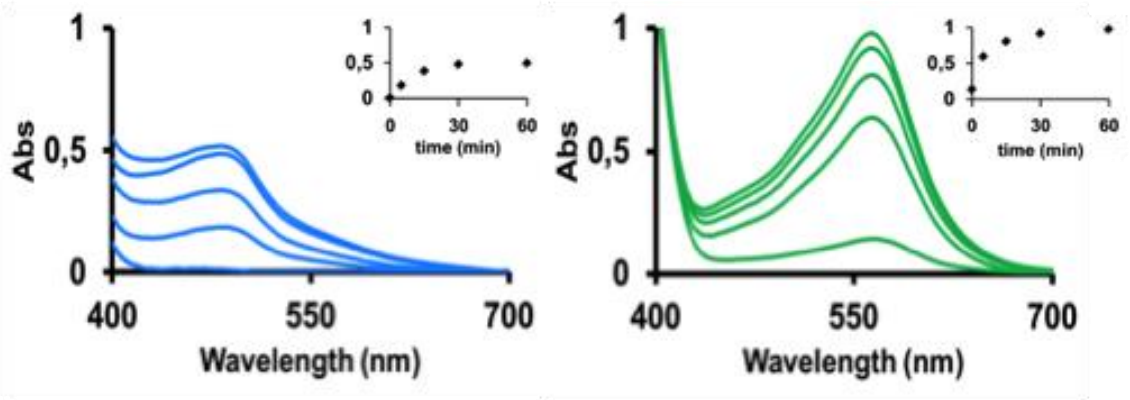

***Figure 3**. UV-vis spectra recorded at different times after the addition of Cu- MT2 + BTA (left) and Cu-MT2 + fz (right) to a mixture of HuFtH + Fe^{II}. Insets correspond to the time dependence of the absorbance at 480 nm (left) and 562 nm (right).*

Based on the initial Cu concentration of the Cu-MT2 sample (41 μM), it can be concluded that almost 90% of Cu was removed from MT2 after 30 min of reaction (35,7 μM final concentration of Cu^{I}-BTA). The same reaction with Cu-MT3 released only 6% of the initially coordinated Cu^{I}. However, the parallel study of HsFt is dramatically different; no absorbance peak developed at 480 nm, highlighting the absence of free Cu^{I} since, in agreement with the high Fe storage capacity of HsFt, there is a very low availability of Fe^{III} in the medium to oxidize either Cu-MT2 or Cu-MT3.

It is therefore reasonable to assume that the Fe^{III} formed after oxidation at the HuFtH ferroxidase center is the agent responsible for oxidizing Cu-MT2 on the basis of three different experiments: (i) The mixtures of HuFtH, Cu-MT2/Cu-MT3 and BTA do not exhibit any significant UV-vis absorption corresponding to Cu^{I}-BTA in the absence of Fe^{II}. This points out that, in the absence of Fe^{II}, neither MT2 nor MT3 are oxidized. (ii) Addition of an Fe^{III} salt, in the same concentration as that generated in the Fe^{II} + HuFtH experiment, to an anaerobic Cu-MT2 solution, but not in one containing Cu-MT3, in the presence of BTA produces Cu^{I}-BTA with a Cu^{I} delivery pattern similar to that of the Fe^{II} + HuFtH + Cu-MT2 experiment (see Experimental). This clearly indicates that Fe^{III} is a powerful oxidant capable of oxidizing the mammalian MT2 isoform in its Cu loaded form, while that of MT3 practically resists this oxidizing environment. (iii) When HuFtH is incubated with Fe^{II} and after 15 min of reaction (once the Fe^{II}

oxidation is almost complete, Figure 1) Cu-MT2 -together with fz- is added to the reaction mixture, the ($[Fe^{II}(fz)_3]^{2+}$) complex forms and its concentration increases with time (Figure 3). This final experiment evidences that after the reduction of the Fe^{II} concentration to almost zero during the Fe reconstitution process of HuFtH, reaction upon addition of Cu-MT2 again raises the Fe^{II} concentration to 59% of the initial value as a consequence of the oxidation of MT2 by Fe^{III}.

In summary, in this paper we demonstrate that part of the Fe^{III} formed at the ferroxidase centers of HuFtH is available, not only for complexation with an Fe^{III} chelator, but also to oxidize Cu-loaded MT2, giving rise to the concomitant release of two toxic metals ions, Cu^{I} and Fe^{II}. The latter reaction does not take place when the apoferritin is a H/L heteropolymer such as HsFt. In this case, all the Fe^{III} formed at the ferroxidase center is unavailable for either Lf complexation or MT oxidation. The chemical scenario we have created is especially significant in the brain, where incorrect Fe uptake by Ft has been suggested to result in the progression of neurological diseases. Hence, Dobson and co-workers proposed that patients with Alzheimer's disease could have a dysfunction in brain Fe storage due to a disruption in the balance of ferritin H- and L- subunit synthesis.[21] In this sense, our results point out that in cells where Cu-MT2 and Ft coexist, there is no danger if the ferritin is L-rich, as it occurs in astrocytes and microglia,[16] and both proteins would preserve their integrity and functionality. However, if this imbalance in L- and H-subunit synthesis leads to the synthesis of pure H apoferritins, and therefore to some events analogous to those we have described here in which the high ferroxidase activity and low Fe storage capacity of a H-rich Ft would provoke Cu^{I} liberation from Cu-MT2, then the presence of two free and toxic metals such as Cu^{I} and Fe^{II}, could produce fatal results for the cell. Interestingly, Cu-MT3 does not react with either HuFtH or HsFt in the presence of Fe^{II} thus making the Cu-MT3 and Ft pair a non-deleterious combination in neurons. This is extremely relevant because in neuron cells Ft is mainly present in H-rich forms,[16] which would lead to a harmful interaction should the predominant MT isoform present be that of MT2. What we wish to underline here is that the process of Fe storage in ferritin affects parallel metal metabolisms depending on the protein shell itself. Following on from that we have shown that an excessive proportion of H-subunits in the ferritin shell

results in a significant decrease in the amount of Fe stored, meaning that there is free Fe^{III} available that is capable of oxidizing Cu-MT2, ultimately leading to the liberation of toxic Fe^{II} and Cu^{I}. As a final conclusion, it is worth highlighting that the current results reconcile the simultaneous presence of ferritins and MT in cells,[12] provided that the correct combination of isoforms is preserved, otherwise metal-related neuronal disorders could be triggered if parting from this ideal combination.

Experimental Section

Materials. Horse spleen apoFt (HsFt) was obtained from Sigma and was exhaustively dialyzed against Milli-Q water using a Spectra/Por Float-A-Lyzer with a molecular weight cut off (MWCO) of 300,000 Da. Recombinant human H-Ft (HuFtH) was prepared as previously described[21,22] and rendered iron free by dialysis against sodium hydrosulfite (dithionite), $Na_2S_2O_4$, and complexation with 2,2'-bipyridyl at pH 6.0[23], to isolate an apoferritin containing 10 Fe/protein. The Cu loaded forms of the mammalian metallothionein isoforms MT2 and MT3 were recombinantly synthesized and characterized (ICP-AES and ESI-MS) as previously reported.[17,18] The final preparations were 0.13 x 10^{-4} M (MT2) and 0.35 x 10^{-4} M (MT3) in 50 mM Tris-HCl, pH 7.5 buffer, and they were deaerated under N_2 flux to avoid the presence of O_2 during the described reactions. Monoferric lactoferrin was purchased from Fonterra. Lf was prepared following the same protocol as reported previously.[24]

Measurement of available Fe^{II}. Batches of 15 fresh solutions for each type of apoferritin, 0.2 μM in 0.15 M HEPES buffer, pH 7.0, and fresh aqueous solutions of $Fe(SO_4)_2(NH_4)\cdot 6H_2O$ (final Fe 0.0353 mM) were mixed. 1 mL of an aqueous ferrozine solution (3-(2-pyridyl)-5,6-diphenyl-1,2,4-triazine-p,p-disulfonic acid monosodium salt hydrate, Aldrich), final concentration 0.935 mM, was added to every sample after 1, 2, 3, 4, 5, 8,10, 15, 20, 30, 60, 100, 200 and 300 min and the UV-visible spectra immediately recorded. Available Fe^{II} concentration was calculated for every sample in the batch from the UV-vis absorbance measured at 562 nm, due to formation of the ($[Fe^{II}(fz)_3]^{2+}$) complex (ε = 27,900 $M^{-1}cm^{-1}$).

Measurement of available Fe^{III}. A batch of four fresh solutions of each apoferritin, 0.2 μM in 0.15 M HEPES buffer containing 10 mM of $NaHCO_3$, pH 7.0, and fresh aqueous solutions of $Fe(SO_4)_2(NH_4)\cdot 6H_2O$ (final Fe 0.353 mM) were mixed. 200 μL of an aqueous solution of Lf (final concentration 200 μM) was added to every sample after 5, 10, 20 and 60 min and the UV-vis spectra recorded. Available Fe^{III} concentration was calculated for every sample of the batch from the UV-vis absorbance measured at 464 nm, due to formation of the $[Fe^{III}(Lf)]$ complex (ε = 2,600 $M^{-1}cm^{-1}$).

Measurement of Cu^{I} during ferritin reconstitution in the presence of Cu-MT. In a parallel experiment, HuFtH and HsFt (0.2 μM) in 0.15 M HEPES buffer, pH 7.0, were incubated with aqueous solutions of $Fe(SO_4)_2(NH_4)\cdot 6H_2O$ (final [Fe] 0.035 mM) at 37 ºC and in aerobic conditions for 15 min. The reaction mixture was then totally deoxygenated under nitrogen flux and kept under an anaerobic atmosphere prior to the addition of Cu-MT2 (100 μL, 5.2 μM, [Cu] 41 μM) or Cu-MT3 (100 μL, 4.7 μM, 40 μM). Then, 10 μL of 0.4 mM BTA (bathocuproinedisulfonic acid disodium salt) was added to the mixture in order to detect Cu^{I} by observation of the UV-vis band at 480 nm due to formation of the $[Cu^{I}(BTA)_2]^{+}$ complex (ε = 14,000 $M^{-1}cm^{-1}$). The same experiments carried out in the absence of Fe^{II} did not produce an absorbance peak at 480 nm for the UV-vis spectra of $[Cu^{I}(BTA)_2]^{+}$.

Measurement of Fe^{III} reduction to Fe^{II} during HuFtH ferritin reconstitution in the presence of Cu-MT2. The previous protocol was followed but using ferrozine instead of BTA as a chelating agent for the purposes of measuring the Fe^{II} concentration. We noted that after 15 min of Fe^{II} reconstitution by HuFtH, the Fe^{II} concentration had dramatically decreased (Figure 1). Therefore the increase of Fe^{II} concentration in this experiment corresponds to the oxidation of Cu-MT2 by Fe^{III} with the subsequent formation of Fe^{II}, which is ultimately detected and quantified by its complexation with fz.

Oxidation of Cu-MT by Fe^{III}. In a parallel experiment, Cu-MT2 (100 μL, 3 μM) and Cu-MT3 (100 μL, 3 μM) were incubated at 37 ºC in a degassed aqueous solution of Fe^{III} acetate (0.02 mM) under Ar. BTA or fz was added to detect and quantify the Cu^{I} or Fe^{II} concentrations.

Acknowledgements

Work supported by the Spanish MINECO and FEDER funds with grants CTQ2012-32236 to J.M. Domínguez-Vera, BIO2012-39682-C02-01 to S. Atrian, and BIO2012-39682-C02-02 to M. Capdevila. The authors from the Barcelona universities are members of the Grup de Recerca de la Generalitat de Catalunya refs. 214SGR-00423. F. C. is grateful to the Spanish MINECO for a FPI Fellowship. We thank the Centres Científics i Tecnològics (CCiT) of the Universitat de Barcelona (ICP-AES) and the Servei d'Anàlisi Química (SAQ) of the Universitat Autònoma de Barcelona (ESI-MS) for allocating instrument time. S. Artime, working at S. Atrian's laboratory, was responsible for the recombinant syntheses of the Cu-MT preparations.

Keywords: Ferritin • Metallothionein • Ferroxidase activity • Fe metabolism

References

[1] a) K. Jomova, M. Valko, *Curr. Pharm. Des.* **2011,** 17, 3460-3473. b) H. Heli, S. Mirtorabi, K. Karimian, *Expert Opinion on Therapeutic Patents* **2011**,21, 819.

[2] a) E. C. Theil, *Curr. Opin. Chem. Biol.* **2011,** 15, 304-311; b) X. F. Liu, E. C.Theil, *Acc. Chem. Res.* **2005**, 38, 167-175.

[3] F. Bou-Abdallah, *Biochim. Biophys. Acta* **2010**, 1800, 719-731.

[4] F. Carmona, O. Palacios, N. Gálvez, R. Cuesta, S. Atrian, M. Capdevila, J. M. Domínguez-Vera, *Coord. Chem. Rev.* **2013,** *257*, 2752– 2764.

[5] N. D. Chasteen, P. M. Harrison, *J. Struct. Biol*. **1999,** *126*, 182-194.

[6] J. M. Bradley, G. R. Moore, N. E. Le Brun, *J. Biol. Inorg. Chem*. **2014**, DOI

10.1007/soo775-014-1136-3 and references therein.

[7] X. Liu, E. C. Theil, *Proc. Natl. Acad. Sci. U.S.A*. **2004**, *101*, 8557–8562.

[8] P . Arosio, R. Ingrassia, P. Cavadini, *Biochim. Biophys. Acta,* **2009,** *1790*, 589–599.

[9] F. Bou-Abdallah, G. Zhao, H. R. Mayne, P. Arosio, N. D. Chasteen, *J. Am. Chem. Soc*. **2005,** *127*, 3885–3893.

[10] H. K. Ebrahimi, E. Bill, P. L. Hagedoorn, W. R. Hagen, *Nat. Chem. Biol.* **2012,** *8*, 941–948.

[11] J. S. Rohrer, R. B. Frankel, G. C. Papaefthymiou, E. C. Theil, *Inorg. Chem.* **1989**, *28*, 3393-3395.

[12] R. Orihuela, B. Fernández, Ò. Palacios, E. Valero, S. Atrian, R. K. Watt, J. M. Domínguez-Vera, M. Capdevila, *Chem. Commun*. **2011**, *47*, 12155-12157.

[13] M. Capdevila, R. Bofill, Ò.Palacios, S. Atrian, *Coord. Chem. Rev.* **2012**, *256*, 46–52.

[14] Ò. Palacios, S. Atrian, M. Capdevila, *J. Biol. Inorg. Chem.* **2011**;*16*, 991–1009.

[15] B. A. Masters, C. J. Quaife, J. C. Erickson, E. J. Kelly, G.J. Froelick, B.P. Zambrowicz, R.L. Brinster, R.D. Palmiter, *J. Neurosci.* **1994**, *14*, 5844-5857.

[16] P. Ponka, C. Beaumont, D. Richardson, *Semin. Hematol.* 1998, *35*, 35.

[17] E. Artells, Ò. Palacios, M. Capdevila, S. Atrian, *Metallomics* **2013**, *5*, 1397-1410.

[18] E. Artells, Ò. Palacios, M. Capdevila, S. Atrian, *FEBS J* **2014**, *281*, 1659-1678.

[19] G. Meloni, V. Sonois, T. Delaine, L. Guilloreau, A. Gillet, J. Teissié, P. Faller, M. Vašák, *Nat Chem Biol*. **2008**, *4*; 366-372.

[20] A. Pagani, L. Villarreal, M. Capdevila, S. Atrian, *Mol. Microbiol.* **2007**, *63*, 256-269.

[21] Q. Q. Pankhursta, D. Hautotb, N. Khanc, J. Dobson, *J. Alzheimers Dis*. **2008**, *13*, 49-Pagina final.

[22] P. Santambrogio, A. Cozzi, S. Levi, E. Rovida, F. Magni, A. Albertini, P. Arosio, *Protein Expression Purification* **2000**, *19*, 212–218.

[23] E. R. Bauminger, P. M. Harrison, D. Hechel, I. Nowik, A. Treffry, *Biochim. Biophys. Acta,* **1991,** *1118*, 48–58.

[24] F. Carmona, V. Muñoz-Robles, R. Cuesta, N. Gálvez, M. Capdevila, J-D. Maréchal, J. M. Dominguez-Vera, *J. Biol. Inorg. Chem.* **2014**, *19*, 439–447.

RESULTADOS/CONCLUSIONES DEL CAPITULO 3 QUE MOTIVARON EL CAPITULO 4.

Los resultados del capítulo anterior ponen de manifiesto que las ferritinas H tienen alta actividad ferroxidasa pero baja capacidad de almacenar hierro. Este hecho adquiere especial importancia en la leche materna, donde la ferritina es predominantemente H y existen elevadas concentraciones de lactoferrina, proteína encargada de captar Fe(III) para privar a los microorganismo patógenos de este metal esencial y evitar así su proliferación.

En el siguiente capítulo, la existencia de este "tándem" lactoferrina – ferritina H en leche materna nos inspiró para llevar a cabo la preparación de materiales formados por ambas proteínas que combinaran de manera sinérgica las funciones de éstas, es decir, un alto poder detoxificante de Fe(II) por parte de la ferritina H y una rápida incorporación del Fe(III) generado en la lactoferrina, actuando estos materiales como secuestradores de hierro en cualquiera de sus estados de oxidación, llevando a cabo por tanto una acción antimicrobiana completa.

La bibliografía contiene ejemplos de materiales y moléculas discretas capaces de actuar como antimicrobianos, todos ellos basados en la captación de Fe(III). En este trabajo desarrollamos un material, inspirado en cómo funcionan las proteínas ferritina H y lactoferrina, para secuestrar cualquier forma de hierro y poder llevar a cabo una acción antimicrobiana más integral.

CAROLVS·RO·IMP·SEMPER·AVG·HISPAN·REX·FUNDATOR·UNIVERSITATIS·GRANATENSIS

CAPÍTULO 4.

A BIOINSPIRED HYBRID SILICA-PROTEIN MATERIAL WITH ANTIMICROBIAL ACTIVITY BY IRON UPTAKE

Fernando Carmona, Daniela Mendoza, Alicia Megía Fernández ,Francisco Santoyo-Gonzalez and José M. Domínguez-Vera

Abstract. A silica–protein hybrid material has been prepared by simultaneous covalent deposition of apoferritin and lactoferrin on functionalized silica. This material exhibits strong antibacterial activity against E. coli due to its high iron-uptake capacity.

As bacteria are able to infect almost all tissues in the human body, they cause a spectrum of illnesses ranging from common skin infections to severe and fatal diseases. Indeed, bacterial infection is one of the leading causes of death in the world. Furthermore, some bacteria have developed aremarkable ability to resist currently available antimicrobials, thus highlighting the need for the development of new antimicrobial agents. A promising strategy in this respect involves inhibiting their ability to obtain the nutrients required for growth.[1] An effective route to combat bacterial infection is to create materials that can compete with bacteria for iron, thereby depriving them of this metal, which they need to proliferate. However, such a route must be more efficient in terms of iron uptake than siderophores, low-molecular-weight iron chelators that are produced and exported by bacteria during periods of nutrient deprivation.[2] A good alternative to the creation of new materials for this purpose is to mimic existing and efficient biological systems. Animals closely regulate iron levels[3] and sequester this nutrient as a mechanism of preventing bacterial proliferation. Two kinds of proteins, namely transferrins (including lactoferrin), which are glycoproteins that remove extracellular Fe(III) due to their high Fe(III) affinity,[4,5] and ferritin, which stores the iron that is not required for immediate metabolic purposes, play a crucial role in this mechanism.[6,7]

Lactoferrin is considered to be one of the key components of the immune system, partly due to its high affinity for Fe(III),[8,9] and ferritin consists of a spherical protein shell (apoferritin) surrounding an aqueous cavity that incorporates Fe(II), which is oxidized during its journey to the cavity to form a Fe(III) mineral core

therein.[6,7] The apoferritin shell is assembled from 24 polypeptide chains of two types, namely heavy (H) (21 kDa) and light (L) subunits (19 kDa). It has traditionally been thought that H-subunits play a key role in Fe(II) oxidation as they contain catalytic ferroxidase centres, whereas L-subunits are associated with Fe(III) nucleation.[6] However, it is interesting to note that pure L ferritin has not been found in iron storage organs. All known ferritins always contain at least a small amount of H subunits (10% in the liver, for example). As such, it seems that the iron uptake and storage process requires the oxidative activity of at least a small number of H subunits. Nevertheless, pure or H-rich ferritin is frequently found in humans, especially in breast milk, the heart or serum, probably due to its strong ferroxidase activity, which helps to protect against toxic Fe(II).[10]

In light of these findings, we considered that H-apoferritin and lactoferrin could be an effective combination for iron uptake. Interestingly, breast milk contains both lactoferrin and apoferritin, the latter of which is an H-rich or H-pure apoferritin.[10] As a result, we supposed that a material capable of confining both H-apoferritin and lactoferrin could constitute an effective system for Fe(II) uptake as Fe(II) would be oxidized by apoferritin to Fe(III), some of which would be stored in its cavity, with the remainder, and any available Fe(III), being captured by lactoferrin. In this sense, it is interesting to note that most previous iron uptake strategies based on molecular recognition technologies[11] involve solids containing immobilized molecules with a well-known affinity for Fe(III), such as desferrioxamine,[12] 3-hydro-xypyridin-4-ones,[13] or EDTA derivatives.[14] Despite the fact that free Fe(II) is markedly more dangerous than Fe(III) as it catalyses the production of reactive oxygen species, which are extremely powerful oxidizing agents that are capable of causing extensive cell damage, no hybrid solids with iron(II) molecules have been reported.

The aim of this work was therefore to create new materials containing both apoferritin (especially H pure) and lactoferrin to remove iron from the media, thus depriving pathological microorganisms of this metal. To achieve this goal, we decided to use a vinyl sulfone silica functionalized with both proteins in a step-by-step manner. The resulting hybrid silica–protein material spatially confines both proteins and mimics breast milk to some extent, thus making it potentially useful as an antimicrobial agent due to the cooperative effect of the apoferritin–

lactoferrin combination for iron uptake.

The functionalization of silica with vinyl sulfone commences with the silanization of commercial silica followed by the Michael-type addition of a bis-vinyl sulfone. This process gives rise to a functionalized silica containing available vinyl sulfone groups to which different biomolecules can be covalently attached (ESI 1).[15]

We initially analysed the reactivity of each protein with the vinyl sulfone silica. Under similar conditions, the two apoferritins studied [horse spleen (HSFt) and H-recombinant (HFt)] showed a higher reactivity than lactoferrin, therefore we first carried out the immobilization of a default apoferritin followed, in a second step, by an excess of lactoferrin (Scheme 1). Both protein immobilizations were performed by incubating the aforementioned proteins with the vinyl sulfone silica in phosphate buffer at pH 7.5.‡ After 24 h of incubation with apoferritin, the resulting solid was exhaustively washed with buffer (1 M NaCl) to remove the non-covalently immobilized apoferritin. UV-visible spectroscopic analysis of the wash solution showed practically no signal for both HSFt and HFt, thus confirming that almost all the apoferritin had bound covalently to the vinyl sulfone and that negligible amounts of protein were retained by non-covalent interactions (Fig. 1). Once the silica–apoferritin material had been isolated, it was incubated with an excess of lactoferrin and, after 24 h, the solid containing both proteins (silica–Ft + Lf hereafter) was rinsed and dried at room temperature.

scheme 1

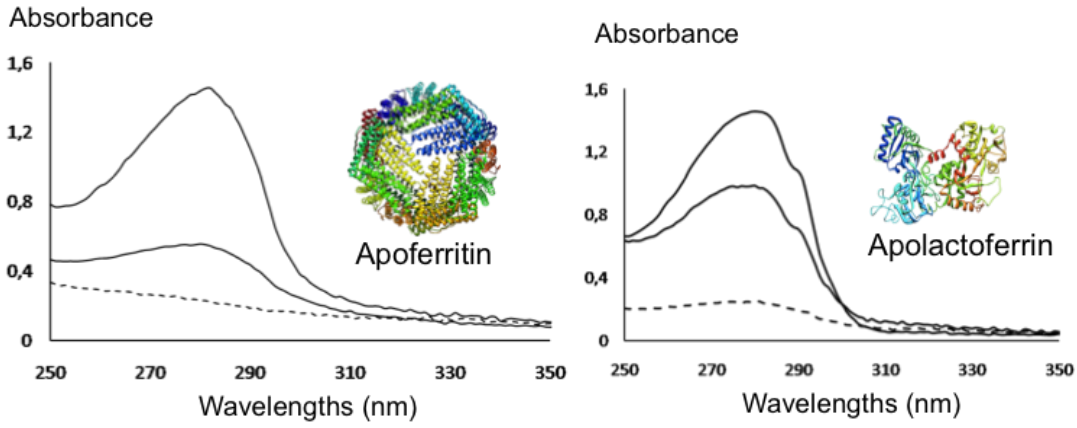

Fig 1. *UV-visible spectra of proteins (H-apoferritin and lactoferrin) before and after incubation with silica (left) and silica–apoferritin (right). Dashed lines correspond to the spectra of the wash solution (non-covalent bound protein).*

From the difference in the absorbance values of both protein solutions at 280 nm before and after incubation with vinyl sulfone silica, and after subtracting the small amount of protein removed upon washing the solid (Fig. 1), values of 33.0 mg (for apoferritin) and 4.6 mg per gram of vinyl sulfone silica (for lactoferrin) were obtained. Note that the absorbance at 280 nm for the solution obtained after washing the silica–HFt + Lf material is minimal. Furthermore, if this solution is mixed with the supernatant solution and dialyzed using a molecular weight cut-off of 100 kDa (larger than the molecular weight of lactoferrin), no absorbance at 280 nm is observed at all, thus confirming that apoferritin is not displaced by the covalent attachment of lactoferrin and that both proteins are definitely fixed to the silica.

Once isolated, the hybrid silica–Ft + Lf materials were incubated with an Fe(II) solution (5 mL, 10 mM) and, after 6 h, the resulting solids centrifuged and washed twice with buffer and 1 M NaCl. The supernatant and wash solutions were mixed and the iron concentration measured by ICP to quantify the iron removal efficacy of the silica–Ft + Lf (silica–HSFt + Lf and silica–Ft + Lf). The results are shown in Table 1 along with values for control samples, functionalized vinyl sulfone silica and silica containing only one protein, either HSFt or Lf.

The best values were obtained with recombinant H-apoferritin and lactoferrin supported on the functionalized silica, which agrees with the expected existence of a cooperative effect of both proteins that leads to a very efficient iron uptake. This effect is lower in the silica–HSFt + Lf material as a result of the lower ferroxidase activity of horse spleen apoferritin with respect to H-pure apoferritin (silica–HFt + Lf). Likewise, it is interesting to highlight the low iron removal efficiency of the silica containing only lactoferrin (silica–Lf), which exhibits a similar yield to the silica containing no protein (silica). This is probably due to the high affinity of lactoferrin for Fe(III) but not for Fe(II). However, in the presence of a protein with ferroxidase activity, such as apoferritin, which oxidizes Fe(II) to Fe(III), lactoferrin multiplies its effectiveness and ultimately makes the apoferritin–lactoferrin combination the best option for iron uptake, especially if the apoferritin exhibits a high ferroxidase activity, as is the case for H-recombinant apoferritin.

In light of these promising results, we decided to check the antimicrobial activity of the silica–HFt + Lf material against *E. coli*. The antimicrobial activity of lactoferrin against *E. coli* has been reported both in solution[16] or immobilized on the surface of a copolymer.[17] However, the antimicrobial activity of our hybrid materials is based on the cooperative effect of two proteins: first by uptake and oxidation of Fe(II) (apoferritin) and ultimately the uptake of Fe(III) (apoferritin + lactoferrin). Our hybrid materials are therefore designed to act as antibacterial agents due to their ability to sequester Fe(II), the most toxic form of iron.

Table 1 Iron removed by the hybrid materials

Material	%Fe removed
Silica–HFt + Lf	96 ± 6
Silica–Ft + Lf	76 ± 7
Silica–HFt	65 ± 9
Silica–Lf	15 ± 5
Silica	12 ± 4

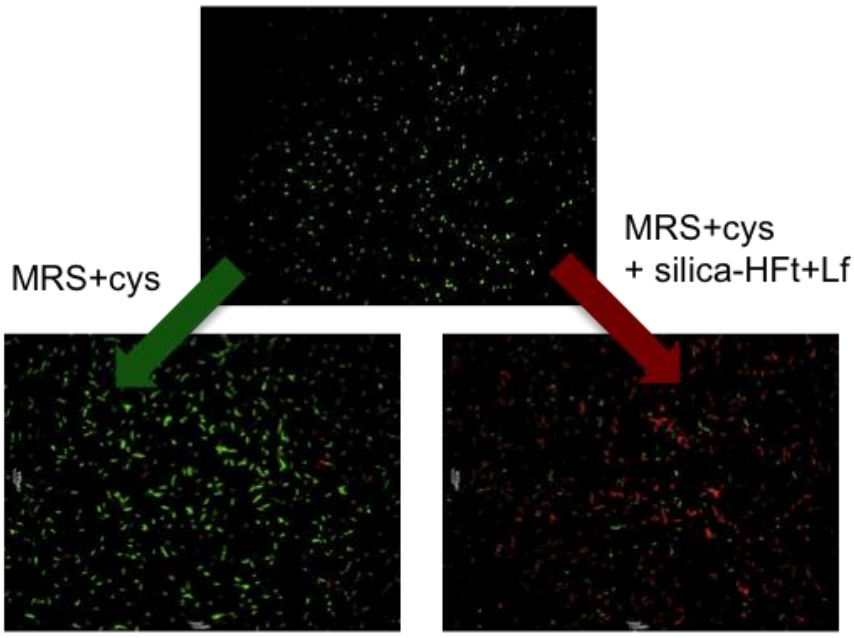

Fig 2. *Fluorescence microscopy images of E. coli proliferation obtained using a Live/Dead Bacterial Viability Kit, where live and dead bacteria exhibit green and red emissions, respectively. Silica–HFt + Lf dramatically inhibits bacterial viability.*

Bacterial inhibition by silica–HFt + Lf was quantified using the Live/Dead Bacterial Viability Kit, counting the number of live (green) and dead (red) bacteria by fluorescence microscopy.‡ The average live/dead ratio (viability v) was used to quantify the bacterial inhibition effect of the hybrid silica–protein material in comparison with control experiments. As can be seen from Fig. 2, the silica–HFt + Lf material dramatically decreases the bacterial viability in MRS + cys (viability v = 0.9), a medium where these bacteria proliferate adequately (viability control v = 60.5).

Interestingly, the silica–Lf material, which only contains lactoferrin and removes small amounts of iron (Table 1), did not significantly inhibit bacterial viability (v = 54.5). Likewise, in agreement with its higher iron uptake ability (Table 1), silica–HSFt inhibits more strongly than silica–Lf (v = 24.1) but is markedly less effective as an antibacterial agent than the silica material containing both proteins (silica–HFt + Lf, viability v = 0.9).

These results demonstrate the antibacterial activity of this novel hybrid silica–HFt + Lf material and confirm that the mechanism of antibacterial activity of this hybrid solid lies in the synergistic action of H apoferritin and lactoferrin for iron uptake.

Conclusions

The results of this study confirm our initial bio-inspired hypothesis that the confinement of apoferritin and lactoferrin supported on a material such as silica is a useful route for iron(II) uptake and therefore for use as an antimicrobial agent. A high antibacterial activity has been demonstrated against *E. coli* K-12, especially when using the silica containing both H-recombinant apoferritin and lactoferrin. Likewise, the correlation between bacterial inhibition and iron uptake confirms that the antimicrobial activity of these materials resides in their iron uptake capacity. Finally, we are convinced that this kind of material may find use as the active ingredient in creams or topical drugs for the treatment of microbial infections in cosmetics and personal hygiene.

This work was supported by MINECO and FEDER (project CTQ2009-09344), Junta de Andalucía (project P07-FQM-02899) and BIOSEARCH SA (contract PostBIO).

Materials and methods

‡ The vinyl sulfone silica[15] (ESI) (100 mg) was incubated with stirring with the protein (2.5 mL, 0.01875 mM) in phosphate buffer at pH 7.5 at 4 ºC. After 24 h, the mixture was centrifuged at 10000 rpm for 10 min at 20 ºC. The solid was washed with buffer containing 1 M NaCl. Both supernatant solutions, from the first centrifugation and washed solid, were mixed and the protein concentration measured by the absorbance at 280 nm (ε^{280}_{HS} = 33 900 and ε^{280}_{HFt} = 27 900 $M^{-1}cm^{-1}$) in the UV-visible spectrum. From the difference in the absorbance values at 280 nm in the initial protein solution and the mixture of supernatant solutions (after centrifugation and after washing), values of 33.0 mg for apoferritin, and 4.6 mg for apolactoferrin per gram of vinyl sulfone silica were obtained.

Preparation of vinyl sulfone functionalized silica–lactoferrin + apoferritin (silica–HFt + Lf and silica–HSFt + Lf): the vinyl sulfone silica (100 mg) was incubated with stirring with apoferritin (HSFt or HFt) (2.5 mL, 0.01 mM) in phosphate buffer at pH 7.5 at 4 ºC. After 24 h, the mixture was centrifuged at 10000 rpm for 10 min at 20 ºC. The solid was washed with buffer containing 1 M NaCl. The resulting solid (silica–Ft or silica–HFt) was incubated with stirring with apolactoferrin (2.5 mL, 0.05 mM) in phosphate buffer at pH 7.5 at 4 ºC. After 24 h, the mixture was centrifuged at 10000 rpm for 10 min at 20 ºC. The solid was washed with buffer containing 1 M NaCl and dried at room temperature. Iron uptake by the hybrid silica–protein materials: the silica–protein (500 mg) was incubated with a solution of $Fe(NH_4)_2(SO_4)_26H_2O$ *(5 mL, 10 mM) for 6 h without stirring and then centrifuged at 10000 rpm for 10 min at 20 ºC. The solid was washed with a 1 M NaCl solution. The supernatant solution from the centrifugation and the washed solution were mixed and the iron concentration measured by Inductive Coupled Plasma. From the ratio between final and initial iron concentration, the yield of iron removal was obtained for each sample (Table 1).*

Inhibition of E. coli K-12: a bacteria culture (400 mL of $1 \cdot 10^7$ *CFU) in MRS + cys was subjected to the hybrid material (100 mg) for 16 h. Quantification of bacterial proliferation was performed by using the Live/Dead Bacterial Viability Kits SYTO9 (green) and propidium iodide (red) (Invitrogen), counting the number of live (green) and dead (red) bacteria in a batch of three experiments using the Image-Pro Plus 6.0 software. The average live/dead ratio (viability v) was used to quantify the effect of the hybrid material on bacterial inhibition by comparing with control experiments where no silica–protein material was present. The presence of silica–HFt + Lf resulted in a decrease in viability to 0.9 with respect to control experiments where the viability was 60.5. Values of 24.1 and 54.5 were obtained for silica–HFt and silica–Lf, respectively.*

Electronic Supplementary Information (ESI)

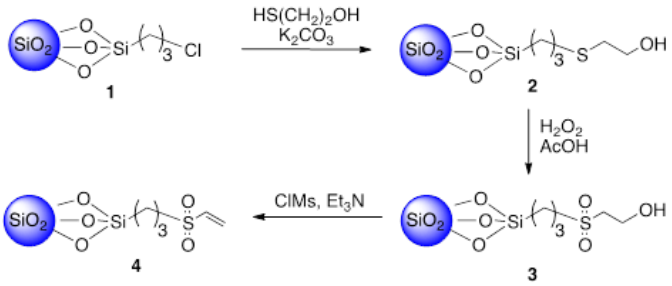

Scheme SI1*. Synthetic route for the preparation of the vinyl sulfone silica.*

Preparation of mercaptoethanol functionalized silica 2 (Scheme 1). Chloro functionalized silica 1 (5.0 g) was suspended in acetonitrile (40 mL) and then 2-mercaptoethanol (3.5 mL) and potassium carbonate (6.9 g) were added. The magnetically stirred suspension was heated at 50 ºC under an Ar atmosphere for 8 h. The reaction mixture was filtered and the white powder washed with hot water (2 x 20 mL) and finally with acetone (2 x 20 mL) and dried under vacuum (1mmHg) at 50 ºC for 16 h giving the mercaptoethanol functionalized silica 2 (4.2 g).

Preparation of ethanol sulfone functionalized silica 3 (Scheme 1). Mercaptoethanol functionalized silica 2 (3.0 g) was suspended in acetic acid (6.0 mL) and then hydrogen peroxide 33% (15.0 mL) was added. The magnetically stirred reaction mixture was kept at room temperature for 24 h in the absence of light. After filtration, the white powder was washed with water (2 x 20 mL), methanol (2 x 20 mL) and finally acetone (2 x 20 mL), and dried under vacuum (1 mmHg) at 50 ºC for 16 h giving the ethanol sulfone functionalized silica 3 (2.9 g)

Preparation of vinyl sulfone functionalized silica 4 (Scheme 1). Ethanol sulfone functionalized silica 3 (2.5 g) was suspended in anhydrous dichloromethane (40 mL). The magnetically stirred suspension was cooled at 0 ºC by means of an ice bath. Methanesulfonyl chloride (0.9 mL) and triethylamine (3.5 ml) were then added. After the addition of the reagents, the reaction mixture was kept at room temperature for 7 h and then filtered. The white powder was washed with methanol (2 x 20 mL) and acetone (2 x 20 mL), and dried under vacuum (1mm Hg) at 50 ºC for 16 h giving the vinyl sulfone functionalized silica 4 (2.4 g).

Proteins. Recombinant H apoferritins were obtained from Molirom and was exhaustively dialyzed against milli-Q water using a Spectra/Por Float-A-Lyzer with a molecular weight cut-off (MWCO) of 300.000 Da. Horse spleen apoferritin and human apolactoferrin were purchased from Sigma and used as received.

References

1 J. J. Bullen, H. J. Rogers, P. B. Spalding and C. G. Ward, FEMS Immunol. Med. Microbiol., 2005, 43, 325–330.

2 E. D. Weinberg, Metallomics, 2010, 2, 732–740. 3 T. Zheng and E. M. Nolan, Metallomics, 2012, 4, 866–880.

4 H. J. Vogel, Biochem. Cell Biol., 2012, 90, 233–244.

5 E. N. Baker and H. M. Baker, Cell. Mol. Life Sci., 2005, 62, 2531–2539.

6 E. C. Theil, Curr. Opin. Chem. Biol., 2011, 15, 304–311; E. C. Theil, R. K. Beheraa and T. Takehiko, Coord. Chem. Rev., 2012, 257, 579–586.

7 N. E. Le Brun, A. Crow, M. E. P. Murphy, A. G. Mauk and G. R. Moore, Biochim. Biophys. Acta, 2010, 1800, 732–744; A. Lewin, G. R. Moore and N. E. Le Brun, Dalton Trans., 2005, 3597–3610.

8 R. D. Baynes and W. R. Bezwoda, Adv. Exp. Med. Biol., 1994, 357, 133–141.

9 D. Legrand, Biochem. Cell Biol., 2012, 90, 252–268.

10 P. Arosio, A. Ponzone, R. Ferrero, I. Renoldi and S. Levi, Clin. Chim. Acta, 1986, 161, 201–208.

11 H. Hiroshi, I. M. M. Rahman, K. Sanae, M. Teruya and F. Yoshiaki, Chemosphere, 2011, 82, 1161–1167.

12 N. A. A. Rossi, M. Ibrahim, J. K. Jackson, H. M. Burt, S. A. Horte, M. D. Scotta and J. N. Kizhakkedathua, Biomaterials, 2009, 30, 638–648.

13 J. Golenser, A. Domb, D. Teomim, A. Tsafack, O. Nisim, P. Ponka, W. Eling and Z. I. Cabantchik, J. Pharmacol. Exp. Ther., 1997, 281, 1127–1135.

14 F. Tian, E. A. Decker and J. M. Goddard, J. Agric. Food Chem., 2012, 60, 2046–2052.

15 M. Ortega-MuÑoz, J. Morales-Sanfrutos, A. Megia-Fernandez, F. J. Lopez-Jaramillo, F. Hernandez-Mateo and F. Santoyo-Gonzalez, J. Mater. Chem., 2010, 20, 7189–7196.

16 Y. Chih-Ching, C.-J. Shen, W.-H. Hsu, Y.-H. Chang, H.-T. Li, H.-L. Chen and C.-M. Chen, Biometals, 2011, 24, 585–594.

17 A. Oyane, Y. Yokoyama, M. Uchida and A. Ito, Biomaterials, 2006, 27, 3295–3303.

RESULTADOS/CONCLUSIONES DEL CAPITULO 4 QUE MOTIVARON EL CAPITULO 5.

En el capítulo siguiente, exploraremos una vía que nos permita entender cómo, al mismo tiempo que nuestro organismo priva de hierro a microorganismos infecciosos, existen bacterias probióticas beneficiosas capaces de captar hierro a expensas del "host" donde proliferan. En particular hemos demostrado, mediante una nueva metodología, que la lactoferrina no sólo no tiene acción bacteriostática frente a estas bacterias beneficiosas sino que además promueve su proliferación actuando como dadora de hierro, justo al contrario de su papel ante microorganismos patógenos.

Concretamente, hemos podido usar el fenómeno de FRET para demostrar que la lactoferrina cede hierro a bacterias probióticas y que además lo hace sin ser internalizada en la bacteria, a diferencia del mecanismo generalizado en el que las proteínas transportadoras de hierro, como la transferrina, ceden hierro a las células a través de su internalización.

CAPÍTULO 5.

MONITORING LACTOFERRIN IRON LEVELS BY FLUORESCENCE RESONANCE ENERGY TRANSFER: A COMBINED CHEMICAL AND COMPUTATIONAL STUDY

Fernando Carmona, Víctor Muñoz-Robles, Rafael Cuesta, Natividad Gálvez, Mercè Capdevila, Jean-Didier Maréchal, José M. Dominguez-Vera

Abstract. Three forms of lactoferrin (Lf) that differed in their levels of iron loading (Lf, LfFe, and $LfFe_2$) were simultaneously labeled with the fluorophores AF350 and AF430. All three resulting fluorescent lactoferrins exhibited fluorescence resonance energy transfer (FRET), but they all presented different FRET patterns. Whereas only partial FRET was observed for Lf and LfFe, practically complete FRET was seen for the holo form ($LfFe_2$). For each form of metal-loaded lactoferrin, the AF350–AF430 distance varied depending on the protein conformation, which in turn depended on the level of iron loading. Thus, the FRET patterns of these lactoferrins were found to correlate with their iron loading levels. In order to gain greater insight into the number of fluorophores and the different FRET patterns observed (i.e., their iron levels), a computational analysis was performed. The results highlighted a number of lysines that have the greatest influence on the FRET profile. Moreover, despite the lack of an X-ray structure for any LfFe species, our study also showed that this species presents modified subdomain organization of the N-lobe, which narrows its iron-binding site. Complete domain rearrangement occurs during the LfFe to $LfFe_2$ transition. Finally, as an example of the possible applications of the results of this study, we made use of the FRET fingerprints of these fluorescent lactoferrins to monitor the interaction of lactoferrin with a healthy bacterium, namely *Bifidobacterium breve*. This latter study demonstrated that lactoferrin supplies iron to this bacterium, and suggested that this process occurs with no protein internalization.

Keywords: Lactoferrin, Iron metabolism, Protein–ligand docking, FRET, Structural analysis

Introduction

Lactoferrin is a glycoprotein (80 kDa) of the transferrin family with a high affinity for iron(III) [1, 2]. Lactoferrin possesses various biological functions, including antibacterial, antiviral, and antiparasitic activities [3]. High lactoferrin levels are found in colostrum and milk, and this protein is also present in most mucosal secretions, including uterine fluid, vaginal, and nasal secretions, as well as in tears [4, 5].

The extraordinary affinity of lactoferrin for iron undoubtedly determines part of its functionality. Indeed, lactoferrin is considered to form part of the innate immune system due to its effects on pathogen growth. Iron is essential for life and is a key nutrient for pathogenic microorganisms, which require this metal to survive and replicate. Life can to some extent be considered a battle for iron, so hosts must deprive undesirable guests of iron in order to combat the infections they cause. As a result, iron uptake by lactoferrin prevents the development of pathogenic microorganisms which cannot then access this metal. This is why blood lactoferrin levels increase markedly during infection. Indeed, lactoferrin concentrations increase in all biological fluids during most inflammatory reactions and viral infections, with the highest levels being detected at the nidus of the inflammation [6].

The clearest evidence that the immune function of lactoferrin is related to its iron affinity is the fact that whereas apolactoferrin (lactoferrin without iron) inhibits the growth of a large number of species of bacteria (such as *Escherichia coli*, some *Pseudomonas, Yersinias, Listeria, Streptococcus*, and *Staphylococcus*), hololactoferrin (iron-saturated lactoferrin) exhibits significantly lower inhibitory activities towards such bacteria [7–9]. The iron loading level of lactoferrin therefore partially determines its functionality.

It should be noted that lactoferrin also has some effects on the immune system that have nothing to do with iron affinity. Thus, lactoferrin exerts antiviral effects by binding directly to DNA (or RNA) and by preventing the entry of viruses into cells, thereby stopping infections at an early stage [10–13].

Lactoferrin can also serve as an iron donor, supporting the growth of certain beneficial bacteria [14, 15]. This occurs in breast milk, where lactoferrin,

Lactobacilli, and *Bifidobacteria* coexist in an environment that is optimized for proliferation.

X-ray diffraction studies, which are only available for the apo and holo forms of lactoferrin, have shown that it consists of one polypeptide chain containing 703 amino acids, which forms two homologous globular domains named the N- and C-lobes. The N-lobe corresponds to amino acid residues 1–333 and the C-lobe to residues 345–692, and the ends of these domains are connected by a short a-helix (Fig. 1). These two homologous lobes are further subdivided into two similarly sized domains known as domain 1 and domain 2 (domains N1 and N2 in the N-lobe and domains C1 and C2 in the C-lobe), and the two iron-binding sites are located within the interdomain clefts of each lobe. In human lactoferrin, when two iron atoms are incorporated into the apoprotein, the C-lobe conformation does not change significantly whereas the N-lobe closes like a hinge to grip the metal. This results in different tertiary structures: iron-free apolactoferrin is characterized by an open conformation of the N-lobe and a closed conformation of the C-lobe, whereas both lobes are closed in the iron-rich hololactoferrin, as shown by X-ray.

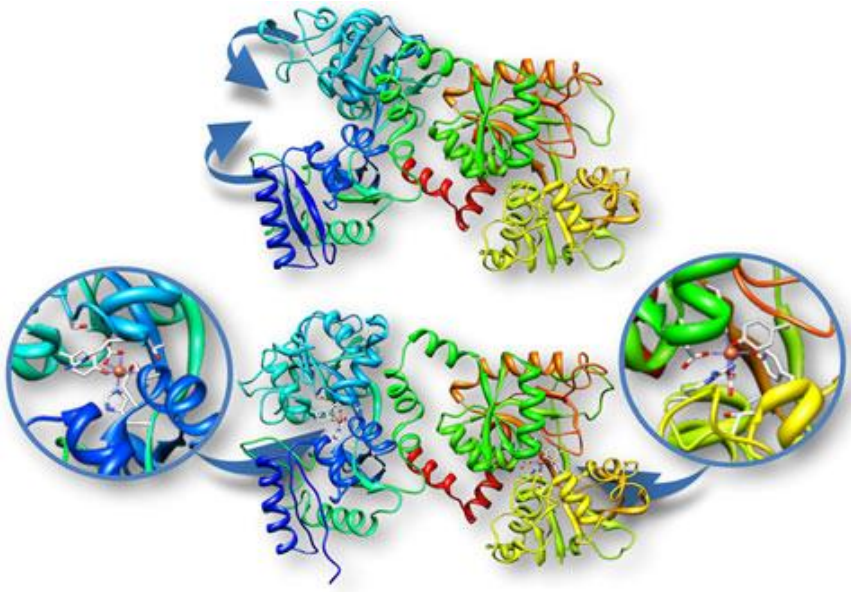

Fig. 1 X-ray structures of Lf and LfFe2. Arrows indicate the conformational movement of the N-lobe when coordinating iron. The iron-binding sites are magnified to highlight the chemical environment of the iron at each site

The chemical environments of the two iron(III) coordination sites are similar and consist of two phenolate oxygens from two tyrosine residues, one imidazole from a histidine residue, one carboxylate from an aspartate residue, and a synergistic adjacent bicarbonate or carbonate, which is stabilized by hydrogen bonding to the peptide chains that surround the active site. Despite this similarity, the two coordination sites of iron(III) can be distinguished kinetically and spectroscopically [18]. The three known forms of lactoferrin, namely apolactoferrin (Lf), the monoferric form (LfFe), and hololactoferrin ($LfFe_2$) differ in their iron loading levels, which determine the functionality of the protein.

The lysine residues on the external surface of lactoferrin can be used to covalently couple molecules [19–22] or clusters [23], permitting new functionality to be added to the protein. This option has been exploited for different applications, including increasing cell internalization levels, oral administration, rheology modulation, and for monitoring toxic non-transferrin bound iron. We use this functionalization to determine the iron loading level of the protein. The idea of incorporating a fluorescent moiety into lactoferrin is of considerable and widespread interest, especially in the field of biomedicine, as adequate functionalization could lead to fluorescence resonance energy transfer (FRET), an effect/process that is commonly used in sensors in biological research [24–26].

In the work described in the present paper, a pair of Alexa Fluor® (AF) fluorophores, AF350 and AF430, were chemically bound to Lf, LfFe, and $LfFe_2$. As the emission band of the AF350 donor overlaps with the excitation band of the AF430 acceptor, simultaneous labeling of these lactoferrin species with both fluorophores (AF350 and AF430) offers the opportunity to achieve FRET, which is strongly dependent on the distance between the AF350 donor and the AF430 acceptor. We show in this work that the FRET yield, which is the ratio of the emission intensities for the acceptor and donor, differs for Lf, LfFe, and $LfFe_2$ because the conformational changes that the protein undergoes during iron incorporation lead to variations in the donor–acceptor distance. As a result, the FRET pattern can be used as an indicator of the tertiary structure of lactoferrin, thus providing information on its iron load. Finally, we made use of this correlation between the FRET pattern and iron loading level to determine the iron

loading state of lactoferrin during its interaction with probiotic bacteria, a process which ends with the transfer of iron from the lactoferrin to the bacteria.

Moreover, we performed a computational study to rationalize this dependency of the FRET pattern on the iron loading level. The reason that this study is interesting is that the evolution of the FRET pattern with the tertiary structure of the protein can be used to probe how, upon the uptake of the first iron(III) ion, the other lobe of the protein is prompted to take up the second iron(III) ion. No definitive answer is available to this question at present.

Materials and methods

Monoferric lactoferrin (LfFe) was purchased from Fonterra (Auckland, New Zealand; ref. no: 81665295/100). The apo and holo forms were prepared from this monoferric lactoferrin.

Preparation of apolactoferrin (Lf)

Lyophilized human milk LfFe (20 mg/mL) was totally desaturated of iron following successive dialysis steps against 0.1 M citric acid/citrate buffer (pH 3.50) using a high retention seamless cellulose tubing membrane with a molecular weight cutoff (MWCO) of 12,000 Da. The citric acid/citrate buffer was changed several times until no characteristic iron lactoferrin absorbance at 464 nm (ε^{464} = 2,500 M^{-1}) was observed. The resulting colorless pale apolactoferrin solution was then dialyzed against phosphate buffer pH 6.80 and subsequently chromatographed (Sephadex G-25, GE Healthcare, Little Chalfont, UK). The concentration of apolactoferrin was measured by UV/vis spectroscopy based on the absorbance at 280 nm (ε^{280} = 92,300 M^{-1}).

Preparation of diferric lactoferrin (LfFe2)

Based on a previously published procedure [27], 20 mg of lyophilized human milk LFe were dissolved in 1 mL of TRIS–Cl buffer pH 6.80 containing 5 mM sodium bicarbonate. This solution was then titrated with Fe citrate at 37 ºC under continuous stirring until the appearance of a characteristic dark reddish solution. Fe citrate was freshly prepared every day following a previously reported

protocol [28].

Iron contents per lactoferrin were calculated directly by UV/vis spectroscopy from the relationship between the absorbance at 464 nm (ε^{464}= 2,500 M^{-1}) and that at 280 nm (ε^{280} = 92,300 M^{-1}). The iron/protein values obtained were 0 (Lf), 1.09 (LfFe), and 1.97 ($LfFe_2$). These values were obtained from triplicate preparations, with less than 8 % variation from the mean observed. The same lactoferrins were used for all subsequent experiments. This means that the iron content of every lactoferrin remained constant throughout the experiment.

Preparation of fluorescent lactoferrins

Lf, LfFe, or $LfFe_2$ (2 mL, 20 mg/mL) was incubated in a buffered PBS solution at pH 8 with an excess of (a) AF350, (b) AF430, and finally (c) a mixture of the AF350 and AF430 fluorophore succinimidyl ester derivatives. The two former assays allowed the molar ratio required for the third reaction to be determined. Specifically, an AF350:AF430:protein molar ratio of 30:15:1 was used to prepare the samples. The labeling reactions were performed at room temperature under continuous stirring for 24 h. The resulting solutions were then exhaustively dialyzed at room temperature for 3 days against several changes of Milli-Q water (Millipore, Billerica, MA, USA) using a high retention seamless cellulose tubing membrane with a MWCO of 12,000 Da, and size exclusion chromatography (Sephadex G-25) was then performed to remove the unbound fluorophores. Protein-containing fractions were isolated. For apolactoferrin samples labeled with both fluorophores, the concentration of AF430 was directly calculated from the absorbance values of the UV–visible spectra at 430 nm (ε^{430} = 16,000 M^{-1}) because the absorbances of apolactoferrin and AF350 are negligible at this wavelength. The concentration of AF350 was obtained from the absorbance at 350 (ε^{350} = 19,000 M^{-1}) by subtracting the absorbance of AF430 at this wavelength. The concentration of lactoferrin was obtained directly from the absorbance at 280 nm (ε^{280} = 92,300 M^{-1}) because the absorbances of both fluorophores at this wavelength can be considered negligible. A similar procedure was performed to determine the number of fluorophores for LfFe and $LfFe_2$, with the UV–visible spectrum of the starting lactoferrin subtracted from each labeled lactoferrin spectrum beforehand. The average number of fluorophores per protein was determined after performing the reaction in triplicate. Values were

very consistent (with less than 5 % variation from the mean) and were rounded to the nearest integer (Table 1). FRET yields from the three samples were also calculated, and standard deviations from the average were less than 3%.

Table 1 Number of fluorophores per lactoferrin (rounded to the nearest integer)

Protein	Only AF350	Only AF430	Combined use of both fluorophores	
			AF350	AF430
Lf	6 (6.16)	6 (6.11)	3 (3.06)	3 (3.02)
LfFe	5 (5.09)	5 (5.09)	3 (3.10)	2 (2.12)
$LfFe_2$	5 (5.09)	5 (4.98)	3 (3.07)	2 (1.97)

The average value calculated after performing the reaction in triplicate is shown in parentheses

All UV–visible spectra were recorded with a Thermo Scientific (Waltham, MA, USA) Spectronic Unicam UV300 spectrophotometer, and all fluorescence spectra were recorded with a Varian (Palo Alto, CA, USA) Cary Eclipse fluorescence spectrophotometer.

Incubation of AF-labeled lactoferrins with Bifidobacterium breve

Human milk *B. breve* (10 mg/mL; Biosearch S.A., Granada, Spain; CECT7263) was incubated with $LfFe_2$-AFs (4.86×10^{-6} M) under anaerobic conditions at 37 ºC in Hank's solution for 1, 2, 3, and 6 h. Bacterial suspensions were then centrifuged at 4,000 rpm and the supernatant solutions were analyzed using a Varian Cary Eclipse fluorescence spectrophotometer. No fluorescence was observed from the bacterial pellets. The iron concentrations of the supernatant solutions were measured by ICP, with values of $>10^{-9}$ M obtained. Likewise, the protein concentrations in the supernatant solutions remained constant (in the range 4-5 $\times 10^{-6}$ M, as measured by UV/vis spectroscopy based on the absorbance at 280 nm; $\varepsilon^{280} = 92{,}300\ M^{-1}$).

Docking study

Protein–ligand dockings were performed using the program GOLD 5.1. A harmonic restraint of 5.5 kJ/mol was added between the Ne of the corresponding lysine

(Lys301 or Lys296) and the C of the carboxylate group of the fluorophore. In the simulations where Lys301 or Lys296 were flexible, the Dunbrack rotamer library was used. The cavity was defined as a 20-Å sphere around Tyr82.

Structural statistics

The two scripts used in this work were written in Python and ported to the UCSF Chimera environment. Both can be obtained for free from the authors.

Supplementary Material (ESM)

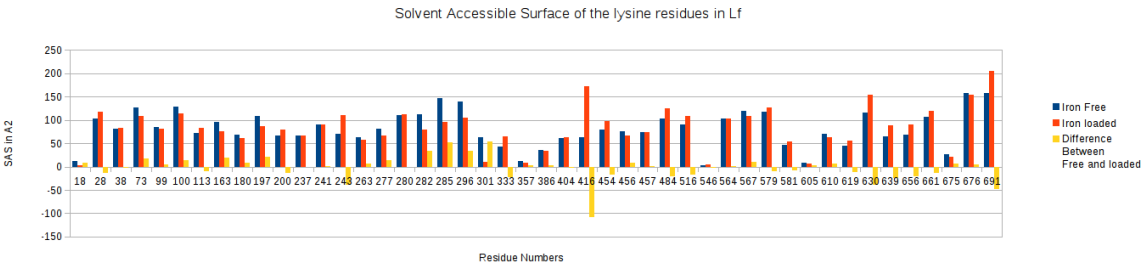

***Figure SI1**. Histogram of SAS values of the 46 Lys residues in Lf. Blue bars corresponds to values obtained for the Lf structure (pdb 1CB6), red bars to LfFe2 structure (pdb 1N76) and yellow bars to the relative difference between iron free and iron loaded conformations.*

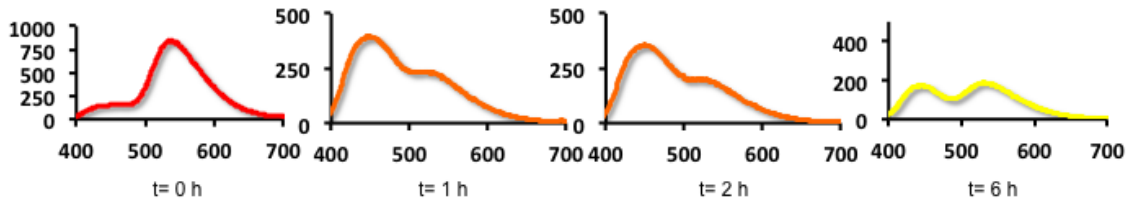

***Figure SI2**. Monitorization of FRET Fluorescence emission spectra for LfFe2-AFs before (left) and after (1, 2 and 6 h) incubation with Bifidobacterium breve.*

Results

Following a known procedure, apolactoferrin (Lf) and hololactoferrin ($LfFe_2$) were prepared from the commercial monoferric form (LfFe). These three forms of lactoferrin with different iron loadings were treated with an excess of each AF fluorophore (or a mixture of both AF fluorophores) for 24 h and then exhaustively dialyzed until no fluorescence was detected in the dialysis reservoir. After isolating the protein-containing fractions, measurement of the UV–vis spectra allowed the final concentrations of each lactoferrin sample and the AF430 and AF350 fluorophores to be calculated. These results yielded the average number of fluorophores per lactoferrin, as shown in Table 1.

Our observations of the reactions of Lf, LfFe, and $LfFe_2$ with AF350 and AF430 allowed us to establish that the number of reaction sites does not depend on the type of fluorophore used, and that they should be reacted with the proteins to determine the stoichiometric ratio (see "Materials and methods"). The fluorescence spectra of the solely AF350- and AF430-labeled lactoferrins showed emission bands centered at 445 and 540 nm upon excitation at 327 and 425 nm, respectively. As expected, the fluorescence properties of AF350 and AF430 were not significantly modified after covalent coupling to lactoferrin.

AF350 and AF430 were chosen for use in this work due to the fact that the emission band of AF350 overlaps with the excitation band of AF430. Therefore, the simultaneous labeling of lactoferrin with both fluorophores (AF350 and AF430) is a good option for achieving FRET. The lactoferrins (Lf, LfFe, and LFe_2) were finally incubated with an excess of a mixture of AF350 and AF430, using the same procedure as employed for the single AFs. The number of AF430 and AF350 moieties in each labeled sample was calculated from the absorbances at 430 and 350 nm in the UV–visible spectra (Fig. 2; see "Materials and methods").

As shown in Table 1, incubation of the lactoferrins (Lf, LfFe, and LFe_2) with an excess of a mixture of AF350 and AF430 yielded similar labeling results. The number of AF350 and AF430 molecules when the lactoferrins were labeled with a single fluorophore was six for Lf and five for both LfFe and $LfFe_2$. Interestingly, the number of AF350 and AF430 molecules in the combined experiments was also found to be also six (3 AF350 + 3 AF430) for Lf-AFs, five (3 AF350 + 2 AF430) for

LfFe-AFs, and five (3 AF350 + 2 AF430) for $LfFe_2$-AFs. All of these results therefore indicate that the fluorophore-labeled apo form of lactoferrin has an extra fluorophore (either AF350 or AF430) than found in fluorophore-labeled LfFe and $LfFe_2$. The three lactoferrins labeled with both AF350 and AF430 exhibited FRET (Fig. 3). Excitation at 327 nm produced emission at 440 and 540 nm. The FRET pattern and efficiency were found to be characteristic of every fluorescent lactoferrin.

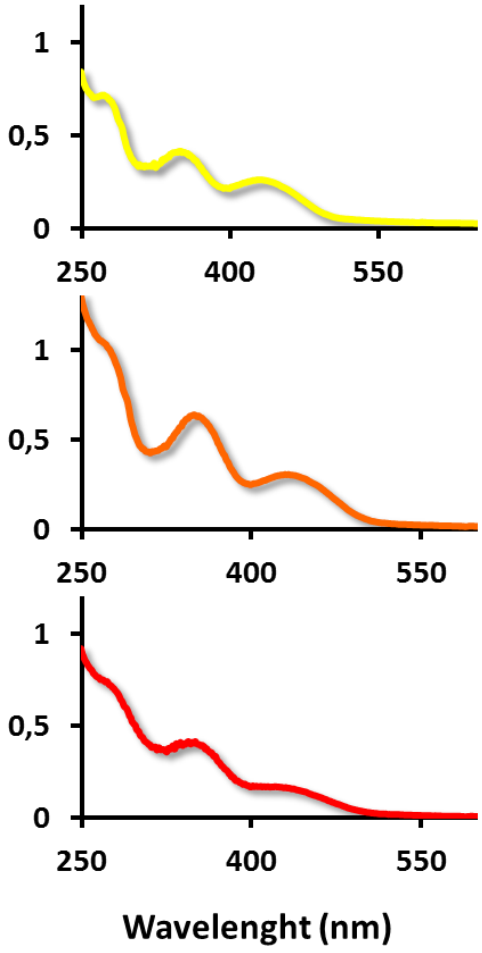

Fig. 2 UV–vis spectra of Lf-AFs indicating the number of AF350 and AF430 moities per protein in the combined AF350+AF430 labeling experiment. Concentrations of AF430, AF350, and protein were calculated from the absorbances at 430, 350, and 280 nm (see "Materials and methods")

In all cases, the emission at lower energy can be attributed to the AF430 acceptor and that at higher energy to the emission of the AF350 donor. In order to evaluate these different efficiencies, the %FRET value of each lactoferrin was calculated using the following equation, which normalizes the intensity of the emission of AF430 (I_{AF430}) with respect to the intensity of the emission from both fluorophores ($I_{AF350} + I_{AF430}$):

$$\%FRET = \frac{I_{AF430}}{I_{AF350} + I_{AF430}} \times 100.$$

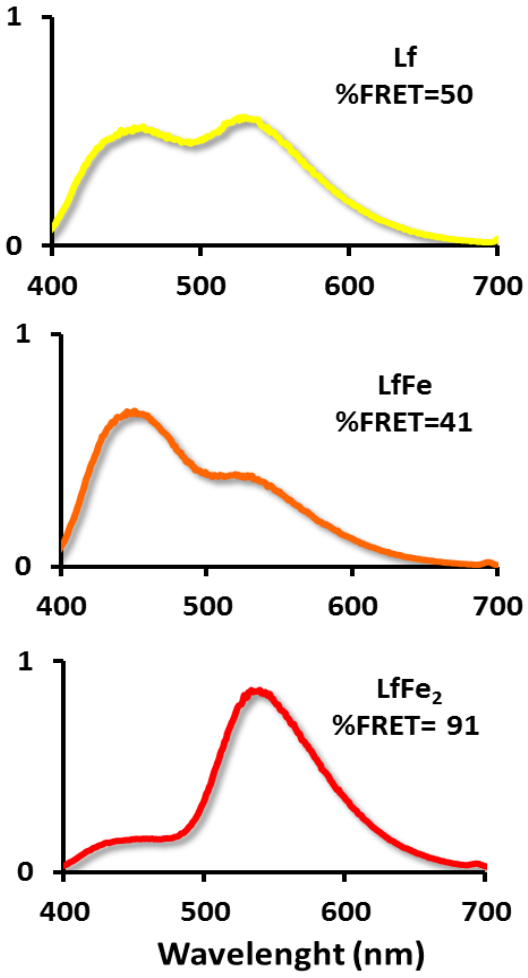

Fig. 3 FRET fluorescence emission spectra of the Lf- AF350+AF430, LfFe-AF350+AF430 and LfFe2-AF350+AF430 samples

The calculated %FRET yield values obtained from the data shown in Fig. 3 imply that the efficiency of the energy transfer between both fluorophores varies. Whereas complete energy transfer from the excited AF350 to AF430 does not

occur in Lf-AFs (%FRET = 50) or in LfFe-AFs (%FRET = 41), practically complete energy transfer occurs in $LfFe_2$-AFs (%FRET = 91). Consequently, the FRET pattern represents a ‘‘fingerprint’’ of the particular fluorescent lactoferrin that produces it, and is related to the conformational changes that occur to the protein upon the incorporation of iron.

Once these results had been analyzed, we aimed to correlate the energy transfer efficiency with the distance between the donor (AF350) and the acceptor (AF430), which obviously should be different in the three iron-loaded forms of Lf.

In order to gain greater insight into the differences observed in the number of fluorophores and the FRET patterns observed among the distinct iron-loaded states of lactoferrin, a computational analysis was performed. Calculations were first employed to ascertain the location of the binding site of the extra AF430 that is present in Lf-3AF350+3AF430 as compared to LfFe- and $LfFe_2$-3AF350+2AF430. Second, computation was used to identify the region (or regions) of the protein that influences the FRET efficiency.

First, a comparative analysis of the solvent-accessible surface (SAS) for the 46 lysines in the X-ray structures of Lf and $LfFe_2$ was performed (see SI1 in the Electronic supplementary material, ESM). As has been reported previously, succinimidyl ester derivatives of AFs are excellent dyes for labeling proteins through reactions with the available lysines [29]. To identify the location of the additional AF430 in the apo-Lf form, we hypothesized that the sixth lysine (i.e., the one to which the additional AF430 binds) should show a dramatic decrease in solvent accessibility when the apo form converts to the holo form of lactoferrin (in other words, upon changing from Lf-AFs to between the donor (AF350) and the acceptor (AF430), which obviously should be different in the three iron-loaded forms of Lf.

In order to gain greater insight into the differences observed in the number of fluorophores and the FRET patterns observed among the distinct iron-loaded states of lactoferrin, a computational analysis was performed. Calculations were first employed to ascertain the location of the binding site of the extra AF430 that is present in Lf-3AF350+3AF430 as compared to LfFe- and LfFe2-3AF350+2AF430. Second, computation was used to identify the region (or regions) of the protein

that influences the FRET efficiency.

First, a comparative analysis of the solvent-accessible surface (SAS) for the 46 lysines in the X-ray structures of Lf and $LfFe_2$ was performed (see SI1 in the Electronic supplementary material, ESM). As has been reported previously, succinimidyl ester derivatives of AFs are excellent dyes for labeling proteins through reactions with the available lysines [29].

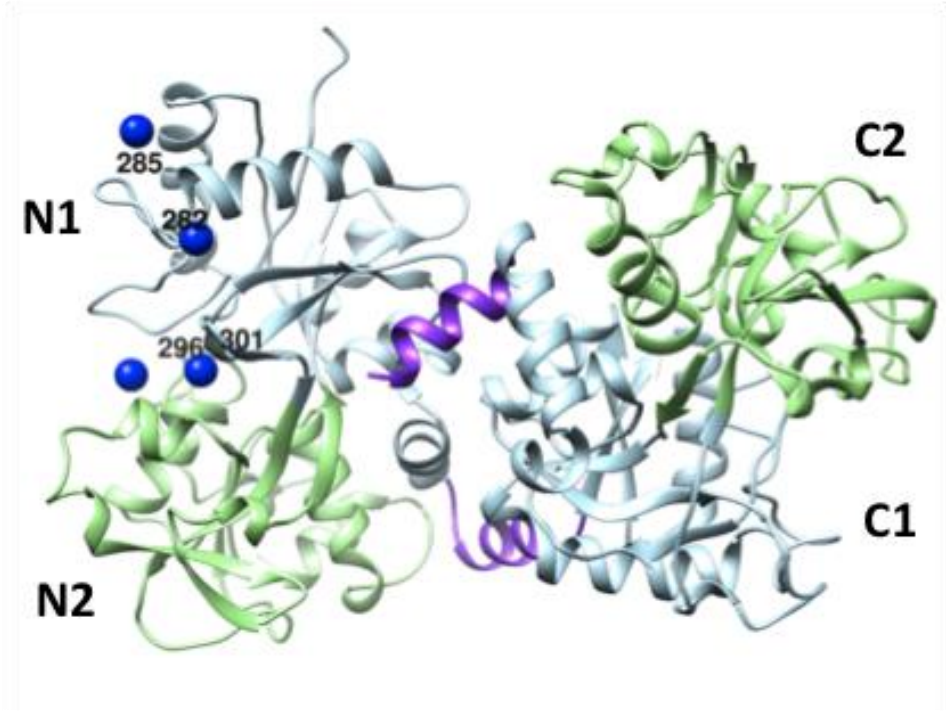

Fig. 4 Locations of the four lysines whose solvent accessible surface (SAS) values decrease the most upon converting from the Lf to the $LfFe_2$ form. The backbones are represented by ribbons. Regions colored green correspond to the C2 and N2 subdomains, and those colored silver correspond to the C1 and N1 subdomains. The lysines of interest are represented as blue spheres at the Ne position and are labeled.

To identify the location of the additional AF430 in the apo-Lf form, we hypothesized that the sixth lysine (i.e., the one to which the additional AF430 binds) should show a dramatic decrease in solvent accessibility when the apo form converts to the holo form of lactoferrin (in other words, upon changing from Lf-AFs to $LfFe_2$-AFs). A program written in Python in house and implemented in the UCSF Chimera environment [30] was designed for this analysis. Such an analysis

could not be done of the monoferric species since no X-ray structure of LfFe was available.

Although most of the lysines were found to be highly exposed to the solvent, four residues (Lys282, Lys285, Lys296, and Lys301) presented a noticeable decrease in SAS during the conversion from Lf to LFe_2. All of these residues are found in the N-lobe, and more specifically in the N1 region of the protein: Lys282 and Lys285 are located at one of the external faces of the subdomain and Lys296 and Lys301 at the entrance and core of the iron-binding site, respectively (Fig. 4). Significantly, Lys282, Lys285, and Lys296 exhibit large SAS values, thereby suggesting that interaction with a fluorophore should be independent of the protein conformation. In contrast, Lys301 exhibited a large SAS value in Lf but a value of almost zero in LFe_2, meaning that this residue changes from being highly exposed in the apo form (Lf) to deeply buried in the holo one ($LfFe_2$).

To better ascertain whether Lys301 is the Lys to which AF430 binds, and to gain a better understanding of its molecular features, protein–ligand dockings of the fluorophore at this site were performed using the available crystal structures of Lf and $LfFe_2$. As stated in the "Materials and methods" section, these calculations were undertaken using the program GOLD and the Chemscore scoring functions [30]. A restraint was added between N of the lysine and the carbon atom of the carbonyl group of the fluorophore during the run in order to achieve geometries consistent with pre-reaction AF430 binding states.

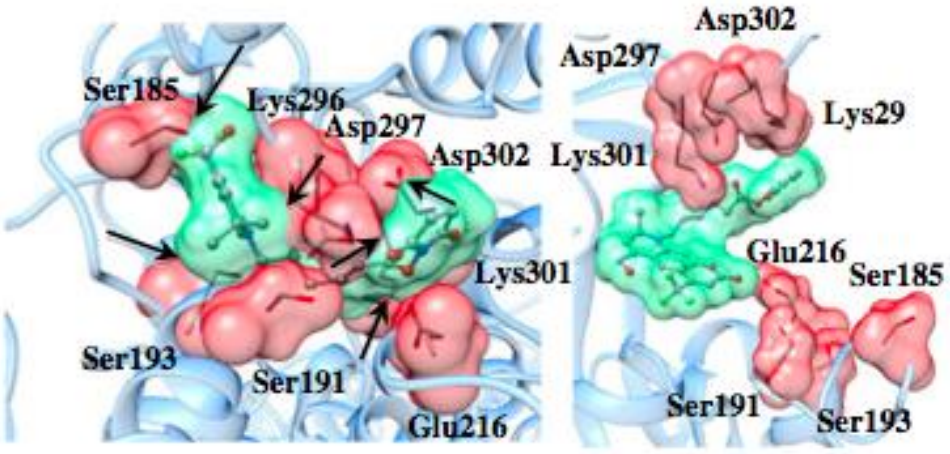

Fig. 5 Lowest-energy solutions for the conformation of AF430 that are consistent with its binding to Lys301 in $LfFe_2$ (left panel) and Lf (right panel). The fluorophores are represented as balls and sticks and the protein residues as sticks. The surfaces are also depicted in order to highlight the residues (red) that show the most steric hindrance with the fluorophore (blue) in $LfFe_2$

The predicted binding affinities for AF430 binding at Lys301 range from 18.8 to –22.1 scoring units on going from Lf to $LfFe_2$, respectively. For calculations performed with the Chemscore function, these values imply a predicted binding affinity that could reach the micromolar range for the former but that binding is impossible for the latter [31].

These findings were further confirmed by repeating the calculations with AF430 on $LfFe_2$, but adding greater flexibility to the Lys301 residue during docking (Fig. 5). Although the predicted affinity of the best binding mode increased at 13.75 U, the binding affinity was still low and was substantially different to that obtained for Lf. Moreover, for the conjugation to occur, Lys301 must escape from a buried situation in $LfFe_2$ (where it interacts strongly with a network of polar interactions with the carboxylic residues E216 and D297) to a conformation that is highly exposed to the solvent. Marked steric hindrance is observed for the environments of the iron-binding sites in the resulting geometry. These results confirm that conjugation of the dye at this position is only possible in the apo form of Lf.

Additional calculations were performed to identify the region of the protein that

could be responsible for the change in FRET efficiency upon shifting from the apo-Lf to the holo-$LfFe_2$ form. These calculations, which considered the variations in the distances between all lysine residues during the transition from Lf to $LfFe_2$, were performed using an additional program written in house in Python and implemented in the UCSF Chimera package [32]. The script provided a 46 x 46 matrix of the entire set of Lys–Lys distances. The comparative analysis of the X-ray structures of Lf and $LfFe_2$ showed that most of the 46 Lys residues have inter-residue distances that only rarely vary by >3 Å on average when the iron loading of the protein changes, thus remaining within the Förster distance range (Fig. 6). However, eight Lys residues, namely Lys99, 100, 113, 197, 200, 237, 241, and 243, showed a different pattern, with variations of between 5 and 10 Å. Also, Lys180 showed variations that were slightly larger than 4 Å.

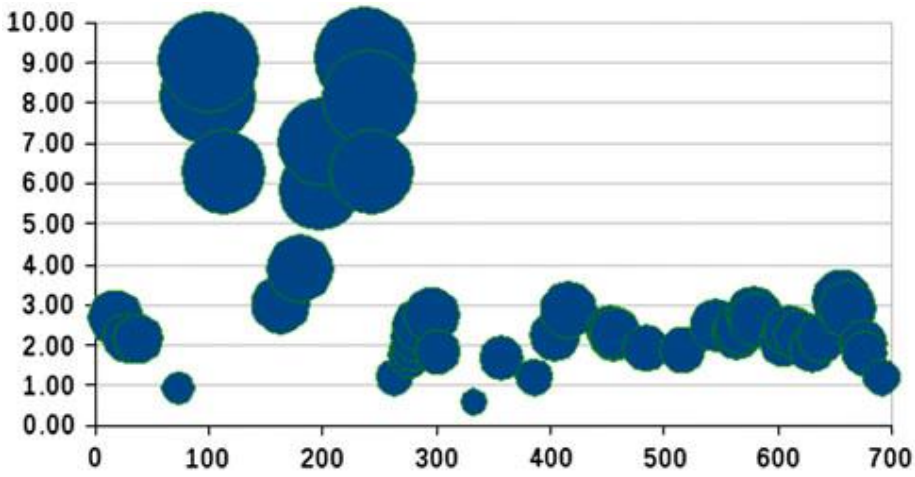

Fig. 6 Bubble chart showing the average variations in inter-residue distances upon transitioning from Lf to $LfFe_2$. The size of each circle is proportional to the magnitude of the variation. Lys residue labels are given on the abscissa

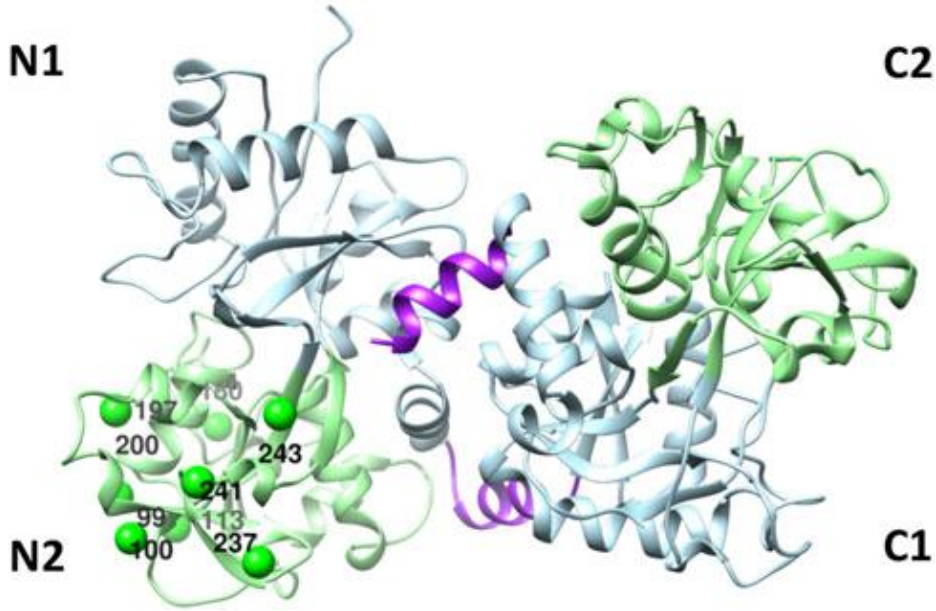

Fig. 7 Locations of the nine lysines whose average variations in inter-residue distance upon transitioning from Lf to $LfFe_2$ exceed 4 Å . The backbones are represented as ribbons. Regions colored green correspond to the C2 and N2 subdomains, and those colored silver correspond to the C1 and N1 subdomains. Putative lysines are represented as green spheres at the Ne position and are labeled

Importantly, these eight residues were all found to be located in the N2 subregion of the N-lobe. This subregion makes the greatest contribution to the conformational transition from Lf to $LfFe_2$ (Fig. 7). Lys301, which was previously identified as the binding site for the "extra" AF430, is located at the interface between the N1 and N2 subdomains. Both of these results suggest that, even upon shifting to the LfFe form of the metalloprotein, a conformational change occurs to the macromolecule consisting of a subdomain rearrangement of the N-lobe.

Using our improved understanding of the relationship between the FRET profile and iron loading, the possibility of using fluorophore labeling to monitor iron loading in lactoferrin-dependent processes was investigated. In particular, we monitored the process by which lactoferrin can supply iron to a healthy bacterium, in this case *B. breve*. The bacteria were incubated with $LfFe_2$-AFs for different durations (1–6 h) and the FRET patterns of the supernatant solutions obtained after bacterial centrifugation were analyzed. After 6 h, the resulting

supernatant solution exhibited a FRET pattern typical of the iron-free Lf-AFs form (Fig. 8). A negligible amount of iron was detected in this solution (concentration below 10^{-9} M), while the concentration of the protein (Lf) remained constant. This finding suggests that all of the iron initially bound to lactoferrin is released and incorporated into the bacteria after this time. Likewise, no fluorescence was observed from the centrifuged bacteria. Interestingly, we observed that the FRET pattern does not change gradually but sharply, in two steps: from $LfFe_2$ to LfFe, and then from LfFe to Lf (SI2).

Discussion

The present study of the FRET signals obtained when functionalizing lactoferrin with two distinct fluorophores, AF430 and AF350, provides not only novel molecular information on the iron-loading state of the protein but also on the mechanisms underlying these iron loading/unloading processes. Furthermore, the results illustrate how this methodology can be useful when performing in vivo and in vitro experiments involving Lf iron release or loading.

Our data show that both the change in the number of fluorophores that can be bound to lactoferrin and the variations in their FRET patterns as a function of the iron loading level of the protein are strongly dependent on the protein conformation. This means that the FRET responses can be used to analyze the iron-dependent conformational change of lactoferrin when it converts from its apo form to its holo (diferric) form, and can shed light on previously unanswered questions about this process.

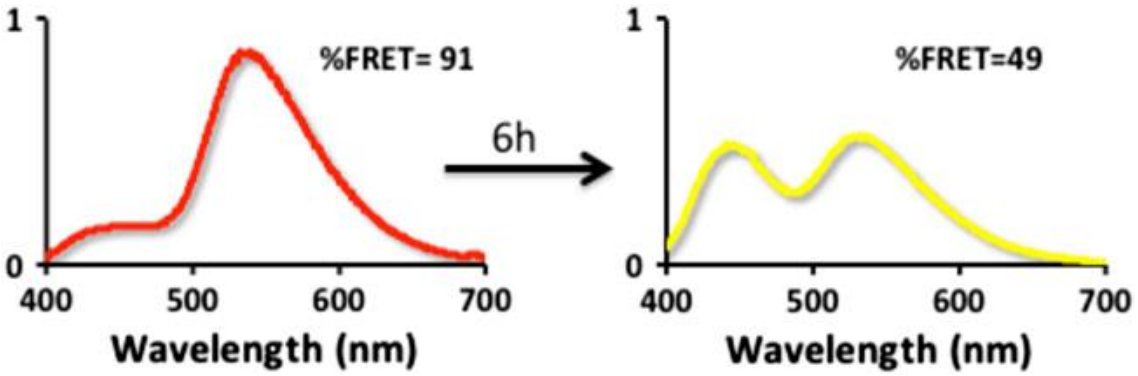

Fig. 8 FRET fluorescence emission spectra for LfFe2-AFs before (left) and after (right) incubation with B. breve for 6 h

More precisely, the FRET responses can be used to probe how, following the uptake of the first iron(III) ion, the other lobe of the protein is prompted to bind the second ion. To the best of our knowledge, none of the information currently available provides a definitive answer to this question.

The results of our computational study, based on an SAS analysis of the Lys residues in Lf and $LfFe_2$, clearly indicate that Lys301 is the only residue that is able to selectively bind AF430 in Lf (but not in LFe_2). This result is supported by those obtained from simulated protein–ligand dockings that explicitly modeled the binding of the fluorophore to the selected amino acid and showed that AF430 can easily access a catalytically consistent orientation for binding at Lys301 in Lf but not in LfFe nor $LfFe_2$ (Fig. 5). Since Lys301 is located at the iron-binding site of the N-lobe and is located at the interface between the N1 and N2 subdomains, it appears that some type of conformational change occurs in this domain as a consequence of the binding of the first iron to the protein. Additional calculations on the available X-ray structures also allowed us to demonstrate that the differences in the FRET patterns obtained for Lf, LfFe, and $LfFe_2$ are likely to be related to the fluorophores attached to the Lys residues located at the N2 lobe. This suggests that the transition between Lf and $LfFe_2$ is likely to involve a major contribution from an interdomain change in the N-lobe.

At this point, it is interesting to note that uptake of the first iron(III) by lactoferrin

has been reported to occur at the C-site, at which point the N-site becomes capable of acquiring a second iron(III) ion [33]. However, the mechanism by which the N-lobe is activated once this first iron(III) ion has been bound to the C-lobe is not well known and the source of debate. To date, it is believed that the binding of the first iron(III) is followed by a series of proton dissociations that probably trigger changes in the conformation of the protein, thereby affecting the N-site and allowing the capture of the second iron(III) [18].

On the one hand, our results suggest that the capture of the first iron(III) ion triggers a partial but significant enough interdomain change at the N-lobe. Lys301, which is located at the interface between the N1 and N2 subdomains, binds an AF430 in Lf but not in $LfFe_2$. The steric hindrance of Lys301 is associated to a certain degree with the closing motion that takes place between the N1 and N2 subdomains upon the shift from the Lf to the LfFe form of the protein, as shown by further SAS analysis.

Therefore, our results show that the binding of the first metal to Lf involves a reorganization of the N2 domain with respect to the N1 one. However, the FRET efficiency remains almost unaffected (50 vs 41 %) by the Lf to LfFe transition, leading us to suspect that the conformational change is relatively limited.

The capture of the second iron(III) by the N-lobe results in a significant conformational change of the protein as a whole. A drastic increase in FRET is observed upon transitioning from LfFe (41%) to $LfFe_2$ (91%). This suggests that a marked change in the N2/N1 interface occurs with the binding of the second iron. In the absence of an X-ray structure for human LfFe, the results of our joint computational–experimental study suggest that the structure of LfFe presents an intermediate conformation of the N-lobe that is mainly characterized by intersubdomain reorganization. This observation is consistent with the recently released structure of an intermediate conformation of di-iron and di-bismuth human transferrin, where the main structural changes were observed at the N2 domain and at the interface between both subdomains [34]. Our interpretations are also consistent with those of other authors, who have envisaged the possibility that cooperativity between the C- and N-lobes occurs via dynamic event modifications of the interlobe chain, rather than the lobes themselves [18, 33].

In addition to the novel information obtained on the molecular mechanism of iron loading by lactoferrin, the present study illustrates how the FRET profile of lactoferrin can be used as a tool to monitor some specific processes of iron metabolism in which this protein plays a relevant role. In particular, lactoferrin may support the growth of some nonpathological but beneficial bacteria [14, 15]. Indeed, lactoferrin coexists with several lactic acid bacteria, such as *Bifidobacterium* and *Lactobacilli*, in breast milk. These Gram-positive anaerobic bacteria proliferate in the human intestinal tract and are classified as probiotic bacteria because of their health benefits [35–37]. Our results confirm that, as for other healthy bacteria, human iron-saturated lactoferrin acts as an iron donor for *B. breve*. The evolution of the FRET pattern of the supernatant solution after the incubation of $LfFe_2$ with the bacteria (Fig. 8) points to complete iron transfer from $LfFe_2$ to the bacteria. Moreover, the fact that the protein concentration in the extrabacterial medium does not significantly change suggests that lactoferrin does not require protein internalization and that, unlike other transferrins, it is not involved in Fe(III) transport by receptor-mediated endocytosis. This kind of iron trafficking has only been observed in certain Gram-negative bacteria [38].

Conclusions

Fluorescent lactoferrins with different iron loading levels were prepared by labeling the proteins with the Alexa Fluor dyes AF350 and AF430. All of the fluorescent lactoferrin samples showed FRET, but interestingly with distinctive patterns. This indicates that energy transfer from the donor to the acceptor fluorophore varies with the iron loading level of lactoferrin. Since the iron loading level of lactoferrin determines its tertiary structure, the FRET pattern of the sample correlates with its iron content. Moreover, the results of our joint experimental-computational study provide an additional piece of evidence relating to the subdomain dynamics of the N-lobe upon iron binding. They are consistent with a cooperative transfer mechanism between the C- and N-lobes of lactoferrin that involves interdomain conformational changes during the transition from the Lf to the LfFe form, although the closed conformation found in $LfFe_2$ is not achieved during this transition.

In a further achievement, we used this FRET to iron level correlation for lactoferrin as a tool to monitor the interaction between human lactoferrin and *Bifidobacteria*. Specifically, we used this methodology to demonstrate that lactoferrin supplies iron to these healthy bacteria and, furthermore, that this process takes place without iron(III) trafficking by receptor mediated endocytosis.

Acknowledgments

This work was supported by MINECO and FEDER (projects CTQ2012-32236, CTQ2011-23336, and BIO2012- 39682-C02-02) and BIOSEARCH SA. F.C. and V.M.R. are grateful to the Spanish MINECO for FPI fellowships

References

1. Vogel H (2012) J Biochem Cell Biol 90:233–244

2. Baker EN, Baker HM (2005) Cell Mol Life Sci 62:2531–2539

3. Baker EN, Baker HM (2009) Biochimie 91:3–10

4. Anderson BF, Baker HM, Norris GE, Rice DW, Baker EN (1989) J Mol Biol 209:711–734

5. Baker EN, Lindley PF (1992) J Inorg Biochem 47:147–160

6. Birgens HS (1985) Scand J Haematol 34:326–331

7. Orsi N (2004) Biometals 17:189–196

8. Byrd TF, Horwitz MA (1991) J Clin Investig 88:351–357

9. Griffiths E, Duffy L, Schanbacher F, Dryja D, Leavens A, Neiswander R, Qiao H, DiRienzo D, Ogra P (2003) Dig Dis Sci 48:1324–1332

10. Arnold RR, Cole MF (1977) Science 197:263–265

11. Valenti P, Antonini G (2005) Cell Mol Life Sci 62:2576–2587

12. Berkhout B, Floris R, Recio I, Visser S (2004) Biometals 17:291–294

13. Kanyshkova TG, Semenov DV, Buneva VN, Nevinsky GA (1999) FEBS Lett 451:235–237

14. Liepke C, Adermann K, Raida M, Mägert H-J, Forssmann W-G, Zucht H-D (2002) Eur J Biochem 269:712–718

15. Sherman M, Bennett S, Hwang FY, Yu C (2004) Biometals 17:285–289

16. Kumar J, Weber W, Mü nchau S, Yadav S, Singh SB, Saravanan K, Paramasivam M, Sharma S, Kaur P, Bhushan A, Srinivasan A, Betzel C, Singh TP (2003) Indian J Biochem Biophys 40:14–21

17. Chug TDY, Raymond KH (1993) J Am Chem Soc 115:6765–6768

18. Bou AF, El Hage Chahine JM (2000) J Mol Biol 303:255–266

19. Moosmann A, Blath J, Lindner R, Mü ller E, Bö ttinger H (2011) Bioconjug Chem. 22:1545–1558

20. Breuer W, Cabantchik ZI (2001) Anal Biochem 15:194–202

21. Nojima Y, Suzuki Y, Iguchi K, Shiga T, Iwata A, Fujimoto T, Yoshida K, Shimizu H, Takeuchi T, Sato A (2008) Bioconjug Chem 19:2253–2259

22. Zalipsky S (1995) Bioconjug Chem 6:150–165

23. Xavier PL, Chaudhari K, Verma PK, Pal SK, Pradeep T (2010) Nanoscale 2:2769–2776

24. Myc A, Majoros IJ, Thomas TP, Baker JR Jr (2007) Biomacromolecules 8:13–18

25. Wang YA, Li JJ, Chen H, Peng X (2002) J Am Chem Soc 124:2293–2298

26. Green M, Howman E (2005) Chem Commun 121–123

27. Bates GW, Billups C, Saltman P (1967) J Biol Chem 242:2816–2821

28. Faller B, Nick H (1994) J Am Chem Soc 116:3860–3865

29. Fernández B, Gálvez N, Sánchez P, Cuesta R, Bermejo R, Domínguez-Vera JM (2008) J Biol Inorg Chem 13:349–355

30. Pettersen EF, Goddard TD, Huang CC, Couch GS, Greenblatt DM, Meng EC, Ferrin TE (2004) J Comput Chem 25:1605–1612

31. Maréchal JD, Yu J, Brown S, Kapelioukh I, Rankin E, Wolf C, Roberts G, Paine M, Sutcliffe M (2006) Drug Metab Dispos 34:534–538

32. Verdonk ML, Cole JC, Hartshorn MJ, Murray CW, Taylor RD (2003) Proteins

52:609–623

33. Pakdaman R, Petitjean M, El Hage Chahine JM (1998) Eur J Biochem 254:144 153

34. Yang N, Zhang H, Wang M, Hao Q, Suna H (2012) Sci Rep 2:999

35. Macfarlane S, Macfarlane GT, Cummings JH (2006) Aliment Pharmacol Ther 24:701–714

36. Shah NP (2000) J Dairy Sci 83:894–907

37. Kaur IP, Chopra K, Saini A (2002) Eur J Pharm Sci 15:1–9

38. Heymann JJ, Weaver KD, Mietzner TA, Crumbliss AL (2007) J Am Chem Soc 129:9704–9712

RESULTADOS/CONCLUSIONES DEL CAPITULO 5 QUE MOTIVARON EL CAPITULO 6.

Como fruto del estudio del metabolismo de hierro en bacterias probióticas, hemos podido constatar la presencia de una o varias moléculas reductoras emitidas por estas bacterias que son capaces de reducir Fe(III) a Fe(II). Este poder de reducción ha sido aplicado a otros iones metálicos y en particular hemos demostrado que estas bacterias probióticas son capaces de reducir Au(III) a Au(0) con la consiguiente formación de nanopartículas de Au que se quedan fijadas en el biofilm de la bacteria.

Por otra parte, trabajos llevados a cabo en el grupo de investigación en el que he desarrollado esta Tesis Doctoral, han puesto de manifiesto que estas bacterias probióticas son capaces de incorporar en su superficie nanopartículas de maghemita.

Hemos prentendido combinar ambas propiedades de estas bacterias probióticas: poder de reducción de Au(III) y capacidad de incorporar nanopartíulas de óxido de hierro en su membrana exterior, para generar bacterias vivas que contengan simultáneamente nanopartículas con propiedades ópticas (debido a la presencia de nanopartículas de Au) y magnéticas (debido a la presencia de nanopartículas de maghemita). Esto nos ha permitido crear el primer material vivo con propiedades magneto-ópticas.

UNIVERSITATIS·GRANATENSIS
CAROLVS·RO·IMP·SEMPER·AVG·HISPAN·REX·FUNDATOR

CAPÍTULO 6.

BIOINSPIRED MAGNETO-OPTICAL BACTERIA

Fernando Carmona, Miguel Martín, Natividad Gálvez, Jose M. Dominguez-Vera

Abstract. "Two-in-one" magneto-optical bacteria have been produced using the probiotic Lactobacillus fermentum® for the first time. We took advantage of two features of bacteria to synthesize this novel and bifunctional nanostructure: their metal-reducing properties, to produce gold nanoparticles, and their capacity to incorporate maghemite nanoparticles at their external surface. The magneto-optical bacteria survive the process and behave as magnets at room temperature.

Keywords: Magnetic Nanoparticles, Gold Nanoparticles, Bioinspired Materials.

Tremendous interest in the possibility of using bifunctional gold-magnetite nanomaterials for biomedical and electronic applications has led to increased research into the synthesis of such materials.[1-8] Synthetic methods usually involve the use of toxic chemicals, high temperatures and pressures, and result in particles that become unstable or aggregate upon interaction with biological media. An alternative approach to traditional synthetic chemistry is the biosynthesis of nanomaterials which employs natural organisms that reduce metal ions into stable nanoparticles.[9-16] Moreover, it should be borne in mind that there is ever increasing pressure to develop green, eco-friendly and economically-viable synthetic routes to nanomaterials. This has resulted in researchers turning towards biological organisms for inspiration.

Microorganisms, such as bacteria and fungi, can be successfully used for large scale production of small particles at an extracellular level.[9-16] Biosynthesized nanoparticles usually exhibit enhanced stability and afford better control over morphology. Furthermore, bio-based fabrication has been shown to be reproducible and includes the possibility of synthesizing hydrophilic nanoparticles.[17]

Despite these advantages, the use of microorganisms as potential nanoparticle biofactories is a relatively new area of research. Most of the known examples

deal with the synthesis of microbial mediated zero-valent metal nanoparticles, especially gold. Gold nanoparticles are in fact formed by a variety of metal-reducing microorganisms. Although the mechanism has not yet been fully elucidated, it is roughly assumed that the biofilm would capture Au(III) ions on its external surface. The Au(III) ions are then thought to be reduced by biomolecules secreted by the bacteria producing Au atoms that would aggregate at specific sites to form nanoparticles.[9]

On the other hand, other bacteria are capable of adsorbing, at extracellular level, amorphous magnetite nanoparticles by a biologically induced process, of which the mechanism is still unknown. Similarly, we have recently reported that the direct adhesion of magnetic nanoparticles onto the biofilm of some bacteria is also a viable route for producing novel magnetic bacteria.[22]

Inspired by the existence of both metal-reducing microorganisms capable of producing extracellular gold nanoparticles from the metal cations and microorganisms that can capture iron oxide nanoparticles at an extracellular level, we have designed a new route that incorporates both processes. In this work we describe the preparation of a new type of ''two-in-one'' magneto-optical bacteria based on maghemite and gold nanoparticles.

The presence of both magnetic and gold nanoparticles in a single nanostructure is a powerful way to combine the properties of two of the most interesting metallic nano-building blocks. On the one hand, magnetic nanoparticles are of paramount importance in biomedicine as diagnostic tools in magnetic resonance imaging, as mediators for hyperthermic cancer treatment, and as drug-delivery vehicles.[23-26] On the other hand, gold nanoparticles are being employed in biomedicine because of their unique optical, electrical and photothermal properties.[27-30] In this context, in recent years, a wide range of gold-magnetic nanoparticles have been developed by a variety of physical, chemical and biological methods, most of them, leading to core-shell Au-magnetite nanoparticles.[31-35]

Here we show that bacteria such as *Lactobacillus fermentum*®, known to have a positive effect on the maintenance of human health since they constitute an important part of natural microbiota, can reduce Au(III) ions to produce discrete extracellular gold nanoparticles and then, in a second step, are able to

incorporate maghemite nanoparticles, also at the external surface, therefore producing bifunctional magneto-optical bacteria. As far as we know, this is the first example of a microorganism simultaneously containing optical gold and magnetic maghemite nanoparticles.

Furthermore, toxicity assessments showed that neither the gold nor the maghemite particles were especially toxic or inhibitory to these bacteria. Thus, using this hybrid natural-synthetic approach, we succeeded in obtaining living bacteria that behave as magnets at room temperature and exhibit optical properties. We found that when an aqueous Au(III) solution was added to a culture of *Lactobacillus fermentum*®, the reaction mixture turned from pale yellow to red within 30 min, indicating the formation of gold nanoparticles (Figure 1). The UV–visible absorption spectrum recorded from the gold- loaded bacteria exhibited a surface plasmon band at 520 nm, which is characteristic of Au nanoparticles, that was not observed for the supernatant after bacteria centrifugation.

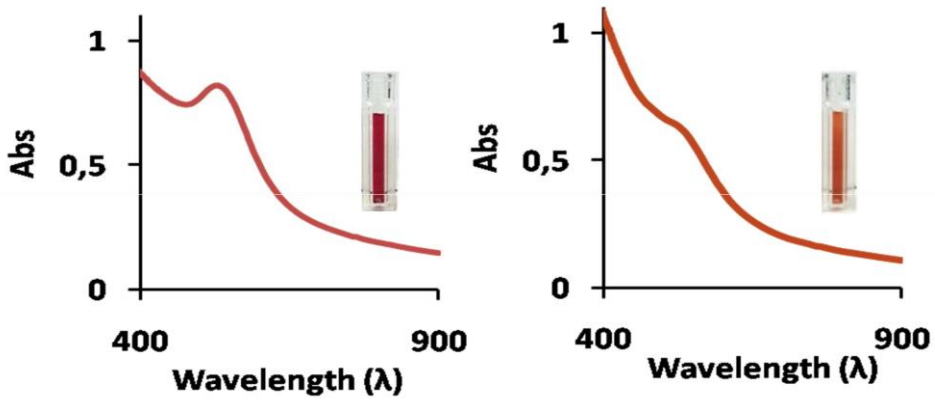

Figure 1*. UV-Vis spectra of just gold and gold+maghemite- labelled Lactobacillus fermentum*®*.*

To gain further insight into the role of *Lactobacillus fermentum*® in gold nucleation, we chemically reduced Au(III) in the absence of the bacteria, but in the presence of the extracellular reductant solution generated by the cultivated

bacteria. For this purpose, *Lactobacillus fermentum*® were cultivated, centrifuged and the supernatant solution isolated. Interestingly, when an aqueous Au(III) solution was added to the supernatant extracted from the *Lactobacillus fermentum*® culture, the reaction mixture changed from pale yellow to produce different colors within 1 h and finally formed a black precipitate, indicating the formation of gold aggregates. Based on these observations, it can be deduced that gold particles are likely produced with the aid of bacterial extracellular reducing agents. In parallel, they also suggest the existence of a chemical site of gold nucleation on the external bacterial surface. This would explain the stability of the gold nanoparticles once incorporated onto the bacteria and also the absence of any size (or color) evolution with time. Purification and physicochemical characterization of the biomolecules involved in the microbial synthesis of gold nanoparticles need to be investigated. Further analytical and proteomic studies are currently being conducted in order to attain a thorough understanding of the mechanism and nature of the reducing agent(s) and the nucleation site.

Having isolated the gold nanoparticle-loaded bacteria, they can serve as precursors for the incorporation of maghemite nanoparticles, thus incorporating magnetic properties to thereby obtain the first magneto-optical microorganisms. A liquid culture of gold-*Lactobacillus fermentum*® was incubated with an acidic solution of maghemite nanoparticles.[36] The resulting bacteria, labeled with gold and maghemite nanoparticles, were collected by centrifugation then dispersed in water to form a reddish-brown solution. This solution was examined by UV-Vis spectroscopy and Transmission Electron Microscopy (TEM). As shown in Figure 1, the surface plasmon resonance remains at the same wavelength, which confirms that gold nanoparticles remain intact after the incorporation of the maghemite ones. In fact, the supernatant liquid after the final isolation of the magneto-optical bacteria did not contain any gold.

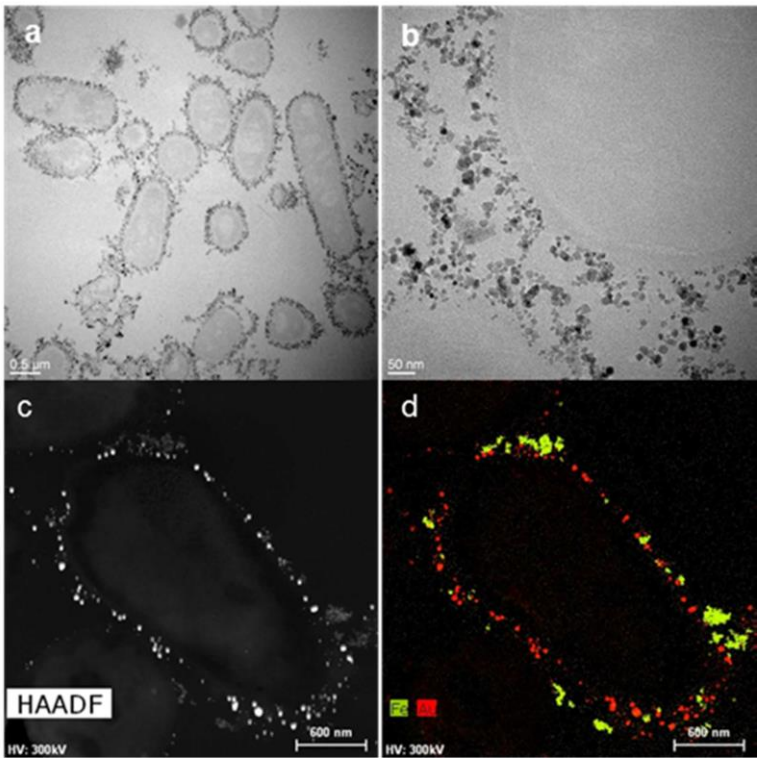

Figure 2. *a) TEM micrograph of a thin epoxy resin section showing the presence of particles at the external surface of the gold+maghemite-labeled bacteria. b) An area of (a) at higher magnification, showing the different contrast of gold and iron-containing nanoparticles. c) HAADF-STEM micrograph of a single bacterium. d) EDX compositional maps of iron (green) and gold (red) collected over the whole HAADF- STEM image in (c).*

Large accumulations of nanoparticles on the external bacterial surface were revealed by TEM (Figures 2a and 2b). Gold and maghemite nanoparticles are attached to each bacterium, as demonstrated by high-angle annular dark field scanning transmission electron microscopy (HAADF-STEM) (Figure 2c) and energy-dispersive X-ray spectroscopy (EDX) (Figure 2d). However, maghemite nanoparticles (in green, Figure 2d) tend to form aggregates while gold nanoparticles are well dispersed throughout the bacteria surface. The intensity of the HAADF-STEM images depends primarily on the atomic number (Z) and thickness of the specimen. A typical HAADF image of the gold+maghemite-labeled bacteria (Figure 2c) shows clear evidence of a different contrast between gold and

iron-containing nanoparticles, which serves to distinguish between the two kinds of particles. Every bacterium contains less-bright particles, corresponding to iron oxide structures with a lower Z, and brighter particles, corresponding to the gold nano-blocks. The presence of both gold and maghemite nanoparticles on each bacterium was unequivocally confirmed when inspected by EDX Au and Fe mapping, as can be seen in Figure 2d. Both gold and maghemite particles had relatively homogeneous size distributions and were approximately spherical. The gold nanoparticles produced were in the size range of 3 - 18 nm, with an average of 7 ± 2 nm whereas the maghemite particles were centered around 10 nm.

Figures 3a and 3b show typical HREM images of agglomerates of maghemite and gold nanoparticles, respectively, surrounding the bacterial wall. Under high resolution HREM the lattice fringes of both nanoparticles can be observed, thus confirming their crystalline nature. Measured d-spacing and electron diffraction patterns were indexed according to the maghemite and gold structures (Figures 3c and 3d, respectively).

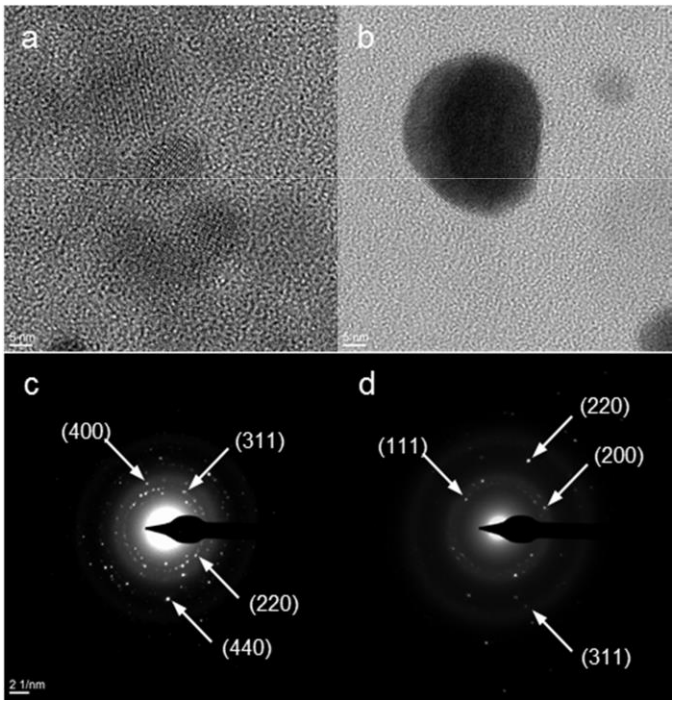

Figure 3. *a) HREM micrograph of maghemite nanoparticles. b) HREM micrograph of a single gold nanoparticle. c) Electron diffraction pattern of maghemite particles of (a) with labeled reflexions. d). Electron diffraction pattern of the gold particle of (b) with labeled reflexions.*

Figure 4 provides clear evidence that the magneto-optical gold+maghemite-*Lactobacillus fermentum*® bacteria have ferromagnetic properties at room temperature as they transfer across a liquid medium placed in the magnetic field of an external magnet. Note that the area of the liquid medium furthest from the magnetic field source is almost colorless, this underlines the fact that both maghemite and gold nanoparticles are collectively associated in the same bacterial platform. Magnetic studies of lyophilized gold+maghemite-*Lactobacillus fermentum*® samples were performed using a superconducting quantum interference device (SQUID). Hysteresis loop with coercivity (10 Oe) is observed at 300 K, indicating a permanent magnetism even at room temperature. The magnetization vs. H curve at room temperature showed a sharp increase, reaching saturation at low fields (Figure 4). These results are indicative of a collective ferromagnetic phase at room temperature. This behavior is also apparent from the

temperature dependence of the field-cooled (FC) and zero-field-cooled (ZFC) magnetization. The data presented a maximum in the ZFC curve at 130 K, which is generally ascribed to the average blocking temperature of the magnetic moment.

Magnetization decreases slightly with increasing temperature but nonetheless shows permanent magnetization at room temperature.

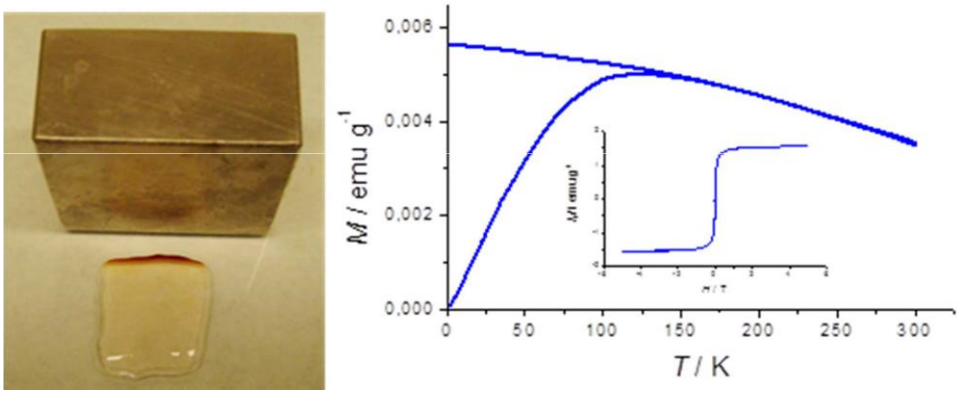

Figure 4. *Field-cooled (FC) and zero-field-cooled (ZFC) curves of lyophilized gold+maghemite- Lactobacillus fermentum® powder. Inset: hysteresis curves at 300 K of lyophilized gold+maghemite-Lactobacillus fermentum® powder. Photo: Application of a magnetic field to an aqueous dispersion of gold+maghemite-Lactobacillus fermentum® produced attraction of the magneto-optical bacteria*

It must be emphasized that isolated maghemite nanoparticles of this size range (10 nm) are superparamagnetic at room temperature and do not show persistent magnetization.[38-39]

However, once they are incorporated into the external bacterial surface, dipole-dipole interactions occur due to the close mutual proximity of the maghemite particles so that the maghemite-gold bacteria behave as ferromagnets at room temperature. This behavior is consistent with results that we have reported previously, in which massive incorporation of maghemite nanoparticles onto the bacteria surface yielded increased magnetic properties.[22]

Additionally, assessment of the antibacterial activity of these particles revealed that they are non-toxic and nor do they significantly inhibit this kind of bacteria.[38] Quantification of bacterial proliferation was performed using Live/Dead Bacterial Viability Kits SYTO9 (green) and propidium iodine (red), by counting the number of live (green) and dead (red) bacteria. The average live/dead ratio was used to quantify the effect of gold and maghemite nanoparticles upon bacterial proliferation by comparing with control cultures in the absence of nanoparticles. The presence of nanoparticles resulted in a slight decrease of the live/dead ratio of 15-25% with respect to control experiments.[40]

As conclusions, it must first emphasize that the putative potential of probiotic bacteria for the biosynthesis of metal nanoparticles is still a relatively unexplored field. Here we describe the first demonstration of the bio-fabrication of discrete gold nanoparticles using the metal-reducing *Lactobacillus fermentum*® bacterial strain. The resulting gold-loaded bacteria can be used, in a second step, as a precursor for the incorporation of maghemite nanoparticles, thus producing for the first time living bacteria that behave as magnets at room temperature and which also exhibit optical properties.

The biosynthesized magneto-optical nanoparticles built around these kinds of organisms may benefit from their large-scale production, and perhaps of their implementation for various biomedical applications through its inclusion in food, where probiotic bacteria are incorporated since they confer health benefits for men.

Notes and references

(1) Quaresma, P.; Osorio, I.; Doria, G.; Carvalho, P. A.; Pereira, A.; Langer, J.; Araujo, J. P.; Pastoriza-Santos, I.; Liz-Marzan, L. M.; Franco, R. *RSC Advances.* **2014**, 4, 3659-3667.

(2) Umut, E.; Pineider, F.; Arosio, P.; Sangregorio, C.; Corti, M.; Tabak, F.; Lascialfari, A.; Ghigna, P. J. *Mag. and Mag. Mater.* **2012**, 324, 2373-2379.

(3) Sheng, Y.; Xue, J. *J. of Colloid and Interf. Sci.* **2012**, 374, 96-101. (4) Bhattacharya, D.; Chakraborty, S. P.; Pramanik, A.; Baksi, A.; Roy, S.; Maiti, T. K.; Ghosh, S. K.; Pramanik, P. *J. Mater. Chem*. **2011**, 21, 17273.

(5) Yu, H.; Chen, M.; Rice, P. M.; Wang, S. X.; White, R. L.; Sun, S. *Nano Lett*. **2005**, 5, 379.

(6) Jain, P. K.; El-Sayed, I. H.; El-Sayed, M. A. *Nanotoday.* **2007**, 2, 18.

(7) Salgueiriño-Maceira,V.; Correa-Duarte, M. A.; Lopez- Quintela, M. A.; Rivas, J. *J. of Nanosci. and Nanotech.* **2009**, 9, 3684- 3688.

(8) Salgueiriño-Maceira, V.; Correa-Duarte, M. A.; Lopez-Quintela,M.A.;Rivas, J. *Sensor Letters*. **2007**, 5, 113-117.

(9) Suresh, A. K.; Pelletier, D. A.; Wang, W.; Broich, M. L.; Moon, J. W.; Gu, B.; Allison, D. P.; Joy, D. C.; Phelps, T. J.; Doktycz, M. J. *Acta Biomaterialia*. **2011**, 7, 2148–2152.

(10) Bhambure, R.; Bul, M.; Shaligram, N.; Kamat, M.; Singhal, R. *Chem. Eng. Technol*. **2009**, 32,1036–41.

(11) Mukherjee, P.; Senapati, S.; Mandal, D.; Ahmad, A.; Khan, M. I.; Kumar, R.; Sastry, M. *Chembiochem*. **2002**, 3, 461–463.

(12) Mukherjee, P.; Ahmad, A.; Mandal, D.; Senapati, S.; Sainkar, S. R.; Khan, M. I.; Ramani, R.; Parischa, R.; Ajayakumar, P. V.; Alam, M.; Sastry, M.; Kumar, R. *Angew. Chem. Int. Ed.* **2001**, 40, 3585–3588.

(13) Ahmad, A.; Senapati, S.; Khan, M. I.; Kumar, R.; Sastry, M. *Langmuir*. **2003**, 19, 3550–3553.

(14) Das, S. K.; Das, A. R.; Guha, A. K. *Langmuir*. **2009**, 25, 8192– 8109.

(15) Ramanathan, R.; Field, M. R.; O'Mullane, A. P.; Smooker, P. M.; Bhargava, S. K.; Bansal, V. *Nanoscale.* **2013**, 5, 2300-2306.

(16) Inbakandana, D.; Venkatesan, R.; Khan, S. A. *Colloids and Surfaces B: Biointerfaces.* **2010**, 81, 634–639.

(17) Bansal, V.; Bharde, A.; Ramanathan, R.; Bhargava, S. K. *Adv. In Colloid and Interf. Sci*. **2012**, 179-182, 150-168.

(18) Roh, Y.; Gao, H.; Vali, H.; Kennedy, D. W.; Yang, Z. K.; Gao, W.; Dohnalkova, A. C.; Stapleton, R. D.; Moon, J. W.; Phelps, T. J.; Fredrickson, J. K.; Zhou, J. *Appl. Environ. Microbiol*. **2006**, 72, 3236–3244.

(19) Zachara, J. M.; Kukkadapu, R. K.; Fredrickson, J. K.; Gorby, Y. A.; Smith, S. C. *Geomicrobiol. J.* **2002**, 19, 179–207.

(20) Zhang, C. L.; Liu, S.; Phelps, T. J.; Cole, D. R.; Horita, J.; Fortier, S. M.; Elless, M.; Valley, J. W. *Geochim. Cosmochim. Acta*. **1997**, 61, 4621–4632.

(21) Perez-Gonzalez, T.; Jimenez-Lopez, C.; Neal, A. L.; Rull-Perez, F.; Rodriguez-Navarro, A.; Fernandez-Vivas, A.; Iañez-Pareja, E.; *Geochim. Et Cosmochim. Acta*. **2010**, 74, 967–979.

(22) Martín, M.; Carmona, F.; Cuesta, R.; Rondón, D.; Gálvez, N.; Domínguez-Vera, J. M. *Adv. Funct. Mater*. **2014**, DOI: 10.1002/adfm. 201303754.

(23) Cheon, J.; Lee, J. H. *Acc. Chem. Res.* **2008**, 41, 1630-1640. (24) Dobson, J. *Nat. Nanotech.* **2008**, 3, 139–143.

(25) Mornet, S.; Vasseur, S.; Grasset, F.; Duguet, E. *J. Mater. Chem.* **2004** 14, 2161–2175.

(26) Laurent, S.; Forge, D.; Port, M.; Roch, A.; Robic, C.; Elst, L. V. Chem. Rev. 2008, 108, 2064-2110.

(27) Daniel, M. C.; Astruc, D. Chem. Rev. 2004, 104, 293.

(28) Pastoriza-Santos, I.; Liz-Marzan, L. M. Meth. Mol. Biol. 2013, 1025, 75-93.

(29) Lim, J. K.; Majetich, S. A. Nano Today. 2013, 8, 98-113.

(30) Dreaden, E. C.; Alkilany, A. M.; Huang, X.; Murphy, C. J.; El- Sayed, M. A. Chem. Soc. Rev. 2012, 41, 2740-2779.

(31) Wang, L.; Park, H. Y.; Lim, S. I.; Schadt, M. J.; Mott, D.; Luo, J.; Wang, X.; Zhong, C. J. J. Mater. Chem. 2008, 18, 2629–2635.

(32) Salgueiriño-Maceira, V.; Correa-Duarte, M. A.; Farle, M.; Lopez-Quintela, A.; Sieradzki, K.; Diaz, R. Chem. Mater. 2006, 18, 2701.

(33) Correa-Duarte, M. A.; Salgueiriño-Maceira, V.; Rodriguez-Gonzalez, B.; Liz-Marzan, L. M.; Kosiorek, A.; Kandulski, W.; Giersig, M. Adv. Mater. 2005, 17, 2014.

(34) Liu, H. L.; Wub, J. H.; Min, J. H.; Kim, Y. K. J. of Alloys and Compounds. 2012, 537, 60–64.

(35) Spasova, M.; Salgueirino-Maceira, V.; Schlachter, A.; Hilgendorff, M.; Giersig, M.; Liz-Marzan, L. M.; Farle, M. J. Mater. Chem. 2005, 15, 2095-2098.

(36) Liquid cultures of *Lactobacillus fermentum*® were grown in MRS broth (Panreac, 413785) at 37 ºC with orbital agitation for 24 h until early stationary phase. Bacteria were then collected via centrifugation and resuspended in Hank's Balanced Salt Solution to a final concentration of 1 mg/mL (3.5x108 CFU/mL). An Au(III) aqueous solution (Gold tetrachloride, Sigma-Aldrich, 99%), was dissolved in Type 1 Milli-Q ultrapure water and then added to the bacterial suspension to give a final concentration of 1 mM. The reaction mixture was kept at 37 ºC and under continuous stirring for 30 min. until the appearance of a characteristic red-wine colored solution, indicating the formation of gold nanoparticles. The resulting gold-biomass was centrifuged at 100 rpm for 30 min. The supernatant exhibited no band in the visible region. The quantity of gold measured by inducively coupled plasma mass spectrometry was zero. Control reactions in the absence of *Lactobacillus fermentum*®, where the culture supernatants of Hank's Balanced Salt Solution and MRS broth both exhibited no color change or absorbance at 520 nm, clearly indicated that the presence of bacteria in the biosynthesis of gold nanoparticles is a prerequisite. An acidic solution (pH 2) of maghemite nanoparticles (1 μL, at 0.95 - 1 M of iron), prepared as previously reported,[39] was added to the gold-loaded *Lactobacillus fermentum*® and maintained at 37 ºC under orbital agitation for 30 min. The reaction mixture was washed with several centrifugation cycles (100 rpm, 5 ºC, 30 minutes), to remove any unbound maghemite nanoparticles, and the final bacterial pellet resuspended in a 50 mM sodium citrate, PBS, Milli-Q water 1:1:4 mixture at pH 5. The resulting gold+maghemite-*Lactobacillus fermentum*® suspension remained stable at room temperature.

(37) The sample of gold+maghemite-*Lactobacillus fermentum*® was embedded in an epoxy resin. Fixation was achieved by adding 2.5% glutaraldehyde in a 0.1 M sodium cacodylate buffer solution at 4 ºC for 4 h. The sample was washed three times in 0.1 M sodium cacodylate buffer for 15 minutes. Then, drying cicles with ethanol and propylene oxide were applied. Finally, the sample was embedded in an

epoxy resin and left overnight at 4 ºC. After ultramicro-cutting, samples were observed with a FEI TITAN G2 microscope.

(38) Valero, E.; Tambalo, S.; Marzola, P.; Ortega-Muñoz, M.; Lopez-Jaramillo, J.; Santoyo, F.; Lopez, J. D.; Delgado, J. J.; Calvino, J. J.; Cuesta, R.; Dominguez-Vera, J. M.; Gálvez, N. J. Am. Chem. Soc. 2011, 133, 4889.

(39) Park, J.; Lee, E.; Hwang, N. M.; Kang, M.; Kim, S. C.; Hwang, Y.; Park, J. G.; Noh, H-J.; Kim, J-Y.; Park, J-H.; Hyeon, T. Angew. Chem. Int. Ed. 2005, 44, 2872.

(40) Quantification of bacteria proliferation was performed by using the Live/Dead Bacterial Viability Kits SYTO9 (green) and Propidium Iodine (red) (Invitrogen), counting the number of live (green) and dead (red) bacteria in a batch of three experiments by the software Image-Pro Plus 6.0. The average live/dead ratio was used to quantify the bacteria proliferation by comparing with control experiments where no nanoparticles were present. The presence of maghemite and gold nanoparticles resulted in a decrease of the live/dead ratio of 15 – 25 % for three independent experiments carried out in Hank's Balanced Salt Solution (Figure SI).

Supporting Information

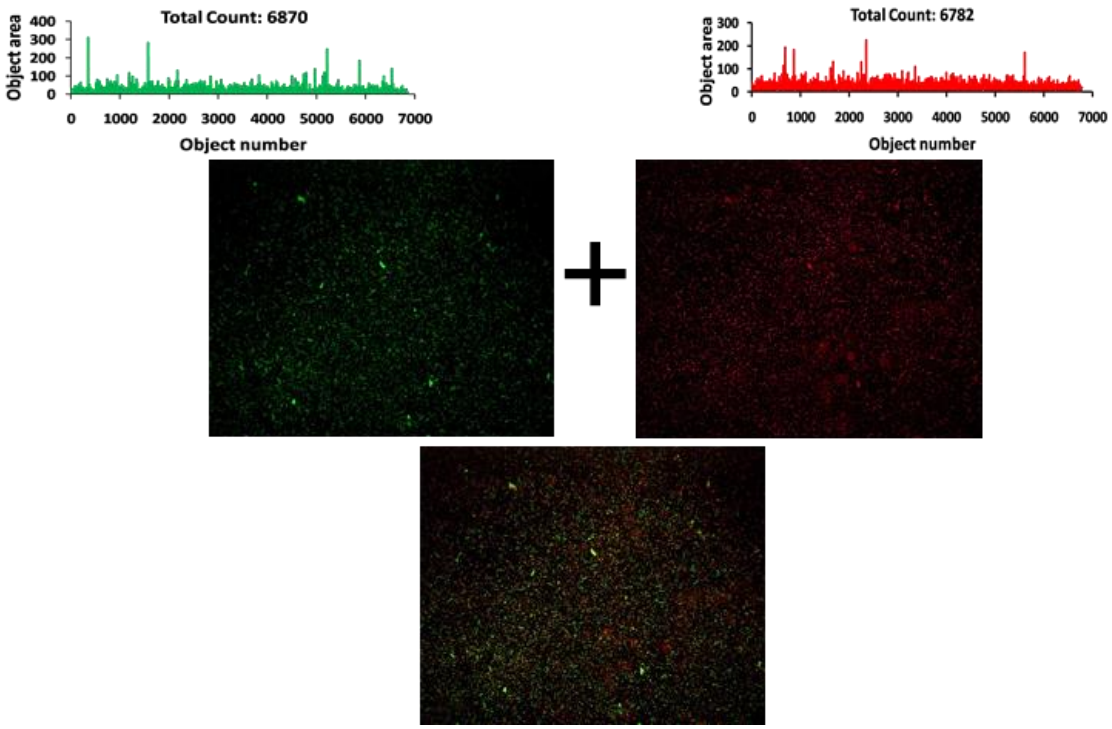

Figure SI-1. *Fluorescence microscopy images of Lactobacillus fermentum®, proliferation obtained using a Live/Dead Bacterial Viability Kit, where live and dead bacteria exhibit green and red emissions, respectively. The ratio live/dead is not significantly modified by the presence of nanoparticles. Whereas the viability of control of Lactobacillus fermentum® is between 1.10-1.20 in Hank's Balanced Salt Solution, it decreases to 1.01 for maghemite+gold-Lactobacillus fermentum®.*

CONCLUSIONES

1. La ferritina H, formada exclusivamente por subunidades H en su cápside proteica, tiene una gran actividad ferroxidasa para oxidar de forma catalítica Fe(II) a Fe(III) pero muy poca capacidad de almacenar Fe(III). Mas allá de entrar en discusiones mecanísticas sobre el proceso de reconstitución de hierro, nuestra investigación se ha centrado en el destino que sigue el Fe(III) generado por la ferritina H, y hemos demostrado que el Fe(III) que no es almacenado queda en una forma biodisponible en el organismo, no ya sólo para un agente quelatante sintético de Fe(III), sino también para biomoléculas de gran tamaño como proteínas. En este marco, hemos demostrado que este Fe(III) generado por la ferritina H es capaz de actuar como oxidante frente a otras metaloproteínas presentes en la célula. Concretamente hemos concluido que el Fe(III) no almacenado es capaz de oxidar a una isoforma de metalotioneína, la MT2, dando lugar a la liberación de iones metálicos Fe(II) y el Cu(I).

2. Por otra parte, hemos puesto de manifiesto que no todas las isoformas de metalotioneínas (MT) de mamífero reaccionan de manera similar con el Fe(III) generado en el proceso de reconstitución de ferritina H. Concretamente, la MT3 no reacciona con dicho Fe(III). Este resultado es de extrema importancia porque "curiosamente" la ferritina H se encuentra en células como neuronas donde la isoforma de la metalotioneína predominante es MT3. En vista de estos resultados, hemos extendido este estudio a otros pares ferritina – MT, y hemos demostrado que para el caso de ferritina mixta H/L no se produce Fe(III) disponible para oxidar a ningún tipo de metalotioneína (MT), incluida la isoforma más reactiva MT2. De nuevo "curiosamente", MT2 sólo coincide fisiológicamente con ferritinas de tipo H/L.

Este complejo entramado de interacciones entre metaloproteínas viene a poner de manifiesto que la elección del par ferritina-metalotioneína debe ser el apropiado en cada célula: ferritinas H con MT3 pero no con MT2, puesto que la presencia de ferritina H y MT2 genera espontáneamente Fe(II) y Cu(I), extremadamente dañinos para la propia célula. Este resultado deja entrever que cualquier disfunción genética que de lugar a la síntesis de una ferritina H en lugar de una H/L en neurona sería fatal para la célula y podría representar el primer estadío del desarrollo de una patología neurológica.

3. La alta actividad ferroxidasa y baja capacidad de almacenamiento de la ferritina H permite entender por qué ferritina H y lactoferrina coexisten en la leche materna. Nuestros resultados ponen de manifiesto que la existencia de este tándem proteico es una estrategia eficaz para llevar a cabo la detoxificación de Fe(II) y la captación de Fe(III) en el organismo en pro de llevar a cabo una actividad antimicrobiana eficaz.
Inspirados en la existencia de este tándem ferritina H + lactoferrina en leche materna, hemos diseñado y sintetizado un material que contiene ambas proteínas inmovilizadas y que funciona extraordinariamente bien como captador de hierro en todas sus formas: el Fe(II) libre es oxidado por la ferritina H mientras que el Fe(III) generado es captado por la lactoferrina. Este efecto sinérgico de ambas proteínas nos ha permitido diseñar materiales con potencial actividad antimicrobiana que representan un nuevo concepto de material destinado a una eficaz defensa contra el desarrollo de microorganismos patógenos al privarle de este metal esencial.

4. Hemos logrado estudiar y monitorizar los cambios conformacionales que tienen lugar en la lactoferrina durante el proceso de incorporación y liberación de Fe(III) de su estructura. Esto se ha hecho a través de espectroscopía de fluorescencia, mediante marcaje con dos fluoróforos AF350 y AF430, que presentan fenómeno de FRET con un rendimiento dependiente de la conformación de la proteína y por ende de su contenido en hierro. Además, hemos hecho uso de la correlación rendimiento del FRET-contenido en hierro de la lactoferrina para demostrar de forma elegante que esta proteína proporciona hierro a bacterias probióticas beneficiosas para la salud, con las que coexiste en la leche materna y que, además, este proceso tiene lugar sin la necesidad de internalización de la proteína por parte de la bacteria.

5. Hemos podido demostrar que al igual que otras bacterias reportadas en la literatura, las bacterias probióticas también emiten una (o varias) moléculas reductoras capaces de reducir metales u otras especies químicas. Concretamente, hemos puesto de manifiesto que estas bacterias son capaces de reducir Au(III) a Au(0) y además controlar el tamaño y deposición del Au(0) como nanopartícula en el biofilm bacteriano. Esto nos ha permitido preparar, aprovechando

conocimientos previos desarrollados en el grupo, bacterias probióticas que contienen simultáneamente nanopartículas de Au (con propiedades ópticas) y nanopartículas de maghemita (con propiedades magnéticas). La bacteria final se comporta como un imán a temperatura ambiente y absorbe en el espectro visible debido a la banda SPR.

Estas bacterias siguen vivas tras la incorporación de las nanopartículas de Au y maghemita. Hasta donde llegan nuestros conocimientos, este es el primer ejemplo de un organismo vivo que presenta propiedades magnéticas y ópticas. Esto abre una nueva vía de para la utilización de bacterias probióticas con propiedades únicas para aplicaciones biomédicas.